Relevance of antibodies targeting the β_1-adrenergic receptor for renal function

Relevanz von Antikörpern gegen den β_1-adrenergen Rezeptor für die Nierenfunktion

Dissertation zur Erlangung des
naturwissenschaftlichen Doktorgrades
der Julius-Maximilians-Universität Würzburg

eingereicht von

Sonja Hartmann

aus
Hirschaid

Würzburg 2014

Submitted on/ eingereicht am: .....

Members of the Committee/ Mitglieder der Promotionskommission:

Chairperson: .....

Primary Supervisor: .....

Supervisor (second): .....

Date of Public Defense/ Tag des Promotionskolloquiums: .....

Date of Receipt of Certificates/ Doktorurkunde ausgehändigt am: .....

Table of Contents

Abbreviations

aa	amino acids
ab	antibody
AC	adenylyl cyclase
ACE	angiotensin converting enzyme
Ach	acetylcholine
ADP	adenosine diphosphate
AHA	American Heart Association
ANG	angiotensinogen
Ang I	angiotensin I
Ang II	angiotensin II
ANP	atrial natriuretic peptide
ANS	autonomous nervous system
APS	ammonium peroxo-sulphate
AR	adrenergic receptor
AT_1	angiotensin receptor type 1
AT_2	angiotensin receptor type 2
ATP	adenosine triphosphate
ATPase	adenosine triphosphate hydrolase
β_1-EC_{II}	second extracellular loop of the β_1-adrenergic receptor
BNP	B-type natriuretic peptide
BSA	bovine serum albumin
BW	body weight
CA	caprylic acid
CAD	cardiac assist device
cAMP	cyclic adenosine monophosphate
CAP	caprylic acid precipitation
cDNA	complementary deoxyribonucleic acid
cGMP	cyclic guanosine monophosphate
CHF	chronic heart failure

CI	cardiac index
cpm	counts per minute
DAG	diacyl glycerol
DCM	dilated cardiomyopathy
DMSO	dimethyl sulfoxide
DNA	desoxyribonucleic acid
EC_I	first extracellular loop
EC_{II}	second extracellular loop
EC_{50}	half maximal effective concentration
EDTA	ethylenediaminetetraacetic acid
ELISA	enzyme-linked immunosorbent assay
FCS	fetal calf serum
FRET	Förster resonance energy transfer
$G_{12/13}$	GTPase-activating G protein
G_{α}	alpha subunit of the G protein
$G_{\beta\gamma}$	beta and gamma subunit of the G protein
GDP	guanosine-5’ diphosphate
GFR	glomerular filtration rate
$G_{i/o}$	inhibitory G protein
GPCR	G protein coupled receptor
G protein	heterotrimeric guanine nucleotide binding protein
$G_{q/11}$	PLC-activating G protein
GRK	GPCR kinase
G_s	stimulatory G protein
GST	glutathione-S-transferase
GTP	guanosine-5’-triphosphate
GTPase	guanosine-5’-triphosphate hydrolase
HF	heart failure
IC	intracellular loop
ICD	interventer cardiac defibrillator
ICM	ischemic cardiomyopathy
IgG	immunoglobulin G

IL	interleukin
IP_3	inositol 1,4,5-triphosphate
i.v.	intravenous
LV	left ventricular
LVBP	left ventricular blood pressure
LVED	left ventricular end diastolic
LVEF	left ventricular ejection fraction
LVES	left ventricular end systolic
MAPK	mitogen-activated protein kinase
MW	molecular weight
NYHA	New York Heart Association
OPD	o-phenylene diamine
PAH	para-aminohippurate
PAS	periodic acid-Schiff
PBS	phosphate buffered saline
PCR	polymerase chain reaction
PFA	paraforme aldehyde
PLB	phospholamban
PLC	phospholipase C
PKA	protein kinase A
PKC	protein kinase C
PNS	parasympathetic nervous system
POD	peroxidase
PRA	plasma renin activity
qPCR	quantitative real-time polymerase chain reaction
RAAS	renin-angiotensin-aldosterone-system
RBF	renal blood flow
RIA	radioimmunoassay
RNA	ribonucleic acid
RNAse	ribonucleic acid hydrolase
RyR	ryanodine receptor
RT	room temperature

SD	standard deviation
SDS	sodium dodecyl sulfate
SDS-PAGE	sodium dodecyl sulfate polyacrylamide gel electrophoresis
SEM	standard error of mean
Serca	sarcoplasmic reticulum calcium ATPase
SNS	sympathetic nervous system
SR	sarcoplasmic reticulum
TBS	tris buffered saline
TEMED	tetramethylethylenediamine
TGFβ	transforming growth factor β
TNFα	tumor necrosis factor α
Tris	tris(hydroxymethyl) aminoethane
TSH	thyroid stimulating hormone

1 Introduction

Dilated cardiomyopathy (DCM) is a non-ischemic heart muscle disease characterized by progressive depression of cardiac function associated with left ventricular dilatation of largely unknown etiology. Over the past decades, evidence has accumulated that functionally active autoantibodies targeting the β_1-adrenergic receptor (β_1-AR) are of pathophysiologic relevance for the disease. Retrospective data of heart failure patients showing an about 3-fold increased cardiovascular mortality risk in anti-β_1-autoantibody (anti-β_1-aab)-positive patients underline the prognostic significance of such antibodies [1]. As β_1-ARs are not restricted to the heart, but are also highly expressed in the kidney, it is tempting to speculate that modulation of renal β_1-ARs by agonist-like anti-β_1-aabs might also contribute to the prognosis of anti-β_1-aabs-positive patients. So far however, the potential pathophysiologic relevance of stimulating anti-β_1-aabs for kidney function has been ignored. Considering the close association between kidney function and cardiovascular disease and mortality [2], and given the fact that β_1-ARs are highly expressed in nephron-segments critically involved in renal function, we hypothesized that stimulating anti-β_1-abs might also impact on kidney function. The present work attempts to further elucidate the (patho-)physiological relevance of anti-β_1-abs for renal function and its relevance in autoimmune DCM.

1.1 The sympathetic nervous system

The sympathetic nervous system (SNS) represents one of the three main components of the autonomous nervous system (ANS), with the others being the enteric nervous system and the parasympathetic nervous system (PNS). It was brought to public awareness in the early decades of the twentieth century by Walter Bradford Cannon, who also coined the term ‘fight-and-flight’ response to stress [3]. However, the first anatomically correct depiction of the SNS was already provided almost three centuries earlier, in 1664 by Thomas Willis [4].

The sympathetic nerves start from the spinal column running towards the middle part of the spinal cord in the lateral horn. The SNS originates at the first thoracic segment of the spinal cord and extends to the third lumbar segment. As the cells of these nerves originate in the lumbar and thoracic regions; the SNS is considered the thoracolumbar part of the ANS.

The PNS and the SNS each consist of two sets of nerve bodies; the preganglionic or presynaptic fibers in the CNS, which synapse to the second set of nerve cell bodies in ganglia outside the CNS. The sympathetic ganglia are adjacent to the spine and consist of the vertebral (sympathetic chain) and prevertebral ganglia, including the superior cervical, celiac, superior mesenteric, inferior mesenteric, and aorticorenal ganglia. These ganglia are connected to the effector organs through long fibers, which innervate tissues in nearly every organ system of the body, including the heart, lungs, blood vessels, sweat glands, eyes, and kidneys (Figure 1).

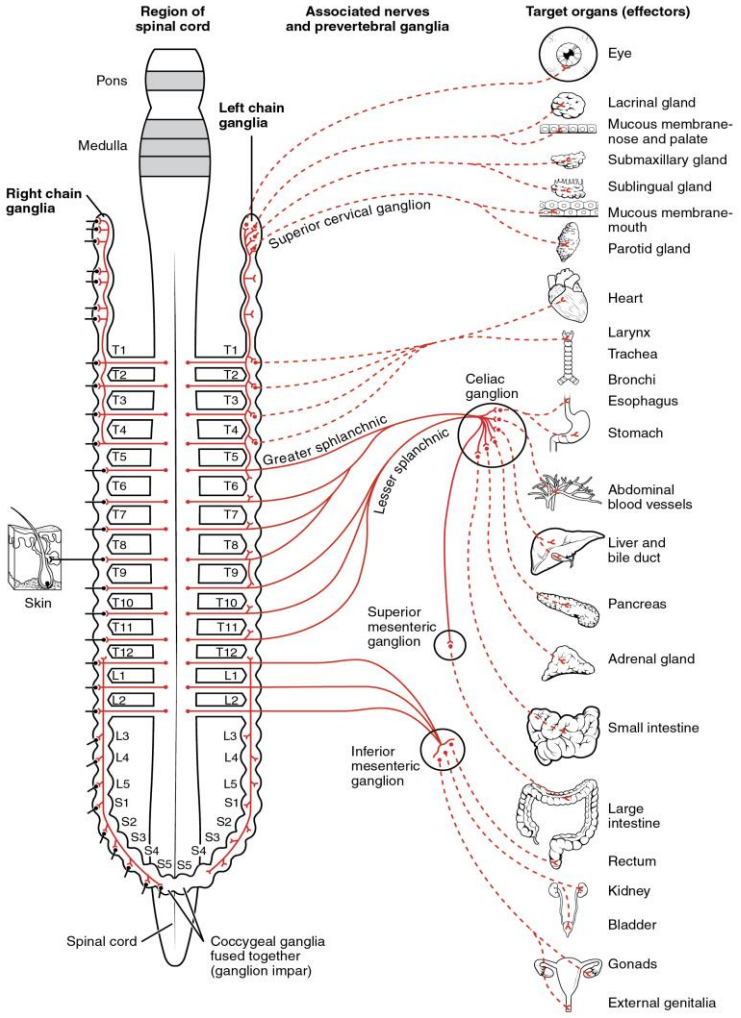

Figure 1: Connections of the SNS, taken from OpenStax College, *Anatomy & Physiology* [5].
Neurons from the lateral horn of the spinal cord (preganglionic neurons) project to the chain ganglia on either side of the vertebral column or to collateral (prevertebral) ganglia that are anterior to the vertebral column in the abdominal cavity. Axons from these ganglionic neurons (postganglionic fibers) then project to target effectors throughout the body.

The transmitter of the presynaptic-sympathetic neurons is acetylcholine. It activates mainly neuronal nicotinic acetylcholine receptors in the cell bodies of the postganglionic neurons, which leads to the secretion of noradrenalin; prolonged activation of the SNS can furthermore elicit the release of adrenalin from the adrenal medulla. The catecholamines noradrenalin and adrenalin mediate most of their effects through binding to α- or β-adrenergic receptors located in peripheral tissues.

The role of the SNS is to secure both basal and stress-related homeostasis. At rest, catecholamines maintain homeostasis by regulating heart rate, blood vessel tone, thermogenesis, and metabolism. When homeostasis is challenged, the SNS gets activated and increases the peripheral levels of catecholamines, which then act to restore a kind of steady state of the internal milieu. This reaction is generally defined as adaption syndrome or stress response [6].

1.2 The β_1-adrenergic receptor as a member of the GPCR superfamily

The β_1-AR belongs to the group of G protein-coupled receptors (GPCR). As one of the largest and most divers protein families in nature, GPCRs play significant roles in a variety of biological and pathological processes, ranging from vision, smell, and taste to neurological, cardiovascular, reproductive, and endocrine functions. Therefore, the GPCR superfamily represents a major target for therapeutic interventions [7, 8]. *De facto,* about 40% of the drugs currently available at the pharmaceutical market are known to target GPCRs [7, 9]. To underline the paramount importance of GPCRs, the 2012 Nobel Prize for chemistry was awarded to Drs. Robert J. Lefkowitz and Brian K. Kobilka for their contribution to the studies of GPCRs [10]. All GPCRs are characterized by seven transmembrane α-helices, which are connected by three extracellular and three intracellular loops (Figure 2). The N-terminal region is located in the extracellular space, where binding of potential ligands takes place. The intracellular regions comprising the C-terminal part of the receptor can interact with guanine nucleotide-binding proteins (G proteins), arrestins, and other downstream effectors. The overall architecture of class A GPCRs – which include all three types of β-adrenergic receptors - is quite similar [11]; however, there are considerable variations in the composition of the intra- and extracellular loops, as well as the length of the respective transmembrane helices.

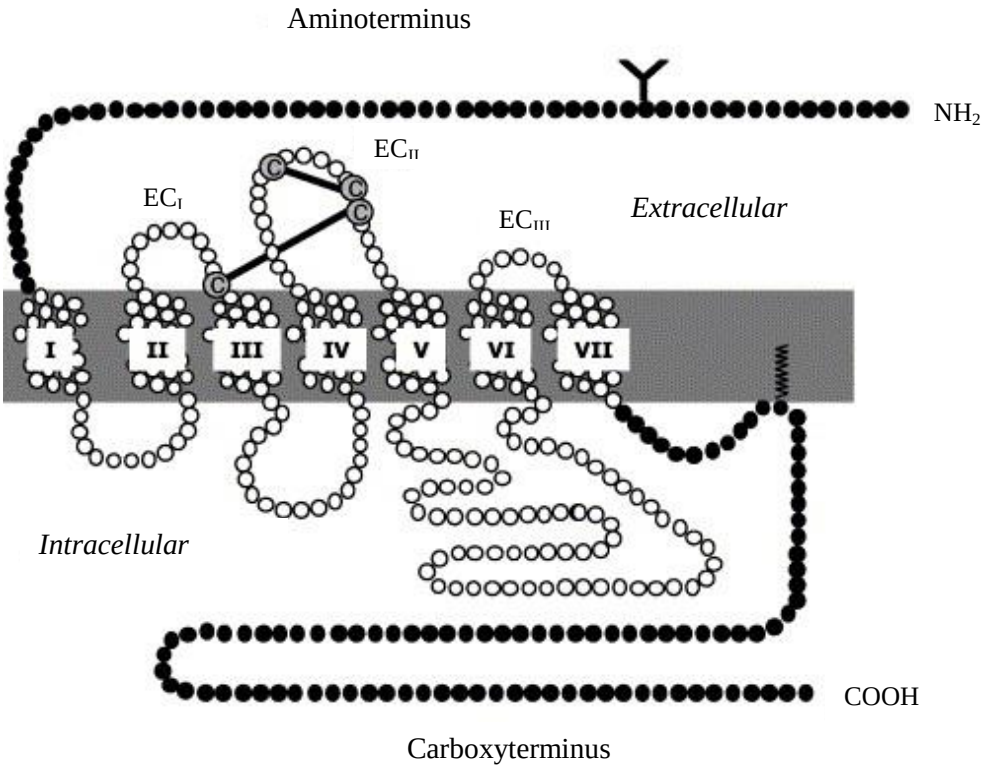

Figure 2: Scheme of the β_1-adrenergic receptor.
Schematic representation of the β_1-AR, adapted from Jahns *et al*. [12].

Extracellular signals are transmitted to the cell cytoplasm by interaction of ligands with their respective membrane receptors. GPCRs can interact with many ligands, ranging from amino acids, ions, and photons over pheromones, ordants, and eicosanoids to peptides, proteins, neurotransmitters, and hormones [13, 14]. Binding of a ligand to a GPCR leads to a ligand-specific conformational change of the receptor molecule. This conformational reorganization depends on the nature of the bound ligand. Under basal conditions, the GPCR is in equilibrium between an active and an inactive conformation [15, 16]. Binding of an agonist is thought to shift this equilibrium towards an activated state, whereas binding of an inverse agonist appears to stabilize the inactive receptor conformation. Pure antagonistic ligands, however, do not affect the conformational balance, but directly compete with agonistic ligands. If agonist-activation or antagonist-inactivation does not achieve maximal receptor responses, the compounds are classified as partial agonists/antagonists.

Upon activation of a GPCR by the binding of an agonist, the signal is transduced into the cytoplasm mainly *via* the activation of G proteins situated at the intracellular side of the membrane [17]. G proteins are heterotrimeric, and are composed of a GDP-binding α-subunit

(G_α) and a dimer consisting of the β- and γ-subunits ($G_{\beta\gamma}$) [18]. Stimulation of the G protein causes an exchange of GDP for GTP, and a subsequent dissociation of G_α from the $G_{\beta\gamma}$-subunit. Both G_α and $G_{\beta\gamma}$ are able to regulate different signaling cascades in the cytoplasm independently [19, 20]. The regulation of downstream signaling cascades is terminated by the intrinsic GTPase function of the G_α-subunit, which hydrolyses GTP to GDP and enables the subunits to reassociate, converting the G protein to its inactive state and translocating it to the membrane [21]. There are four different G_α-subunits which induce different effects; G proteins are therefore subdivided into the following families:

G_s	activation of adenylyl cyclase (AC)	→ increase of cAMP levels
$G_{i/o}$	inhibition of AC	→ decrease of cAMP levels
	stimulation of phosphodiesterase 6 (PDE6)	→ degradation of cGMP
$G_{q/11}$	stimulation of phospholipase C (PLC)	→ formation of IP3 and DAG
		→ Ca^{2+} release
$G_{12/13}$	stimulation of RhoA proteins	→ stimulation of Rho kinases

In addition to the canonical GPCR signaling pathways, a group of molecules referred to as β-arrestins may regulate GPCR activity. After phosphorylation of an activated GPCR by GPCR kinases (GRKs), β-arrestins are recruited to the plasma membrane where they bind to the phosphorylated receptor. Their binding results in uncoupling of the G protein from its receptor, leading to termination of G protein-mediated signaling [22]. Subsequent actions may comprise receptor desensitization, internalization, or the regulation of β-arrestin mediated signaling pathways, depending on the conformational interaction between the receptor and the arrestin molecule, as well as the nature of the phosphorylation of the receptor [23-25].

One subfamily of GPCRs are the adrenergic receptors (ARs). They are divided into two discrete groups, α and β, which, again, are subdivided into several subtypes [26, 27]. The α-receptors have the subtypes α_1 and α_2, the β-receptors are subdivided into β_1-, β_2-, and β_3-ARs [28]. ARs are targets of catecholamines - especially adrenalin and noradrenalin - released by the SNS. $Alpha_1$-ARs are $G_{q/11}$-coupled and, therefore, upon stimulation activate phospholipase C (PLC), subsequently increasing intracellular Ca^{2+} levels. $Alpha_2$-ARs, being $G_{i/o}$ coupled, decrease cellular cAMP levels by inhibition of adenylyl cyclase (AC) [29]. All β-AR-subtypes use AC activation as signal transduction mechanism, and are hence coupled to G_s [30]. $Beta_1$-ARs

are mainly expressed in the heart, and their activation generally triggers myocyte inotropy, chronotropy, and lusitropy. The effects of β_2-ARs include mediation of relaxation of vascular and other smooth muscles [31]. The β_3-subtype is mainly located in adipose tissue and regulates lipolysis and thermogenesis.

The β_1-AR represents the predominant β-AR subtype in the heart (75-80%) [32] and is also expressed in other tissues, like the kidney and the brain [33-35]. Beta$_1$-ARs are considered key mediators of the SNS, inducing the so-called fight-and-flight response described above (section 1.1). Binding of the endogenous agonists noradrenalin and adrenalin, or any other (synthetic) agonist into the transmembrane binding pocket activates the β_1-AR. The subsequent conformational change and activation of $G\alpha_s$ results in an increase in intracellular cAMP levels. In cardiomyocytes, this triggers a signaling cascade leading to phosphorylation of a number of proteins that are essential for cardiac function (Figure 3). In the end, Ca^{2+}-influx into the cell increases direct activation of L-type Ca^{2+} channels [36, 37], an increase in Ca^{2+} -reuptake into the SR through phospholamban and SERCA [38], which together modulates myofilament Ca^{2+}-sensitivity (troponin I) [39].

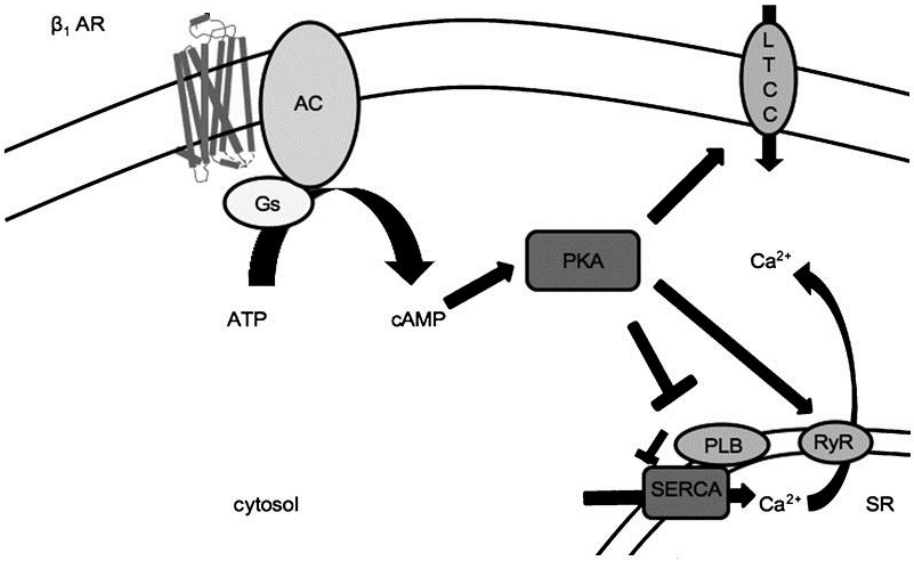

Figure 3: Signaling cascade of the β_1-AR, adapted from Jahns, R. *et al.* [40].

Binding of an agonist to the β_1-AR leads to the activation of $G\alpha_S$, resulting in an increase of cAMP by AC. The subsequent activation of PKA leads to the phosphorylation of LTCC and RyR, which increases intracellular Ca^{2+} levels. Moreover, PKA inhibits PLB, thereby prohibiting the reuptake of Ca^{2+} back into the SR.

All these effects together result in an increase in contractility (positive inotropy), beating rate (positive chronotropy), and excitability of the membrane, facilitating the generation of action potentials (positive bathmotropy). Moreover, conduction velocity of the AV node increases (positive dromotropy), as well as diastolic relaxation of the heart muscle (positive lusitropy).

In the kidney, the cAMP cascade activated after stimulation of β_1-ARs in the juxtaglomerular apparatus leads to an increase in the secretion of renin [41]. The enzyme renin cleaves the zymogen angiotensinogen and thereby converts it into angiotensin I (Ang I). Ang I is then converted into angiotensin II (Ang II), the major bioactive substance of the renin-angiotensin-aldosterone system (RAAS). It exerts several systemic physiological effects, including vasoconstriction and a subsequent rise in blood pressure (Figure 4). This underscores that, in the end, stimulation of the β_1-adrenergic system ensures systemic blood supply and addresses all organ systems necessary in a situation of acute stress (e.g. "flight-and-fight" conditions).

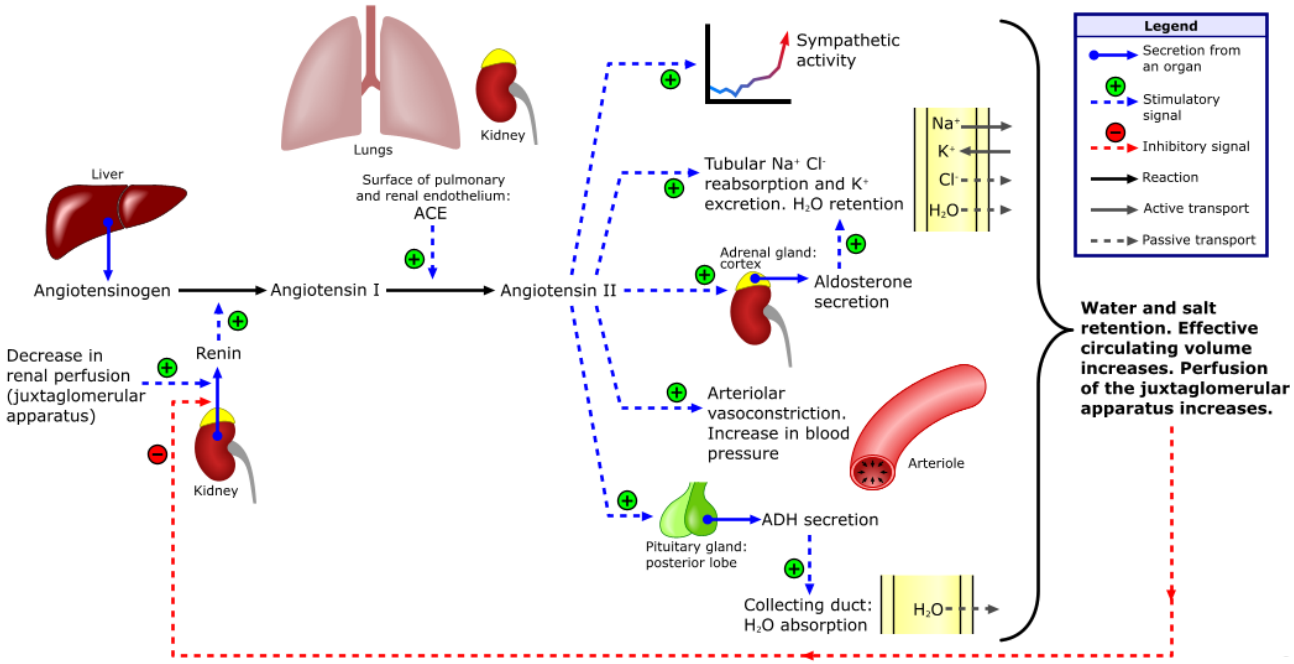

Figure 4: The renin-angiotensin-aldosterone system, adapted from Rad, A. [42].
Scheme of the effects of the RAAS on sympathetic activity, salt excretion, and blood pressure regulation.

1.3 The role of the β_1-adrenergic receptor for kidney function

Since the first renal denervation studies, it is known that the β-adrenergic system is critically involved in the regulation of a number of important physiological processes in the kidney [43, 44]. The specific distribution of β_1-ARs along the nephron was derived from localization studies utilizing autoradiography [45, 46], *in situ* hybridization [47], and immunofluorescence imaging [35]. These studies revealed that the main segments or cell types of the nephron expressing β_1-ARs were juxtaglomerular and mesangial cells, the distal tubules, the cortical thick ascending limb (TAL) of the Henle loop (macula densa), the intercalated cells localized in the collecting duct as well as the renal arteries and afferent arterioles; very few β_1-ARs were also detected in the proximal tubules (Figure 5). From these localization data, the following potential roles of β_1-ARs in the regulation of renal function have been hypothesized:

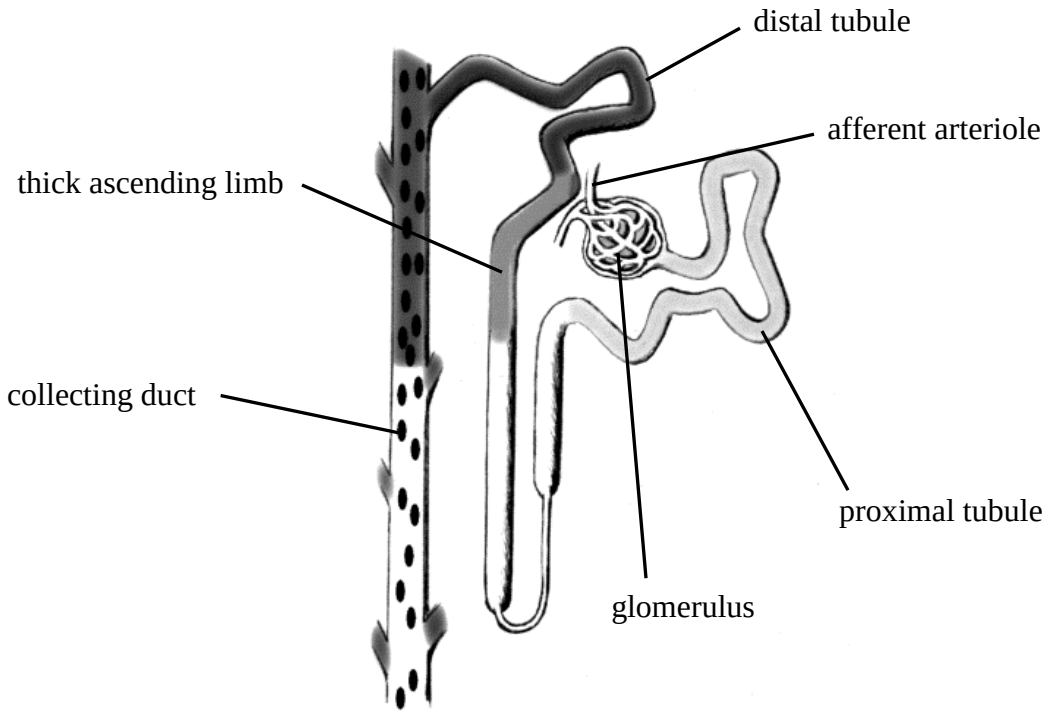

Figure 5: Scheme indicating the major locations of the β_1-ARs in the rat nephron, adapted from Boivin V. *et al*. [35]

Simplified scheme of the rat nephron indicating the areas expressing β_1-ARs. Significant amounts of β_1-ARs were found in the renin-producing juxtaglomerular granular cells (in the wall of the afferent arteriole), the mesangial cells, proximal tubular cells, cortical TAL segments (including macula densa cells), all portions of the distal tubular nephron segments, and the intercalated cells of the collecting duct system (depicted as dark dots).

Renin, an aspartyl-protease, is the key regulator of the RAAS, which is critically involved in salt, volume, and blood pressure homeostasis of the body. The release of renin is regulated by a variety of local and systemic factors. Generally, renin secretion is controlled by three intracellular second messengers: cAMP, cGMP, and Ca^{2+}, with cAMP being the main stimulator of renin release [48, 49]. Thus, all mechanisms that increase intracellular cAMP stimulate renin secretion, like β-adrenergic agonists [50-52], prostaglandins [53], dopamine [54], or adrenomedullin [55]. Especially the stimulation of β_1-ARs by catecholamines is physiologically relevant for the release of renin [52]. The high amount of β_1-ARs localized in the glomerulus and the juxtaglomerular apparatus support these findings.

Besides the juxtaglomerular cells, renin secretion is regulated by the macula densa, which is also part of the juxtaglomerular apparatus and located at the cortical TAL of the Henle loop. The macula densa cells have an important function by sensing changes in tubular fluid composition, generating and sending signals to the juxtaglomerular apparatus which control renal blood flow (RBF) and glomerular filtration rate (GFR) through tubuloglomerular feedback (TGF) and renin release [56, 57]. Any inappropriate increase of the NaCl concentration in the distal tubule is responded to with the secretion of a vasopressor acting on the adjacent afferent arteriole resulting in a decrease in GFR as part of the TGF mechanism. Low tubular NaCl-concentrations sensed by the macula densa induce renin release. Tubular salt sensing by the macula densa involves apical NaCl transport mechanisms, including the $Na^+/K^+/2Cl^-$ cotransporter, which is the primary NaCl entry mechanism. Both the macula densa cells and the premacula densa TAL cells express significant amounts of β_1-ARs. Studies performed on mouse TAL showed that catecholamines are able to influence the active transport of sodium from the lumen into the interstitium [58, 59], indicating that the macula densa mechanism represents another, indirect fashion of β-AR-mediated stimulation of renin secretion through reduction of the amount of sodium excreted.

A high density of β_1-ARs was found also in the smooth muscle cells of the renal arteries and afferent arterioles. As described above, the stimulation of the β_1-adrenergic system leads to an increase in intracellular cAMP and subsequently contraction of smooth muscle cells. Taken together, these findings imply that the β_1-adrenergic system might play an important a role in the regulation of GFR and the perfusion of the kidney as a whole [35], particularly since it has been demonstrated that vasoactive substances such as catecholamines lower the glomerular capillary ultrafiltration coefficient by reducing blood flow in capillary loops and the capillary surface area [60, 61].

Thus, β_1-ARs situated both at the glomerulus and the juxtaglomerular apparatus might also affect systemic blood pressure through the aforementioned mechanisms.

The last part of the nephron, the collecting duct, serves to control the body's electrolyte and fluid balance. It consists of two different cell types, the intercalated cells and the principal cells. The main function of the intercalated cells is Cl^- and K^+ reabsorption and the contribution to the acid-base-homeostasis of the body by secreting H^+ and HCO_3^-; to do so there are two different types of intercalated cells, the acid-excreting α- (or type A) intercalated cells and the base-excreting β-intercalated cells (type B intercalated cells) [62-64]. Alpha-cells, abundant in the outer medullary collecting duct (OMCD), absorb HCO_3^- *via* H^+ secretion, whereas β-cells secrete HCO_3^- *via* apical Cl^-HCO_3 exchange [65]. The β_1-ARs which are expressed in the collecting duct are clearly restricted to the α-intercalated cells. This could mean that stimulation of β_1-ARs leads to an increase in acid excretion, and is therefore able to influence the pH of the urine.

1.4 Dilated cardiomyopathy

1.4.1 Definition

According to the American Heart Association, cardiomyopathies are defined as "*a heterogeneous group of diseases of the myocardium associated with mechanical and/or electrical dysfunction that usually (but not invariably) exhibit inappropriate ventricular hypertrophy or dilatation and are due to a variety of causes that frequently are genetic"* [66]. Following the most recent classification, the four major types of cardiomyopathy are dilated cardiomyopathy, hypertrophic cardiomyopathy, restrictive cardiomyopathy, and arrhythmogenic right ventricular cardiomyopathy. They can be divided into two groups, depending on the predominantly involved organs. In case the clinically relevant disease processes are solely or predominantly restricted to the heart muscle, the disease is classified as primary cardiomyopathy. Secondary cardiomyopathies on the other hand are systemic disorders with involvement of the myocardium [66].

Primary cardiomyopathies can be subdivided into genetic, acquired and mixed (predominantly non-genetic) forms; the latter including dilated cardiomyopathy (DCM). DCM is defined as a myocardial disease with dilatation and reduced contractility of the left or both ventricles [67], and represents the most common form of cardiomyopathy. During the progression of the disease,

ventricular and supraventricular arrhythmias may occur, a further decrease in contractile function, thromboembolism, and ultimately sudden or heart-failure related death. With an estimated prevalence of 1:2500, DCM is the third most common cause of heart failure and represents the most frequent indication for heart transplantation [66]. It can be caused by a variety of agents and conditions, including viruses, bacteria, toxins, systemic disorders, and genetic mutations in genes encoding myocyte structural proteins. Determination of the actual cause in individual cases remains difficult or impossible, leaving a relevant number of DCM cases classified as "idiopathic".

Clinically, heart failure is classified depending on the severity of the patient's symptoms, most commonly according to the New York Heart Association (NYHA) Functional Classification, using four states of disease-severity based on the patient's limitations during physical activity [68]:

Class	New York Heart Association Functional Classification
I	Patients have cardiac disease but without the resulting limitations of physical activity. Physical activity does not cause undue fatigue, palpitation, dyspnea, or anginal pain.
II	Patients have cardiac disease resulting in slight limitation of physical activity. They are comfortable at rest. Physical activity results in fatigue, palpitation, dyspnea, or anginal pain.
III	Patients have cardiac disease resulting in marked limitation of physical activity. They are comfortable at rest. Less than ordinary physical activity causes fatigue, palpitation, dyspnea, or anginal pain.
IV	Patients have cardiac disease resulting in inability to carry on any physical activity without discomfort. Symptoms of cardiac insufficiency or of the anginal syndrome are present even at rest.

1.4.2 Pathophysiology

The pathophysiology of DCM mainly concerns cardiac function. However, it is well known that the heart and the kidney closely interact with each other [69], a phenomenon called cardio-renal crosstalk. The following section describes the pathophysiological features of this disease on the heart and on the kidneys in more detail.

1.4.2.1 Cardiac phenotype

Although DCM may be asymptomatic at early stages of the disease, most symptoms are typical for heart failure (HF). The symptoms of HF can range from shortness of breath, cough, and fatigue to orthopnea, paroxysmal nocturnal dyspnea, and severe edema.

As the perfusion of various organs is reduced due to the decrease in cardiac output and ventricular stroke volume, two compensatory mechanisms are activated. First, the activation of the SNS leads to the release of noradrenalin and adrenalin from the adrenal medulla, which activate β_1-ARs in the heart. This stimulation results in an increase of cAMP followed by an accumulation of Ca^{2+} in the cytosol and increasing contractility. However, chronic stimulation of β_1-ARs corresponding to a constantly enhanced sympathetic tone may result in a considerable decrease of this positive inotropic effect. This is – in part – explainable by the desensitization and/or internalization of stimulated β_1-AR [70, 71]. In addition, recruitment of inhibitory G_i proteins to the plasma membrane might have some influence [72, 73]. Second, the so-called Frank-Starling mechanism gets activated, in which the increased ventricular diastolic volume enhances stretch of the myofibers in order to increase the subsequent stroke volume [74].

In the long run, these compensatory mechanisms are mostly not efficient enough to prevent the effects of chronic adrenergic overstimulation on the heart. Chronic adrenergic challenge has a negative impact on the myocardium, resulting in progressive myocyte degeneration (apoptosis and/or necrosis) and contractile dysfunction, followed by the development of clinical HF-symptoms.

1.4.2.2 Renal phenotype

Renal function plays a central role in many aspects of the pathophysiology and also in the treatment of HF. As cardiac function deteriorates, GFR and RBF decrease [75, 76], filtration

fraction and sodium filtration decline, while tubular reabsorption increases, leading to sodium and water retention. Impaired perfusion of the kidneys leads to activation of the RAAS [77], further increasing the retention of water and sodium, and enhancing both renal and peripheral vascular tone. All these effects are further amplified by the sympathetic activation which usually accompanies HF. The RAAS, in combination with the increased release of vasopressin, causes a cascade of potentially deleterious long-term effects. An increase of Ang II causes vasoconstriction (including efferent renal vasoconstriction) [78] and boosts the production of aldosterone. Aldosterone is a strong stimulator of myocardial and vascular collagen deposition and fibrosis [79, 80], and also further enhances the reabsorption of sodium in the distal nephron. Other direct effects of Ang II include the release of vasopressin and noradrenalin, and triggering apoptosis.

Clearly, heart and kidney functions closely interact with each other. HF is one of the well-known cardiovascular complications of end-stage renal failure; on the other hand, chronic kidney disease is very common in HF patients. The prevalence of chronic kidney disease is very high in patients with a low left ventricular ejection fraction [81-84]. It has been shown that HF patients with renal dysfunction have a significantly poorer prognosis than patients with preserved renal function, despite similar NYHA functional classes and LVEF [75, 85, 86]. Therefore, renal dysfunction has emerged as one of the strongest prognostic factors in HF. This interdependent relationship has come to be known as the “cardio-renal syndrome” [87].

1.4.3 Therapeutic possibilities

Therapeutic possibilities are mainly confined to the standard treatment of heart failure, as it is recommended for instance by the *European Society of Cardiology* [88, 89]. Therapy includes general measures like weight reduction, low sodium and restricted fluid intake, moderate physical activity, and abstinence from nicotine and alcohol, as well as pharmacotherapy. Pharmacotherapy encompasses various groups of drugs, including diuretics, β-blockers, ACE inhibitors, aldosterone antagonists, Ang II receptor blockers, cardiac glycosides, and inotropes.

ACE inhibitors like enalapril and captopril, count as basic therapeutic agents in DCM and are applied in all stages of HF. They inhibit the formation of Ang II by blocking the enzyme responsible for the conversion of Ang I to Ang II. Thereby, arteriolar resistance decreases, venous capacity increases and cardiac output as well as cardiac index decrease. In the kidney, the

resistance of blood vessels decreases, and natriuresis increases. Several studies were able to show that patients with NYHA classes II through IV benefit from the application of ACE inhibitors, regarding symptomatology, physical loadability, hospitalization, and mortality [90, 91].

Beta-blockers represent a cornerstone in the therapy of HF. They block the accessibility of β-ARs for catecholamines, thereby lowering heart rate and blood pressure. As conclusively shown by several meta-analyses of β-blocker trials, their application is associated with a 30% reduction in mortality, 40% reduction in hospitalization, and 38% decrease in sudden death in CHF patients [92, 93].

If a patient exhibits signs of water retention, the application of *diuretics* is imperative. The diuretic effect is usually achieved by increasing the excretion of sodium, which osmotically binds water. Of the five groups of diuretics available, thiazides and loop diuretics are utilized regularly to clear edema.

Regarding HF-therapy, the beneficial effects of *aldosterone antagonists* have been underestimated for a long time. The Randomized Aldactone Evaluation Study (RALES) and the Eplerenone Post-Acute Myocardial Infarction Heart Failure Efficacy and Survival Study (EPHESUS) could show the beneficial effects of aldosterone antagonists in patients with systolic heart failure [94-96]. In these studies, both spironolactone and eplerenone were able to decrease mortality rate in patients with severe HF symptoms (NYHA class III and IV), particularly after acute myocardial infarction. Both agents block the effects of aldosterone by binding to its receptor, resulting in an increased excretion of water and sodium, while potassium is retained.

Angiotensin II receptor blockers (AT_1 receptor blockers), also called sartans, are another group of pharmaceuticals interfering with the RAAS. Blockade of the AT_1-receptor causes, among others, vasodilatation and reduces secretion of vasopressin and aldosterone. Although Ang II receptor blockers showed no clinical advantage over ACE inhibitors [97-99], at least some of the well-known ACE side effects occur less often when the AT_1-receptor is blocked directly.

Only two substances of the large group of herbal *cardiac glycosides* are in clinical use today: digitoxin and digoxin. They inhibit the Na^+/K^+-ATPase, thus acting positively inotropic and negatively chronotropic. They are usually applied in combination with ACE inhibitors, β-blockers, and diuretics.

Inotropes are substances causing a positive inotropic effect, mainly by increasing intracellular cAMP levels. Their application in HF/CHF is not recommended as they have been consistently

shown to increase mortality [100, 101]. Only in acute or decompensated HF, inotropic therapy is recommended to lower end-diastolic pressure and to improve diuresis.

Aside from pharmaceutical therapy, the option of surgical interventions exists. Such procedures include cardiac assist device surgery, implantable cardioverter defibrillator (ICD) therapy, biventricular pacemaker surgery, and heart transplantation.

According to recent studies, insertion of a *biventricular pacemaker* is a promising approach to lower hospitalization and mortality rate in HF patients [102, 103]. This device is designed to pace both ventricles, thus improving the synchrony of contraction of the left ventricle. It is still unclear however, if HF-patients ultimately benefit from this approach.

*ICD*s are designed to prevent sudden death from serious arrhythmias known as ventricular tachycardia or fibrillation. They are generally recommended in patients with hypertrophic cardiomyopathy at high risk for sudden death, but also in children with dilated cardiomyopathy and serious ventricular arrhythmias documented. Although some single studies could show that ICD-implantation may decrease cardiovascular mortality in DCM [104], their majority failed to show a significant effect on all-cause mortality [105-107].

Cardiac assist devices (CAD) improve blood supply to the body, allowing other organ systems to recover from the stress caused by heart failure. They are usually used as a bridge to transplant, and are therefore rather conceived as temporary means of support.

Heart transplantation remains as a last resort in HF when other current treatment options have failed. To date, the 5-years survival rate is about 80% [108], compared to the event-free survival rate of 50 to 60% of HF-patients under standard pharmaceutical treatment [109, 110].

1.5 Autoimmune DCM

In DCM, a number of alterations of the immune system have been found, including auto-reactivity against cardiomyocytes, decreased natural killer cell activity, and abnormal activity of suppressor cells. Thus, autoimmune mechanisms are thought to play a key role in the pathogenesis of this disease [111-114]. In particular, auto-antibodies directed against certain cardiac proteins might play a pivotal role: A significant number of DCM patients has been shown to possess antibodies against e.g. sarcomeric [115-118], mitochondrial [119, 120] or membrane proteins [121-123]. Especially aabs targeting M_2 muscarinic receptors, β_1-ARs, and the myosin heavy chain have been detected in DCM patients independently by several groups [116, 121, 123-

127]. Among these aabs, those directed against the β_1-AR proved to have a particular relevance from a pathophysiologic point of view [128-131]. In particular, aabs that target the β_1-EC_{II} seem to play a key role in the pathogenesis of DCM [132, 133]. They have been shown to be associated with significantly poorer left ventricular function [122], a higher prevalence of serious ventricular arrhythmias [134], and a higher incidence of sudden cardiac death [135]. However, it is still unclear whether patients develop heart disease because of the presence of harmful anti–β_1-EC_{II} aabs, or whether they develop these aabs as a result of cardiac tissue injury.

An autoimmune disease is defined as a disease in which autoimmunity plays a directly causative or a significant contributory role. The autoimmune genesis of a disease is assumed when the *Witebsky postulates* are fulfilled [136]. According to these postulates, direct evidence requires reproduction of the disease by transfer of homologous pathogenic abs or pathogenic T cells from one to another of the same species. Indirect evidence for the autoimmune etiology of a disease requires a corresponding self-antigen to be identified and an analogous immune response to be induced in an experimental animal, which, finally, must also develop a similar disease [137]. All of these criteria have been fulfilled in the case of stimulatory anti-β_1-AR (auto-) antibodies [131]. In the human, anti-β_1-aabs are frequently found in patients suffering from idiopathic DCM, their presence being associated with reduced cardiac function, ventricular arrhythmias, and increased cardiovascular mortality [1, 122].

1.6 Therapeutic options in autoimmune DCM

In addition to the standard therapy recommended for heart failure (see section 1.4.3), the treatment of autoimmune DCM comprises therapeutic approaches successfully used in other kinds of autoimmune diseases.

A strategy widely applied in all kinds of autoimmune diseases is *immunosuppression*. For the treatment of DCM with immunosuppressants, both positive and negative effects have been reported; their indication is therefore considered controversial. One study in DCM-patients treated with prednisone showed a significant improvement of LVEF after 3 months, which was no more seen at 9 and 15 months of follow-up [138]. Studies on the effects of other immunosuppressant drugs like azathioprine and cyclosporine carried out in children showed an improvement of several histological parameters only if prednisone was combined with azathioprine or cyclosporine, but not with prednisone monotherapy [139, 140]. As chronic

treatment with corticosteroids generally entails undesirable side-effects (e.g. Cushing's syndrome, osteoporosis), this kind of treatment is not recommended in DCM.

Increased inflammatory markers (TNF-α, IL-1, IL-6) in patients with DCM suggested that treatment with *anti-inflammatory immunomodulators* might be a therapeutic option. Especially the cytokine TNF-α seems to play a role in the development of DCM. Pilot studies showed that patients treated with TNF-α antagonists (Etanercept) or blockers (Pentoxifylline) slightly improved in functional NYHA-classes and LVEF [141, 142]. However, there are a number of immunologic side-effects to consider that preclude routine application.

Immunoadsorption, a special form of apheresis, attempts to eliminate IgG extracorporeally by employing specific immunosorbent substances. The patient's plasma circulates through specific columns which selectively bind and eliminate IgG. Given the half-life of IgGs (approximately 21 days), several sessions of apheresis – preferentially on consecutive days - are necessary to remove an adequate amount of IgG [143]. This technique turned out to be useful in primarily B cell-mediated autoimmune DCM [144, 145]; however, as immunoadsorption of IgG does not affect the B cells themselves, the reappearance of aabs must be monitored. Also, it is possible that the effect of this treatment is rather attributable to the Ig replacement following immunoadsorption [146, 147].

Mature B cells producing antibodies constitute another potential therapeutic target in autoimmune DCM. Monoclonal antibodies recognizing B cell-specific antigens such as CD20, CD22, and CD19, have been initially developed to treat non-Hodgkin's lymphoma. Hence, a number of therapeutic anti-B cell antibodies have been developed that either deplete or modulate B cells (e.g. rituximab (anti-CD20), epratuzumab (anti-CD22), alemtuzumab (anti-CD52)). Due to the severe immunological side-effects, this approach is, again, not recommended.

A more recent approach attempts the direct neutralization of aabs with *aptamers* [148]. These synthetic, highly structured, single- or double-stranded oligonucleotides bind to their corresponding target molecules with high specificity, thereby modulating the target's function. Due to their low immunogenicity and toxicity, some aptamers have already entered the clinical pipeline [149, 150].

Perhaps the most elegant mechanistic approach is the use of *cyclic peptides*. Such peptides have been designed to scavenge receptor-stimulating aabs directly in the circulating blood by competing with their auto-antigens [151]. The advantage of this method is the selective elimination of potentially causative aabs, while protective aabs remain unaffected. In our

laboratory, we succeeded in preventing the development of auto-immune DCM in immunized rats by injecting cyclic peptides mimicking the β_1-EC_{II} epitope [40, 152, 153]. In addition, our group was able to show that cyclic compared to linear peptides more closely mimic the conformation of the native loop of the target-receptor, thus more effectively bind aabs; moreover such peptides are less degraded *in vivo* because of their cyclic nature. Specific cyclic peptides might thus represent a new promising approach in the treatment of human β_1-aabs-associated DCM.

1.7 Aims of the present work

The purpose of this thesis was to investigate the effects and pathophysiologic relevance of stimulatory abs directed against the β_1-AR on renal function, and their possible contribution to the hypertensive phenotype observed in our rat model. The results of the present work will provide the so far first data on the relationship between β_1-AR-directed autoimmunity and kidney function, helping to gain better insight into the underlying pathophysiology and, thus, contribute to conceive strategies to preserve renal function and/or to circumvent renal effects of simulating anti-β_1-abs. The results obtained from our rat-experiments might even strengthen the rationale for the current development of novel pharmacotherapeutic agents neutralizing sympathomimetic anti-β_1-aabs.

2 Materials & Methods

2.1 Materials

Chemicals, solvents, enzymes, kits, and buffers used in the here presented work are listed in the Appendix.

2.2 Methods

2.2.1 Generation of fusion proteins

An essential pre-requisite for the present thesis was the induction of anti-β_1-abs in rats. This was achieved by injection of fusion proteins containing the second extracellular loop of the human β_1-AR. As a result of monthly immunization, the animals develop functionally active anti-β_1- EC_{II}-abs.

For the generation of the fusion proteins, an overnight culture of the *E.coli* strain expressing the β_1-ECII/GST construct [154] was prepared in LB broth containing ampicillin. The next day, 800 ml LB broth + ampicillin was inoculated with 100 ml of the overnight culture and was left to grow at 30 ℃ shaking to an OD_{600nm} of 1.0 – 1.4. Expression of protein was induced by adding 1 mM IPTG. Induction was stopped by centrifugation (10 min, 5000 rpm) and the pellet was resuspended in 30 ml of lysis buffer. Cells were disrupted using a French Pressure Cell Press (SLM Aminco, Rochester, New York, USA). After addition of RNase, TritonX, and EDTA, the lysate was centrifuged (15 min, 700 rpm, 4 ℃), and the supernatant was filtered through a 45 µm filter and loaded onto glutathione-sepharose columns. After washing with PBS, bound proteins were eluted and dialysed overnight against PBS. Then, protein concentration was determined by the Bradford dye-binding method. Purity of the fusion protein in the eluates was checked by SDS-PAGE; the expected molecular weight was approximately 30 kDa (GST moiety (26 kDa) + β_1-EC_{II} moiety (3.5 kDa)).

2.2.2 Animal model

For the purpose of this study an established immune rat model was used. Six-week-old male Lewis/CrlBR rats (n=80) were obtained from Harlan Laboratories (Venray, Netherlands) and housed in temperature and humidity-controlled scantainers. Care of the animals was performed in accordance with the Committee on Animal Research of the regional government (Regierung von Unterfranken, Würzburg, Germany). The animals were permitted free access to standard rat chow and tap water. The rats were subcutaneously injected monthly over a period of 18 months with the afore-mentioned fusion protein (n=40) or 1x PBS (n=40, control animals).

Solution control animal:	1x PBS	250 µl
	Freud's adjuvant (incomplete)	250 µl
Solution β_1-animals:	Fusion protein	50 µg
	1x PBS	250 µl
	Freud's adjuvant (incomplete)	200 µl
	Freud's adjuvant (complete)	50 µl

The development of anti-β_1-EC_{II}-abs was monitored every month by ELISA (see section 2.2.5).

2.2.3 Collection of 24 hour urine samples

Analysis of urine composition is a standard procedure to monitor possible alterations in renal function. Parallel to venous blood-sampling, urine samples of each rat were collected for 24 h using metabolic cages (Figure 6). These allow for separate collection of urine and feces for further analysis. The urine flows through the floor down the sides of a funnel placed beneath and further into a collection tube placed on ice. Fecal pellets drop separately into a second vial. The feeding and watering compartments are incorporated outside the cage to minimize contamination. Each animal was put into a metabolic cage for exactly 24 h. After measuring of the volume, urine was transferred into falcon tubes and stored at -20 ºC until further analysis.

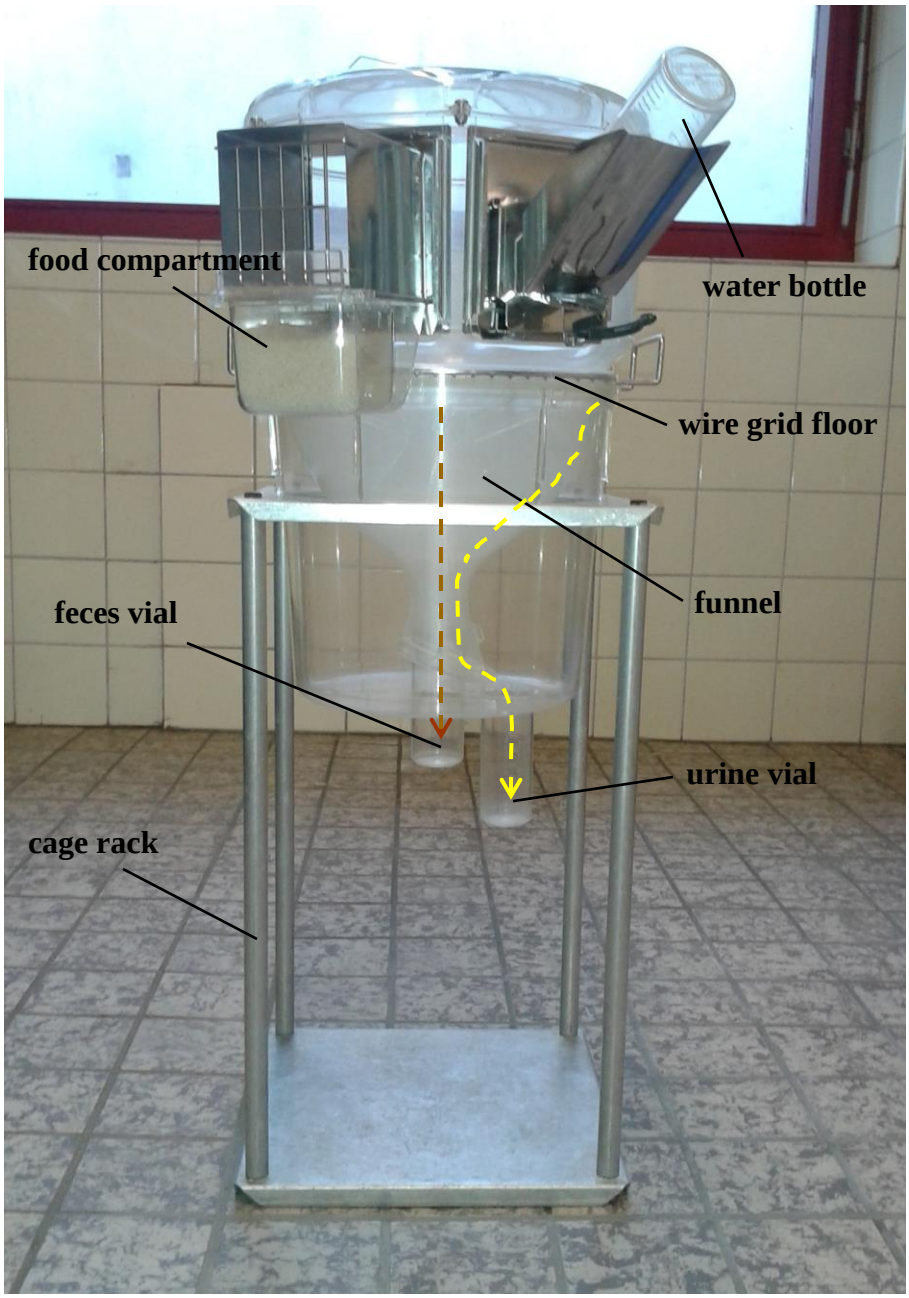

Figure 6: Metabolic cage for rats.

Example of a metabolic cage used in the present work. The rat is put into the transparent polycarbonate cage stacked on the top of a funnel. Urine flows along the sides of the funnel into a collecting vial (yellow arrow). Feces fall directly through the wire grid floor into a second vial (brown arrow).

2.2.4 Blood taking

In order to determine the effects of anti-β_1-EC_{II}-abs on renal function, blood samples were regularly taken throughout the experiment, as blood markers – especially electrolytes - can be strongly regulated by the kidneys. Blood samples were taken at time points 1, 2, 3, 6, 9, 12, 15, and 18 months after the start of immunization. For this purpose, the rats were put into a plastic tube to facilitate handling (Figure 7). Approximately 1 ml of blood was taken out of one of the three tail veins using a 1 ml hypodermic syringe (BD Plastipak, S. Agustín del Guadalix, Madrid, Spain) with a 26 GA 3/8" cannula. Half of the blood was transferred into a small serum tube (BD Microtainer SST Tube, S. Agustín del Guadalix, Madrid, Spain), the rest into a tube containing EDTA (BD Microtainer K2E Tube, S. Agustín del Guadalix, Madrid, Spain) and placed on ice. Red blood cells were separated from the serum by centrifugation (1350 x g, 2 min). Obtained serum was stored at -20 ºC until further use.

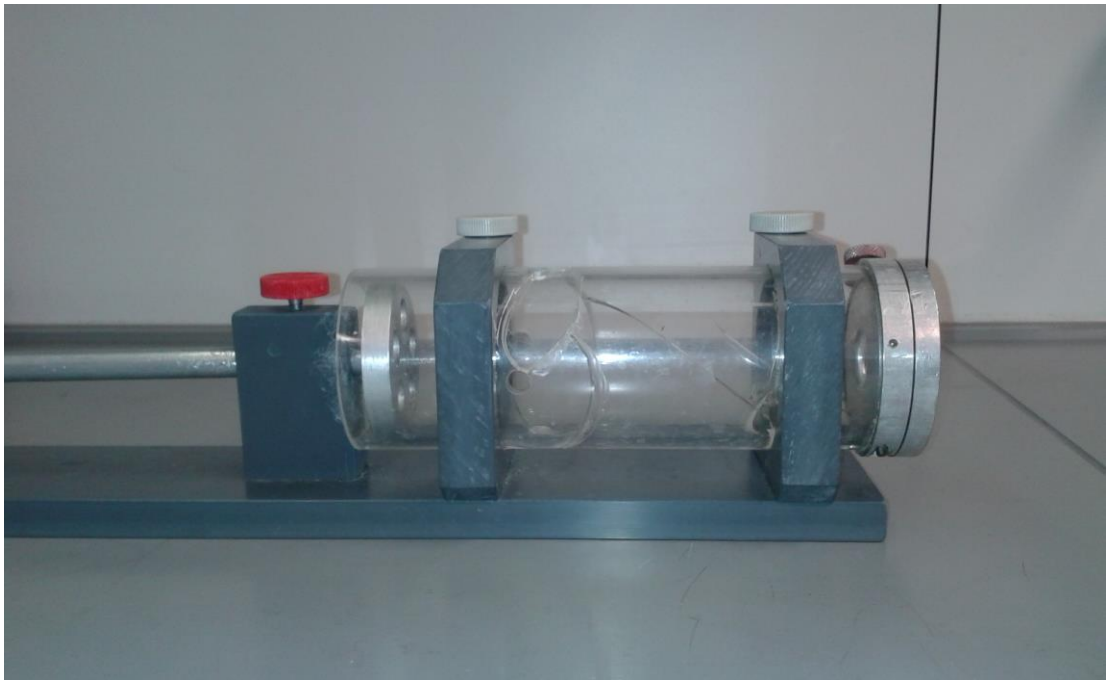

Figure 7: Acrylic glass tube for taking blood.

The rat is put into the tube with a central hole in the metal plate at the tail side to facilitate collection of blood samples. The length of the tube can be adjusted according to the size of the animal by adjusting the metal plate on the head side (left).

2.2.5 Enzyme-linked immunosorbent assay (ELISA)

The ELISA is an analytical tool in biomedical research for the detection and quantification of specific antigens or antibodies in a given sample. It uses the basic immunological concept of an antigen binding to its specific antibody, which allows the detection of very small quantities of antigens such as proteins, peptides, hormones, or antibodies in a liquid sample. Enzyme-labeled antigens and antibodies are utilized to detect the biological molecules. We performed ELISAs to determine the titer of anti-β_1-EC_{II}-abs induced in immunized rats. 3 µg/ml of a peptide corresponding to the β_1-EC_{II} domain served as antigen and were coated onto 96-well micro titer plates (NUNC, Roskilde, Denmark) at 50 µl/well in 0.1 M carbonate-bicarbonate coating buffer (pH 9.6). After overnight incubation at 4 °C, plates were washed three times with 1x PBS + 0.1% Tween20, pH 7.4, and then blocked with 3% milk in PBS-Tween20 for 2 h at 37 °C. After washing with PBS-Tween20, rat sera (diluted 1/1000 to 1/16000 in 3% milk) were added to the wells in duplicates and incubated for 2 h at 37 °C. Then, the plates were washed with PBS-Tween20 to remove unbound molecules and biotin-conjugated affinity-purified $F(ab)_2$ goat anti-rat IgG whole molecule (Dianova GmbH, Hamburg, Germany) was added and incubation at 37 °C continued for 90 min. Then; the plates were washed and horseradish peroxidase (HRP)-conjugated streptavidin (Dianova GmbH, Hamburg, Germany) was added. After another washing step, ortho-phenol-diamine (OPD) in 0.1 M diethanolamine buffer (pH 9.8) was added. OPD serves as substrate for HRP and yields a water-soluble yellow-orange reaction product. After 30 min, the enzymatic reaction was stopped using 3 M sulfuric acid, and OD was measured at 490 nm in an ELISA plate reader (Molecular Devices Corporation, Sunnyvale, USA). Controls included sera from non-immunized animals and rat IgG whole molecule as standard.

2.2.6 Analysis of blood and urine samples

Electrolyte content of the urine and serum samples was determined using the Cobas Integra 800 analyzer. The test for determining Ca^{2+} in serum/urine is based on the principle of complex formation between Ca^{2+} ions with the chelator NM-BAPTA. The sample is mixed with a reagent containing a NM-BAPTA indicator. The calcium ions in the sample form a complex with the NM-BAPTA indicator at a 1:1 stoichiometry. This leads to a color-change which can be measured photometrically. In a second step, the calcium-NM-BAPTA complex reacts with EDTA. EDTA snatches the calcium ion from the calcium-NM-BAPTA complex releasing NM-

BAPTA, which is measured photometrically at 340 nm. The change in absorbance is directly proportional to the calcium concentration present in the sample.

Sodium and potassium were determined with an ion-selective electrode (ISE) by measuring the difference in potential between the ISE and a reference electrode. The output potential is proportional to the amount or concentration of the selected ion present in the solution.

The ISE consists of an ion-specific half-cell and a reference half-cell. The ion-specific cell gives a potential against the reference cell depending on the specific ion concentration. When the specific ion concentration changes (in the sample or an ion standard), the respective potential changes as well. The relationship between the potential measured with the ISE and the ion concentration in the sample can be expressed using the Nernst equation:

$$E = E_0 - 2.303 \times \frac{RT}{nF} \times \log a \quad (Eq. 1)$$

E = Measured potential between the ion selective and the reference electrode

E_o = Measured potential between the ion selective and the reference electrode

R = Universal gas constant (R = 8.314 J mol^{-1} K^{-1})

T = Temperature in K (Kelvin)

F = Faraday constant (96485 C mol^{-1})

n = Electrical charge of the ion

a = Activity of the measured ion

R and F are constants, and the electrical charge of the ion to be measured is known as well. Therefore the equation can be simplified to:

$$E = E_0 - S \times \log a \quad (Eq. 2)$$

with S = $-2.303 \times \frac{RT}{nF}$ (slope of the ISE).

Using a series of calibrating solutions the response curve or calibration curve of an ion-selective electrode can be measured and plotted as the signal (electromotive force) *versus* the activity of the analyte.

pH values of the 24 h urine samples were determined with a blood gas analyzer, which functions as an ISE as well. It measures the concentration of free hydrogen ions and hence the pH.

Total protein in the urine samples was measured with the Cobas Integra 800 by turbidimetry, a method for determining the concentration of a substance in a solution by measuring the loss of intensity of transmitted light due to the scattering effect of the particles in the sample. In our case, bivalent copper ions react with peptide-bonds of proteins in the test solution to form a characteristic crimson Biuret-complex. The color intensity is directly proportional to the protein concentration in the sample and can be determined by measuring the gain of extinction at 552 nm.

Urinary albumin was determined by immunonephelometry. Albumin forms complexes in an immunochemical reaction with a specific antibody. These complexes scatter a beam of light passed through the sample. The intensity of the scattered light is proportional to the concentration of albumin in the test sample based on a standard curve of known concentrations.

In total, a volume of 100 µl serum and 4 ml of urine was needed per animal to perform all measurements. Values determined in the urine samples were based on the total urine volume collected within 24 h.

2.2.7 Plasma Renin Activity Radioimmuno-Assay (PRA RIA)

Renin is one of the most important parameters regarding kidney function, especially in connection with the adrenergic system. A very precise method for measuring renin activity in blood is a radioimmuno-assay. This assay is based on the fact that renin catalyzes the hydrolytic cleavage of angiotensinogen to angiotensin I (Ang I), dependent on the activity of renin in this sample. The amount of produced Ang I competes with a known amount of radio-labeled Ang I for a limited number of antibody-binding sites. After incubation, the amount of labeled Ang I bound to the antibodies coated on the tubes is inversely related to the concentration of unlabeled Ang I within the sample. Blood used for this assay was collected on ice in EDTA tubes, centrifuged (13500 x g, 2 min) and kept below 4 °C prior to the assay. We used the Plasma Renin Activity RIA of DiaSorin (Dietzenbach, Germany) according to the manufacturer's instructions. In short, 200 µl of serum was mixed with 5 µl PMSF and 25 µl generation-buffer. 115 µl of this mixture were incubated for 90 min at 37 °C, the rest was kept on ice. Afterwards, a 50 µl aliquot

of each sample was transferred into tubes coated with an anti-Ang I antibody, and 500 µl of [^{125}I]-Ang I was added. After 4 h of incubation, the supernatant was aspirated and [^{125}I]-Ang I bound to the coated antibodies was measured with a γ-counter. To determine renin activity, first, a calibration curve was obtained by plotting the calibrator values as a function of Ang I concentration in a semi-logarithmic fashion. From this reference curve, the amount of Ang I generated in the sample was derived. Renin activity was calculated according to the formula

$$PRA = \frac{\left(ng\ 37\ ^{\circ}C - ng\ 4\ ^{\circ}C\right) \times 1.12}{hours\ of\ incubation} = ng/ml/h \quad (Eq.3)$$

2.2.8 Echocardiography

Development of the cardiac phenotype of immunized and control rats was monitored by echocardiography in a blinded manner. Echocardiography was performed at months 0 (baseline), 1, 3, 6, 9, 12, 15, and 18 in all rats under light anesthesia (10 mg of ketamine and 0.2 mg of xylazine per kg BW). After shaving of the chest, the animals were placed on a specially designed table. Echocardiograms were obtained by a commercially available system (Visual Sonics, Vevo LAZR) equipped with a 17.5-MHz phased array transducer (Visual Sonics, RMV 716-013). M-mode tracings were recorded in the parasternal long and short-axis views through the aortic valve at the base of the aortic leaflets and through the anterior and posterior left ventricular wall at the level of the papillary muscles. Wall thickness and LV internal dimensions were measured directly on the screen (online) according to the guidelines of the American Society of Echocardiography [155]. Pulsed-wave Doppler spectra of mitral inflow and LV outflow were recorded from the apical four and five chamber view, respectively.

2.2.9 Hemodynamic measurements

Subsequent to blood and urine collection n=10 animals (5 per group) were anesthesized intraperitoneally with 10 mg of ketamine and 0.2 mg of xylazine per kg BW and placed dorsally recumbent on a heating plate. A 1.8 F high-fidelity catheter (Millar Instruments Inc., Houston, Texas, USA) was inserted into the right carotid artery. The catheter was slowly advanced into the left ventricle until the pressure-volume curve was seen on the monitor. LV pressure tracings were

recorded digitally over 30 min and analyzed off-line (PowerLab, AD Instruments, Castle Hill, Australia).

2.2.10 Measurement of renal filtration function

Following cardiac catheterization, renal function of the animals was assessed by catheterization of the bladder. To estimate GFR and RBF, inulin and para-aminohippurate (PAH) clearances were determined, respectively. FITC-labeled inulin and PAH (2 mg/ml of each substance dissolved in 0.9% NaCl) were applied through the carotic artery (infusion with 0.12 ml/min for 30 min). Thereafter, the bladder was cannulated with a PE-50 catheter. Having obtained a steady state after 30 min of infusion, urine was collected for 20 min, followed by blood sampling. The samples were centrifuged and stored at –20 °C. Then, both kidneys were harvested and dissected according to the planned molecular and histological analyses.

GFR is defined as the fluid volume filtered by the glomeruli within a certain time period. It can be determined by the inulin clearance, as this substance is neither reabsorbed nor secreted or metabolized, and has no effect on filtration function. GFR is calculated according to the equation

$$GFR = \frac{V \times U(Inulin)}{S(Inulin) \times t}[ml/min] \quad (Eq. 4)$$

V = urine volume [ml]
U(Inulin) = inulin concentration in urine [µg/ml]
S(Inulin) = inulin concentration in serum [µg/ml]
t = time [min]

Urine and serum samples were diluted 1:500 with measuring-buffer (see section 8.1.2) and the inulin concentration was determined by fluorescence spectrometry (excitation 480 nm, emission 520 nm). The emission-signal is directly proportional to the inulin concentration derived from a standard curve.

PAH is filtered freely and excreted completely by the kidney. Its clearance equates to the RPF, which is calculated as follows:

$$RPF = \frac{V \times U(PAH)}{S(PAH) \times t} \; [ml/min] \quad (Eq. 5)$$

V = urine volume [ml]
U(PAH) = PAH concentration in urine [µg/ml]
S(PAH) = PAH concentration in serum [µg/ml]
t = time [min]

PAH concentration was determined photometrically *via* a modified version of the Anthrone method [156]. First, urine and serum samples were deproteinized with 0.33 M perchloric acid, followed by stepwise addition of sodium nitrate (1 mg/ml), ammonium amidosulfonate (5 mg/ml), and 32% HCl-solution. Second, n-(1-naphthyl)ethylenediamine dihydrochloride was added to the solution, allowing PAH to react with this substance to form a violet complex. The reaction was stopped after 10 min by adding 100% EtOH. Extinction of the samples was measured photometrically at 550 nm.

The transport of anions from the blood to the proximal tubular cells is the rate-determining step of the secretion of organic anions. As mentioned above, PAH is partly transported *via* this way into the urine. To determine accurately which fraction of PAH is secreted exclusively by the proximal tubule, we calculated the PAH net secretion (PNS):

$$PNS = (U(PAH) \times UO) - (S(PAH) \times GFR) \; [\mu g/min] \quad (Eq. 6)$$

UO = urinary output [ml/min]
U(PAH) = PAH concentration in urine [µg/ml]
S(PAH) = PAH concentration in serum [µg/ml]
GFR = glomerular filtration rate [ml/min]

2.2.11 Histology

To analyze the effects of stimulating anti-β_1-EC_{II}-abs on kidney morphology and structure, tissues from immunized ab-positive *versus* 0.9% NaCal-injected control rats were analyzed histologically.

The harvested kidneys were fixed immediately in 4% (vol/vol) paraformaldehyde (PFA) in dH_2O for 24 h and further processed for paraffin embedding. For histology, tissues were cut into cross-sections of 2 µm thickness and dried over night at 45 ℃.

2.2.11.1 Histochemical staining

Prior to staining, paraffin sections were deparaffinized and rehydrated according to the following protocol:

Deparaffinization:	1)	Xylene	4 min
	2)	Xylene	4 min
	3)	Xylene	4 min
Rehydration:	4)	Ethanol 100%	2 min
	5)	Ethanol 100%	2 min
	6)	Ethanol 100%	2 min
	7)	Ethanol 70%	2 min
	8)	dH_2O	4 x 30 s

For assessment of fibrosis, the samples were incubated in 0.1% Sirius Red in a saturated solution of picric acid for 45 min at RT, followed by a dehydration and clearing step:

1)	Ethanol 70%	1 min
2)	Ethanol 100%	2 min
3)	Ethanol 100%	2 min
4)	Ethanol 100%	2 min
5)	Ethanol 100%	2 min
6)	Xylene	3 min
7)	Xylene	1 h

To improve handling and visibility under the microscope and for preservation purposes, the specimens were embedded with Eukitt mounting medium (Fluka, Seelze, Germany), covered with a glass cover slip and dried overnight at RT.

For morpho-histological assessment of the glomeruli, we used hematoxylin- and eosin (HE)-stained sections. The deparaffinized and rehydrated cross-sections were first stained with hematoxylin for 10 min; after rinsing the sections in running tap water for another 10 min, they were counterstained with eosin for 50 s and rinsed with distilled water. After dehydration and clearing, the specimen were mounted with Eukitt and dried overnight.

Glomerulosclerosis is another key feature in renal pathologies and occurs especially in hypertension. Glomerulosclerosis was assessed in PAS-stained renal cross-sections. After pretreatment of the paraffin sections as described above, the specimens were stained according to the following protocol:

1) Periodic acid (1%)	10 min
2) Tap water	10 min
3) dH_2O	2 x 2 min
4) Schiff's Reagent	15 min
5) Warm tap water	5 min
6) dH_2O	1 min
7) Hematoxylin	10 min
8) Running tap water	10 min

These steps were followed by dehydration, clearing and mounting, as described above.

In addition, kidney sections were stained with Masson-Goldner-Trichrome (MGT) following standard procedures. MGT is composed of three different dyes (1/2/3 = Azophloxine/Orange G/Light Green SF) which allow easy differentiation of various tissue components (1/2/3 = cytoplasm and muscle fibers/erythrocytes/connective tissue). In general, the nuclei are counterstained with Weigert's iron hematoxylin. In our study, we used MGT-staining to assess tubulointerstitial fibrosis. Staining was performed according to the following protocol

1)	Hematoxylin	10 min
2)	Running tap water	10 min
3)	Acetic acid (1%)	30 s
4)	Azophloxine solution	10 min
5)	Acetic acid (1%)	30 s
6)	Orange G solution	1 min
7)	Acetic acid (1%)	30 s
8)	Light Green SF solution	2 min
9)	Acetic acid (1%)	30 s

Dehydration, clearing and mounting was performed as described above.

2.2.11.2 Morphometric Analysis

The amount of total fibrosis was determined on Sirius red-stained kidney sections (200 x magnification). A complete cross section - divided into four areas - of five animals per group and time-point were analyzed in a blinded manner by semi-automated image-analysis using Photoshop CS4 (Adobe, San José, California, USA). Fibrosis was assessed by automated count of the dark-red pixels representing the deposition of collagen; the color threshold was pre-set according to the intensity of the staining. Total fibrosis was expressed as percentage of the whole cross sectional area.

Similarly, perivascular fibrosis was determined in 10 areas per cross section depicting blood vessels (200 x magnification). The amount of fibrosis is given as percentage of the area of the respective blood vessel.

HE-stained sections of glomeruli cut at the macula densa (showing both *vas afferens* and *vas efferens*) served to analyze the glomerular area. Glomerular images (400 x magnification) were digitized, the Bowman capsule and the glomerular tuft were traced and their respective areas were determined using the imaging software Image J (NIH, Bethesda, Maryland, USA) [157]. From each kidney, 25 glomeruli were analyzed. Furthermore, the glomeruli were assessed for glomerulosclerosis. The extent of glomerulosclerosis was graded according to the PAS-positive depositions and/or glomerular lesions within the glomeruli [158], given in percent:

Grade 0: no sclerosis

Grade 1: < 25% of the glomerulum positive for PAS deposits/glomerular lesions

Grade 2: 25 - 50% of the glomerulum positive for PAS deposits/glomerular lesions

Grade 3: 50 - 75% of the glomerulum positive for PAS deposits/glomerular lesions

Grade 4: 75 – 100% of glomerulum positive for PAS deposits/glomerular lesions

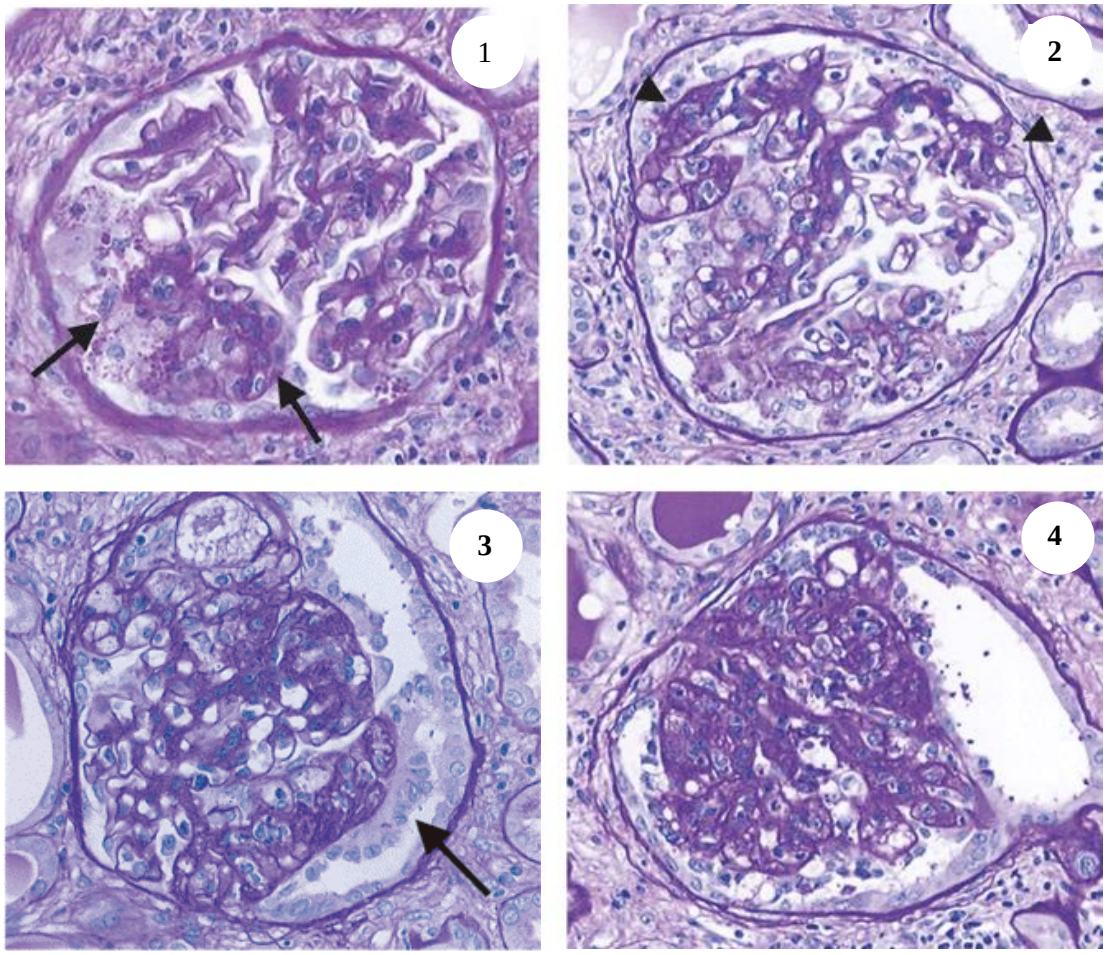

Figure 8: Grades of glomerulosclerosis, adaped from Dijkman *et al.*[159].

Exemplary images of different grades of (focal segmental) glomerulosclerosis, depending on the presence of PAS-positive deposits and glomerular lesions.

The glomerulosclerotic index was calculated by multiplying the grade of sclerosis with the number of affected glomeruli and dividing it by the total number of the analyzed glomeruli.

To assess interstitial injury, MGT-stained 2µm kidney-sections were analyzed (400 x magnification). Interstitial damage was defined as tubular atrophy or dilatation, deposition of extracellular matrix (ECM), or interstitial fibrosis. For each kidney, 20 randomly selected fields of vision were graded on a scale of 0 to 3 according to the Banff Quantitative Criteria for Interstitial Fibrosis [160] [161]:

Grade 0: interstitial fibrosis in < 5% of the cortical area

Grade 1: interstitial fibrosis in 6 - 25% of the cortical area

Grade 2: interstitial fibrosis in 26 – 50% of the cortical area

Grade 3: interstitial fibrosis in > 50% of the cortical area

2.2.11.3 Spectrophotometric assessment of total fibrosis

Total fibrosis was furthermore established spectrophotometrically using a modified method after Lopez-De Leon *et al* [162]. Deparaffinized and rehydrated cross-sections were air-dried for 10 min and stained with 0.1% Fast Green FCF und 0.1% Sirius red in saturated picric acid for 45 min at RT. Excess stain was washed off with distilled water. Cross-sections were dried for 10 min at RT and incubated for 3 min in a 1:1 solution of 0.1N NaOH and 100% methanol for destaining. 200 µl of this solution was transferred into a 96-well plate. Extinction was measured at wavelengths 540 nm and 605 nm. The amount of fibrosis was determined using the following equations:

$$E(Collagen) = E(540\,nm) - 0.291 \times E(605\,nm) \quad (Eq.7)$$

$$E(unspecific\ protein) = E(605\,nm) \quad (Eq.8)$$

$$A(Collagen) = \frac{E(unspecific\ protein)}{38.4} \times 1000 \quad (Eq.9)$$

$$A(unspecific\ protein) = \frac{E(unspecific\ protein)}{2.08} \times 1000 \quad (Eq.10)$$

$$C(Collagen) = \frac{A(Collagen)}{A(Collagen) + A(unspecific\ protein)} \quad (Eq.11)$$

E(Collagen) = extinction of collagen

E(unspecific protein) = extinction of unspecific proteins

E(540 nm) = extinction at 540 nm

E(605 nm) = extinction at 605 nm

A(Collagen) = amount of collagen [µg/cross-section]

A(unspecific protein) = amount of unspecific proteins [µg/cross-section]

C(Collagen) = collagen concentration [µg/mg]

2.2.12 Reverse transcription

Screening of organ-specific gene expression is a fast way of getting a first insight into organ-specific pathways and mechanisms that may be altered under certain (pathophysiological) conditions. Total RNA from frozen kidney tissues was prepared using the RNeasy Mini Kit of Qiagen. About 25 mg of tissue was lysed in 600 µl RLT buffer plus β-mercaptoethanol. Cell-debris were pelleted by centrifugation (10000 x g, 3 min) and the supernatants were mixed with a same volume of 70% ethanol, and run over the RNeasy silica membranes to bind RNA. After washing with 350 µl of washing buffer, any remaining DNA was removed by DNase treatment on RNeasy spin columns. After washing, total RNA was eluted with 50 µl of RNase-free water. Obtained RNA was quantified spectrometrically (Nanodrop, peqlab, Erlangen, Germany). Complementary DNA (cDNA) was transcribed from RNA templates using the High Capacity RNA to cDNA Kit (Applied Biosystems, Foster City, CA, USA) and random hexamer primers.

Reaction Master Mix:	10 µl Reverse Transcription Buffer
	4 µl 25 x dNTPs
	10 µl 10 x random primers
	5 µl MultiScribe^{TM} Reverse Transcriptase (50 U/µl)
	21 µl nuclease-free H_2O
Reaction Mixture:	6 µl RNase-free H_2O
	4 µl Reaction Master Mix
	10 µl RNA (0.1 µg/µl)

Mixtures were vortexed, briefly centrifuged and reverse transcription was performed according to the following profile:

Thermal cycler conditions:	25 ℃	5 min
	42 ℃	30 min
	85 ℃	5 min
	4 ℃	∞

Thereafter, plate was cooled down on ice and centrifuged again. CDNA was diluted to 5 ng/µl and stored at -20 ℃.

2.2.13 Quantitative real-time polymerase chain reaction

Quantitative real-time PCR (qPCR) is a variant of the classic PCR approach. For our study, the intercalator-based method of qPCR, also known as SYBR green method [163], was applied. As DNA dye, the Brillant III Ultra-Fast SYBR Green QPCR Master Mix (Agilent Technologies) was utilized. QPCR was performed in 384-well plates using primers designed for conserved regions of the genes (see section 8.1.3).

QPCR reagent mixture	0.2 µl forward primer (20 pmol/µl)
	0.2 µl reverse primer (20 pmol/µl)
	3.6 µl nuclease-free PCR grade H_2O
	6.0 µl MasterMix

Components were mixed and 10 ng cDNA was added. After brief centrifugation and an initializing phase of 3 min at 95 ℃, the plate was incubated for 40 cycles using the following conditions:

Cycling profile:	95 ℃	5 s
	60 ℃	10 s

The reactions were performed in triplicate and the relative expression levels were calculated according to the standard curve method [164]. Obtained data were normalized to the expression of the endogenous housekeeping genes GAPDH, Hprt1, or Pgk1. The logarithm of the RNA concentration of individual markers was derived from standard curves. Expression is given as the ratio of RNA target/RNA endogenous control.

2.2.14 Isolated perfused kidney

Experiments on isolated perfused kidneys were performed to detect direct anti-β_1-EC_{II}-ab effects on kidney function outside an entire organism prone to hide or counter-regulate smaller effects. In this *ex vivo* model, the kidney is isolated from the systemic vasculature, removed from the animal, and perfused through the renal artery with a blood/plasma-similar medium. By collection of the venous effluates after passage through the kidney, possible effects of drugs or other substances added to the perfusion medium on, e.g. renin-secretion can be assessed.

For our experiments, male BL6 mice with an average weight of 30 g were used as donors. Animals were anesthetized by intraperitoneal injection of 5-ethyl-5-(1-methylbutyl)-2-thiobarbituric acid (100 mg/kg) and ketamine HCl (80 mg/k) and placed dorsally on a heating plate at 37℃. The abdominal cavity was opened by a midline incision and the aorta was exposed and clamped distal to the right renal artery; this strategy guaranteed that the perfusion of the right kidney was not disturbed during the subsequent insertion of the perfusion cannula into the abdominal aorta distal to the clamp. The mesenteric artery was ligated, and a metal perfusion cannula (0.8 mm OD) was inserted into the abdominal aorta. After removal of the aortic clamp, the cannula was advanced to the origin of the right renal artery and fixed in this position. The aorta was ligated proximal to the right renal artery, and perfusion was started *in situ* with an initial flow rate of 1 ml/min. With this technique, significant ischemia of the right kidney can be avoided. The basic perfusion medium consisted of a modified Krebs-Henseleit solution, supplemented with all physiological amino acids at 0.2–2.0 mM, 6 g/100 ml bovine serum albumin, 1 mU/100 ml vasopressin 8-lysine, and freshly washed human red blood cells with a hematocrit of 10%. Ampicillin (3 mg/100 ml) and flucloxacillin (3 mg/100 ml) were added to inhibit any bacterial growth in the medium. The perfusate was continuously dialyzed against a 10-fold volume of the same components without erythrocytes and albumin to improve the

functional preservation of the buffer. Oxygenation of the perfusion medium was ensured by purging the dialysate with 94% O_2 and 6% CO_2.

Finally, the right kidney was excised, placed in a thermostated moistening chamber, and perfused with a constant pressure of 100 mmHg. The perfusion pressure was monitored within the perfusion cannula (Isotec pressure transducer, Hugo Sachs Elektronik), and the pressure signal was used for feedback control (model SCP 704, Hugo Sachs Elektronik) of a peristaltic pump. Finally, the renal vein was cannulated with a 1.5-mm-OD polypropylene catheter and the venous effluent was collected in order to assess renin activity and venous blood flow. Perfusate flow was calculated by collection and gravimetric determination of the venous effluent. After constant perfusion pressure was established and the flow rates of the perfusate remained stable, the antibody solutions to be tested were added to the dialysate.

We tested both normal serum and fractionated serum for its effect on renin secretion. For either approach, blood obtained while harvesting the organs of the immunized animals (see section 2.2.10) was used. After collection into serum tubes, blood was centrifuged at 2000 x g for 10 min to remove erythrocytes. The supernatants of five anti-β_1-EC_{II}-ab-positive and corresponding control animals were pooled to obtain the required amount of serum. For the fractionated serum, the serum samples were centrifuged at 4000 x g for 30 min using a centrifugal filter unit with a cut-off of 100 kDa. The purpose was to obtain a fraction of serum containing antibodies without any other substances having a potential effect on renin secretion, as e.g. catecholamines. Other macro-molecules (>100 kDa) remaining in this fraction - as α_2-macroglobulin or coeruloplasmin - do not affect renin secretion. Both, the whole serum pool and the >100 kDa-fraction were tested for their antibody-content by ELISA (see section 2.2.5) and diluted with 0.9% NaCl to an equal concentration of 500 µg/ml prior to the perfusion experiments. After adding perfusion buffer, the final concentration of the antibodies was 1/33.

To determine renin activity, the collected venous effluent samples were centrifuged at 1500 x g for 10 min and the supernatant ("plasma") was used for further analysis. Samples were incubated for 1.5 h at 37 °C with plasma from bilaterally nephrectomized male rats as a renin substrate. Generated Ang I was determined by radioimmunoassay (for more details see section 2.2.7). Renin secretion rates are given as the product of renin activity and venous flow rate.

2.2.15 Statistics

Data are expressed as mean ± SEM. Statistical significance was assessed by a two-tailed student's t-test using GraphPad Prism software (GraphPad Software, Inc., La Jolla, CA, USA). When applicable, two-way ANOVA and post hoc tests were performed. A p-value of < 0.05 was considered significant, $p < 0.01$ as highly significant.

3 Results

3.1 Cardiac phenotype

The present work is based on the fact that stimulating antibodies targeting the β_1-EC_{II} (anti-β_1-EC_{II}-abs) induce cardiac dilatation and failure in rats. As a member of the GPCRs, the β_1-AR exerts its effects *via* coupling to stimulatory G_s proteins, which are localized on the inner side of the plasma membrane. Binding of agonists, such as noradrenalin or adrenalin, to cardiac β_1-ARs results in a sequential activation of G_s proteins, adenylate cyclase (which generates cAMP) and the cAMP-dependent protein kinase A (PKA) [30]. PKA subsequently phosphorylates key regulators of the excitation/contraction machinery of the heart, like phospholamban, the ryanodine receptor, L-type Ca^{2+} channels, and troponin T; in short, the mechanisms necessary to increase cardiac inotropy and chronotropy [165]. As anti-β_1-EC_{II}-abs have been shown to act as agonists, they should be able to induce similar effects at kidney level [133].

After induction, anti-β_1-EC_{II}-abs apparently behave like mild β_1-agonists; they induce a transient significant elevation of systolic blood pressure and an increase in contractility (+dp/dt). After this initial "hypertensive phase", left ventricular systolic blood pressure constantly decreased from the sixth month of immunization on in immunized, antibody-positive animals, whereas blood pressure in control rats remained unaltered (Figure 9B). LV-contractility showed an analogous pattern (Figure 9A). Thus, it appeared that anti-β_1-EC_{II}-ab-positive animals showed a clear cardiac functional deficiency, documented both by echocardiography and by cardiac catheterization. Interestingly, the heart rate was seemingly not affected in our rat model (Figure 9C), due to the fact that in the rat, cardiac β_1-ARs have a higher impact on contractility and relaxation than on beating rate [166, 167].

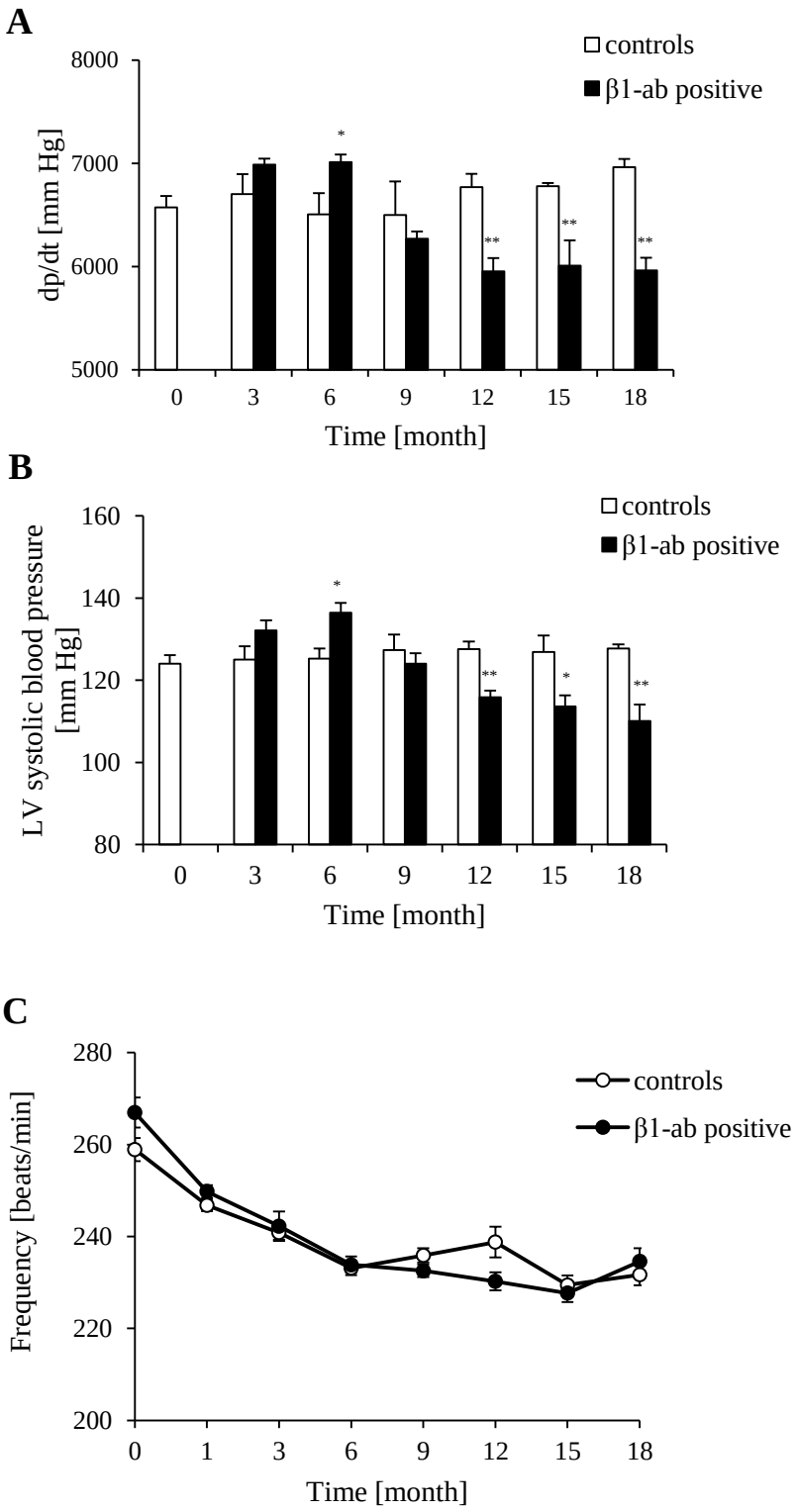

Figure 9: Hemodynamic parameters of immunized anti-β_1-EC_{II}-ab-positive *versus* control rats.

(A) Contractility (+dp/dt) and (B) left ventricular systolic blood pressure of anti-β_1-EC_{II}-ab-positive rats (black, n=5) and corresponding control animals (white, n=5), obtained by LV catheterization at 0, 3, 6, 9, 12, 15, and 18 months after immunization. (C) Heart rate was determined by echocardiography every three months. Error bars indicate mean values ± SEM. *$p < 0.05$, **$p < 0.01$.

3.2 Generation of anti-β_1-EC_{II}-antibodies

With regard to the initial hypertensive phenotype, we analyzed whether renal effects of stimulating anti-β_1-EC_{II}-abs might contribute to the observed increase in blood pressure. Therefore, we induced antibodies targeting the second extracellular loop of the β_1-AR in a Lewis-rat model by the injection of fusion proteins. Generation of the antibodies was monitored by testing blood samples of the immunized animals by ELISA.

Antibodies against β_1-ARs emerge about one month after the start of immunization (Figure 10). The peak-titer is reached after about four months of immunization. Thereafter, the titer decreases slightly until reaching a steady level of about 800 µg/ml; due to monthly antigen-boosts, this amount of circulating antibodies remained constant throughout the second half of the experiment.

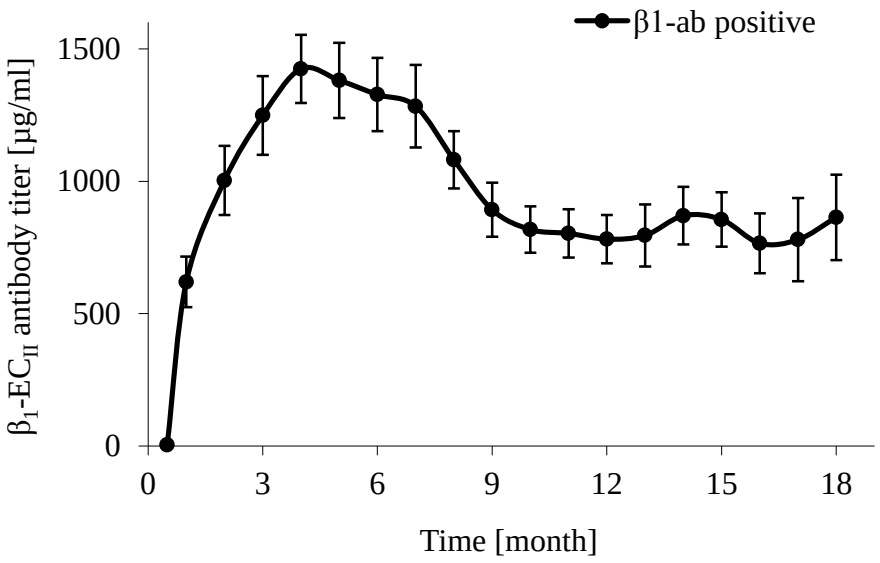

Figure 10: Titer-course of anti-β_1-EC_{II}-abs in immunized animals during the experiment.
Antibody titers were determined monthly by ELISA. The curve shows mean titers ± SEM.

3.3 Development of DCM

Regarding cardiac function, left ventricular dilatation and functional impairment in anti-β_1-EC_{II}-ab-positive animals started after about six months of immunization and progressed continuously during the course of the experiment (Figure 11).

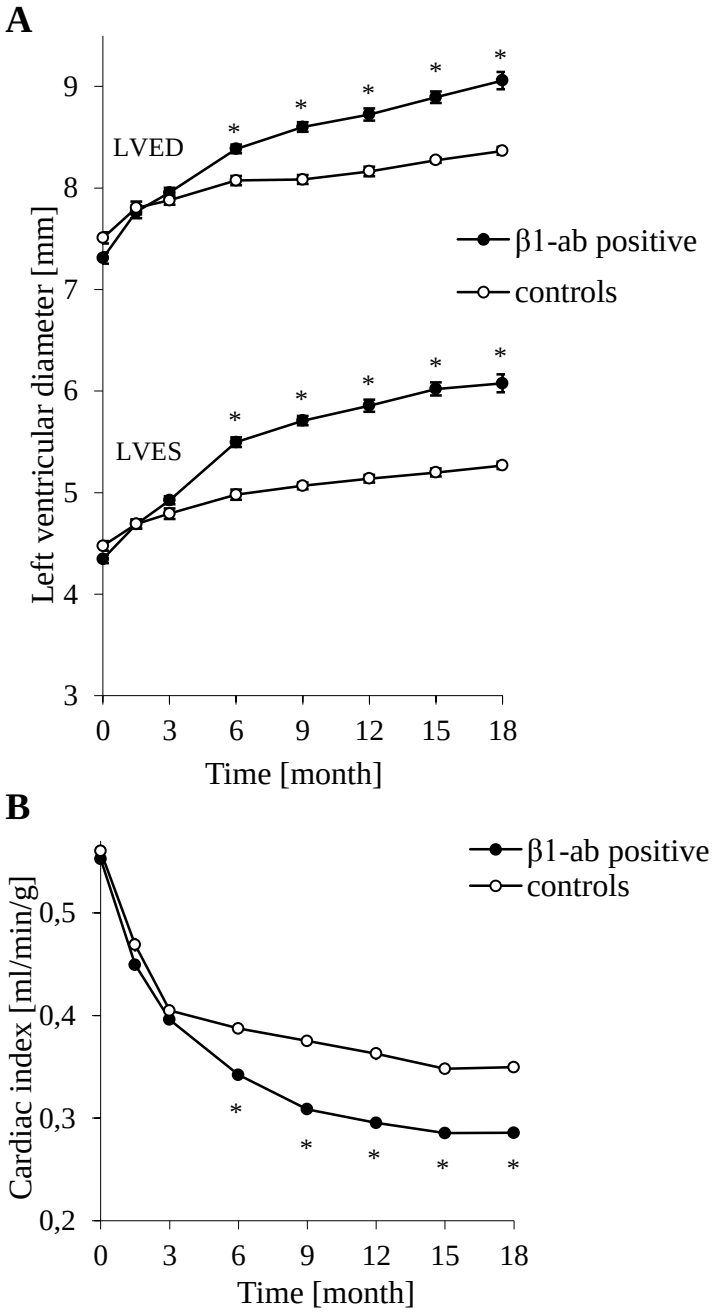

Figure 11: Echocardiographic results of immunized anti-β_1-EC_{II}-ab-positive *versus* control rats.

Time course of echocardiographically determined LVES and LVED (A) and cardiac index (B) of anti-β_1-EC_{II}-ab-positive rats (black, n=20) and corresponding control animals (white, n=20). Data were obtained at time-points 0, 1, 3, 6, 9, 12, 15, and 18 months after immunization. Error bars indicate mean values ± SEM. *$p < 0.001$.

3.4 Drinking behavior

Thirst is a subjective perception that provides the motivation to drink, which may arise from deficiency in either intra- or extracellular fluid volume. Depletion of water in intra- or extracellular compartments triggers the activation of various compensatory reactions. These include the secretion of vasopressin, stimulation of the RAAS, sympathetic activation, etc., and aim to minimize changes in body fluid volume; however, they do not restore the body fluid volume to its original state. The sensation of thirst (and the associated motivation to drink) is, therefore, an important component of a coordinated sequence of physiological responses which maintain the volume and composition of body fluids.

Activation of the SNS and the subsequent release of renin into the circulation may induce the generation of Ang II. One of the effects of this octapeptide is the stimulation of the hypothalamic thirst centers [168]. Regarding our model, the activation of the SNS by circulating anti-β_1-EC_{II}-abs could have led to an increase in need for drinking water, which could – at least in part – contribute to the observed rise in blood pressure. As shown in Figure 12, this was not the case in our model. Over 18 months, the amount of water drunk by the rats was comparable in both groups.

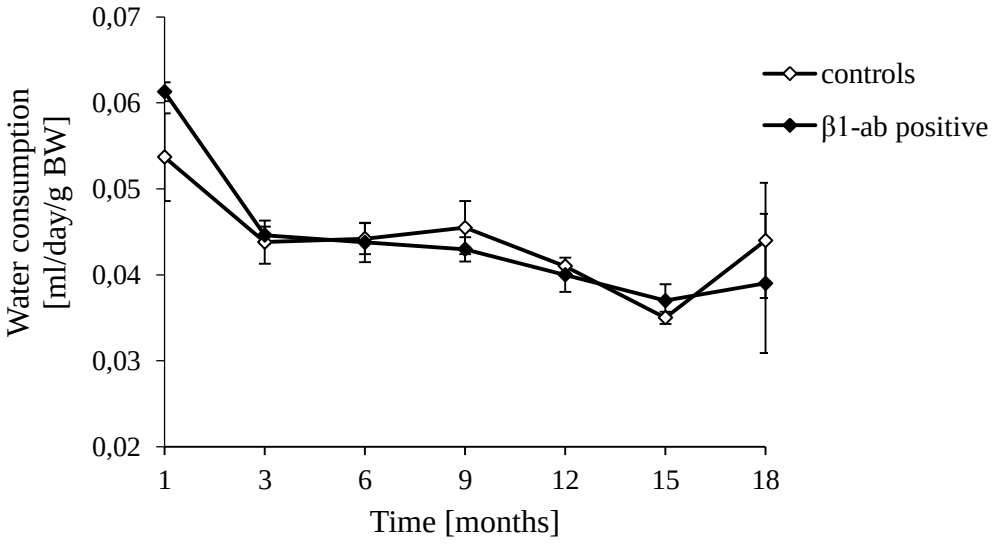

Figure 12: Water consumption of the anti-β_1-EC_{II}-ab-positive and corresponding control animals.

Amount of water consumed by the immunized anti-β_1-EC_{II}-ab-positive and control rats, measured every three months throughout the whole experiment. Data are given as milliliter of water consumed in 24 h per gram of bodyweight. Error bars represent mean ± SEM.

3.5 Urine volume

The kidneys are the most important organ for maintaining water homeostasis. Most of the water is reabsorped in the proximal convoluted tubule and the loop of Henle; only the fine adjustment takes place in the distal tubules. The amount of urine excreted depends on a string of parameters. Of particular importance is a hormone named vasopressin, also called antidiuretic hormone (ADH). This neurohypophyseal hormone is crucial for the regulation of water conservation in the body [169]. This is mainly due to the capacity of this hormone to increase the permeability for water in the distal portion of the nephron, thus enabling the reabsorption of up to 10% of the water filtered by the glomeruli. The main function of ADH includes increasing water permeability of distal tubule and collecting duct cells in the kidney, thereby increasing water reabsorption and excretion of more concentrated urine. This is achieved through water channels like Aquaporin-2 inserted into the apical membrane of cells from the distal tubule and collecting duct. Aquaporins increase the amount of water reabsorbed from the filtrate back into the circulation. Vasopressin also increases transcription of the aquaporin-2 gene, resulting in an increase in the total number of aquaporin-2 molecules in the collecting duct; this process is mediated by coupling of Vasopressin to the Vasopressin-2 (V2) receptor and the subsequent generation of cAMP [170]. As described in section 1.2, cAMP activates PKA by binding to its regulatory subunits, thus enabling it to add phosphate groups to proteins (including the aquaporin-2 protein) and thereby altering their function. This cAMP-mediated vasopressin-effect gave rise to our hypothesis, that stimulating anti-β_1-EC_{II}-abs might have an influence on urine excretion.

Figure 13 depicts the urine volumes of the animals, collected as described above (section 2.2.3). Throughout the experiment, there were no significant differences in urine volume between immunized anti-β_1-EC_{II}-ab-positive and corresponding control animals.

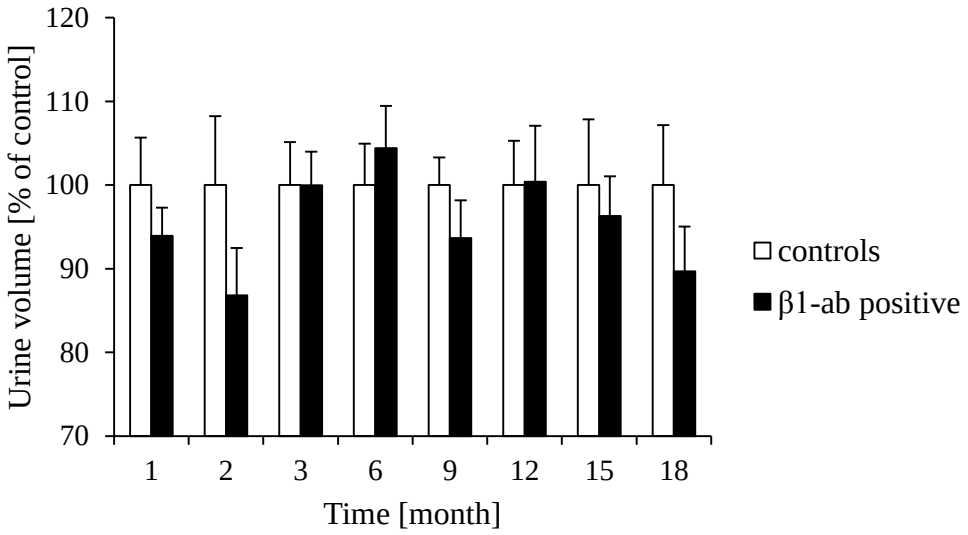

Figure 13: Urine volume, excreted within 24 h.

Urine volume excreted by anti-β_1-EC_{II}-ab-positive (black) and control rats (white). Columns depict the urine volume excreted, calculated as percent of controls, set at 100%. Error bars represent ± SEM.

3.6 Functional changes

As already mentioned in section 1.3, β_1-ARs are involved in a number of physiological processes in the kidney. These may range from the adjustment of urinary pH values to the regulation of electrolyte reabsorption, and the activation of the RAAS to readjust GFR and RBF. In the following sections, different parameters are presented and the potential effect of stimulating anti-β_1-EC_{II}-abs on these parameters is analyzed.

3.6.1 Urinary pH values

A high amount of β_1-ARs have been found in the collecting duct [35]. The collecting duct comprises the distal parts of the CCD, the OMCD, and the IMCD. The role of the β_1-ARs located in this area is still under investigation. However, as the main task of this portion of the nephron is the final adjustment of the urine composition, in particular the acid-base equilibrium, the current main hypothesis is that β_1-ARs may influence the urine pH to some extent.

Extracellular pH and systemic acid-base status are crucial for normal organ and cellular function. An altered acid–base status is e.g. associated with higher morbidity and mortality in patients with chronic kidney disease [171], and the extracellular pH affects bone density and stability, as mild

chronic metabolic acidosis has been suspected to contribute to osteopenia and osteoporosis [173]. Thus, it is essential to keep extracellular pH tightly in the physiologic range of pH 7.36 – 7.44 to secure normal organ and body function. Even though the acid-base status is influenced by the activity of different organs like intestine, bone, and skeletal muscle, the kidneys play an important role in controlling and maintaining the systemic acid-base status. This is achieved by three linked mechanisms: the reabsorption of filtered bicarbonate, the excretion of acids, and the *de novo* generation of ammonium and bicarbonate.

As mentioned above, the fine-tuning of renal acid or base excretion is achieved in the various segments of the collecting duct involving various cell types and distinct transport proteins. It is generally accepted that the so called type A intercalated cells secrete acid, whereas the non-type-A (betimes referred to as type B) intercalated cells excrete bicarbonate [174, 175]. Several studies have shown that β_1-adrenergic stimulation enhances the secretion of H^+ and, therefore, serves as regulator of the acid-base transport in the collecting duct [176-178].

Figure 14 shows the urinary pH values of immunized anti-β_1-EC_{II}-ab-positive and corresponding control animals: the urine pH did not differ significantly throughout the experiment.

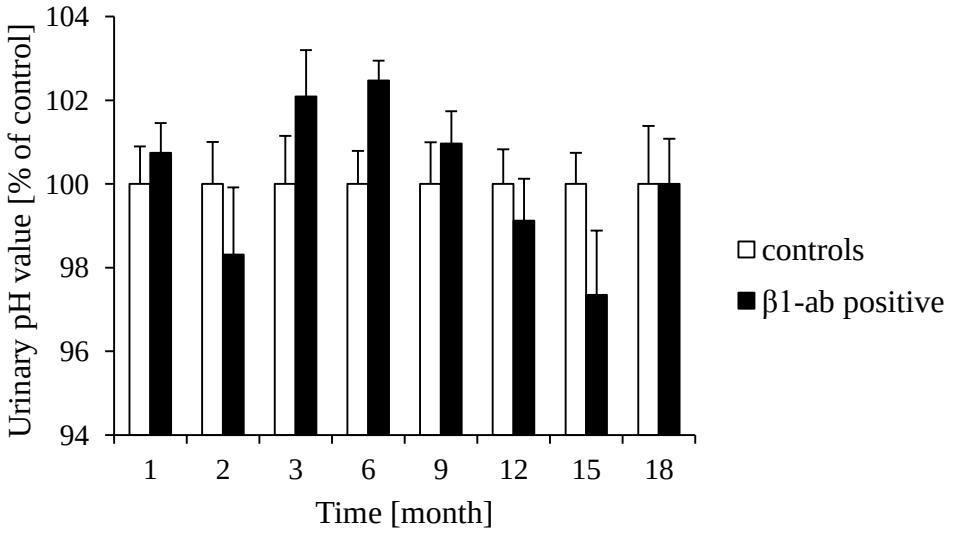

Figure 14: pH values of 24 h urine.

Urinary pH values measured in 24 h urine in n=20 animals per group and time point. Columns represent the means ± SEM (error bars), given in percent of the urine pH of the controls, set at 100%.

3.6.2 Electrolytes

The equilibrium of electrolytes is crucial for almost all aspects of organ function. The rate of reabsorption and excretion of electrolytes is solely regulated by the kidneys; the mechanisms involved are rather complex. Reabsorption and secretion occurs in all compartments along the nephron, and can be affected by a string of hormones, drugs, and other effectors, depending on the current conditions of the body. $Beta_1$-ARs are also involved in the regulation of electrolyte reabsorption/secretion, albeit indirectly.

3.6.2.1 Sodium

Sodium is the predominant ion of the extracellular fluid. It is a so-called non-penetrating solute, and due to its ability to produce osmotic pressure, it is important for maintaining blood pressure and volume. Sodium reabsorption and excretion is mainly regulated by aldosterone and the RAAS, respectively, and changes in the ECF volume, as described before (section 1.4.2.2).

Sodium concentration was measured simultaneously in serum and 24 h urine samples. In general, determination of electrolytes in the serum is considered to be more accurate. Whereas Na^+ concentration in the sera of immunized anti-β_1-EC_{II}-ab-positive *versus* control rats did not significantly differ throughout the experiment, it should be noted that three and nine months after immunization, Na^+ reabsorption was significantly increased (Figure 15).

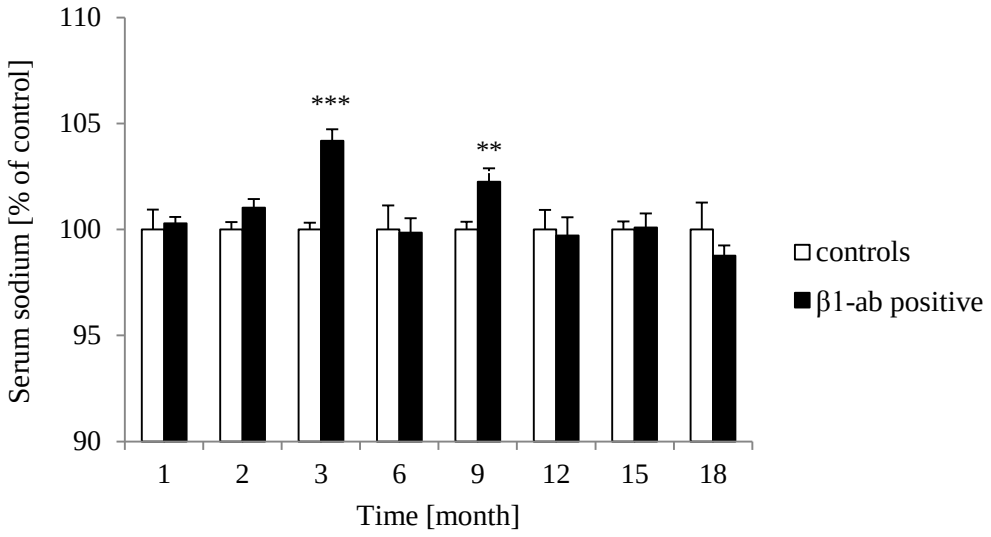

Figure 15: Sodium concentration in the blood.

Columns represent serum sodium concentrations of immunized anti-β_1-EC_{II}-ab-positive animals, given as percentage of the corresponding control animals (white), set at 100%. Error bars represent ± SEM. **p < 0.01, ***p < 0.005.

In contrast, sodium concentrations in 24 h urine samples did not differ significantly. The electrolyte levels of both animal groups were comparable during the 18 months study-period (Figure 16).

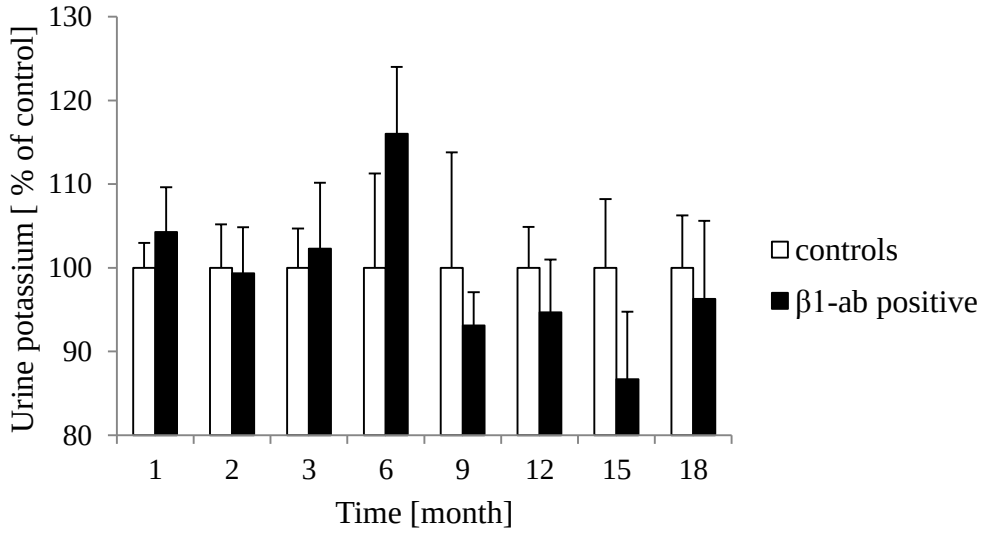

Figure 16: Sodium concentration in 24 h urine samples.

Urine samples of each animal were collected on ice for 24 h. Columns represent urine sodium concentrations of immunized anti-β_1-EC_{II}-ab-positive animals given as percentage of the corresponding control animals (white), set at 100%. Results were adjusted to the total urine volume. Error bars depict ± SEM.

3.6.2.2 Calcium

Calcium is essential for sustaining life in the organism and regulates a variety of signaling processes. Calcium is absorbed throughout the nephron with the principal reabsorption sites being the proximal tubules, the thick ascending limb, and the distal tubules. Whereas the bulk of passive calcium reabsorption occurs at the beginning of the nephron, the fine adjustment of calcium recovery occurs downstream in the thick ascending limb and in the distal tubules. Activation of β_1-ARs stimulates the active reabsorption of Ca^{2+} in the distal convoluted and connecting tubules [179].

The levels of free serum calcium in both control and immunized antibody-positive animals remained almost constant throughout the experiment. However, one and two months after immunization, serum calcium was significantly decreased in anti-β_1-EC_{II}-ab-positive rats compared to their corresponding controls (Figure 17).

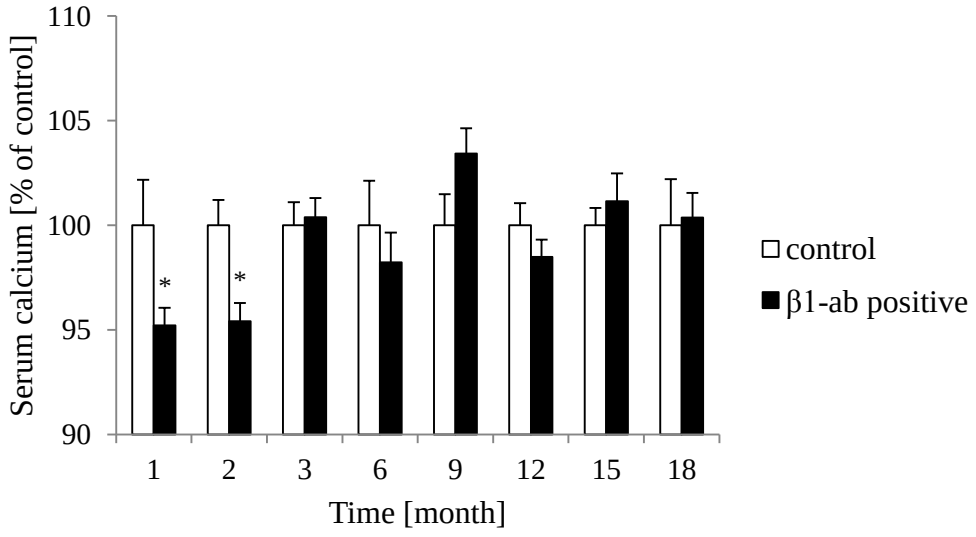

Figure 17: Serum calcium concentration.

Concentration of free calcium ions in the serum. Columns represent serum calcium concentrations of immunized anti-β_1-EC_{II}-ab-positive animals (black) given as percentage of the corresponding control animals (white), set at 100%. Error bars depict mean ± SEM. *$p < 0.05$.

In contrast, the concentration of free Ca^{2+} in 24 h-urine samples gave different results: 6 months after immunization, the excretion rate of calcium was significantly higher in anti-β_1-EC_{II}-ab-positive animals compared to their controls, whereas 12 months after immunization, the

concentration of Ca^{2+} in the urine of the immunized rats was significantly lower compared to the corresponding control animals (Figure 18).

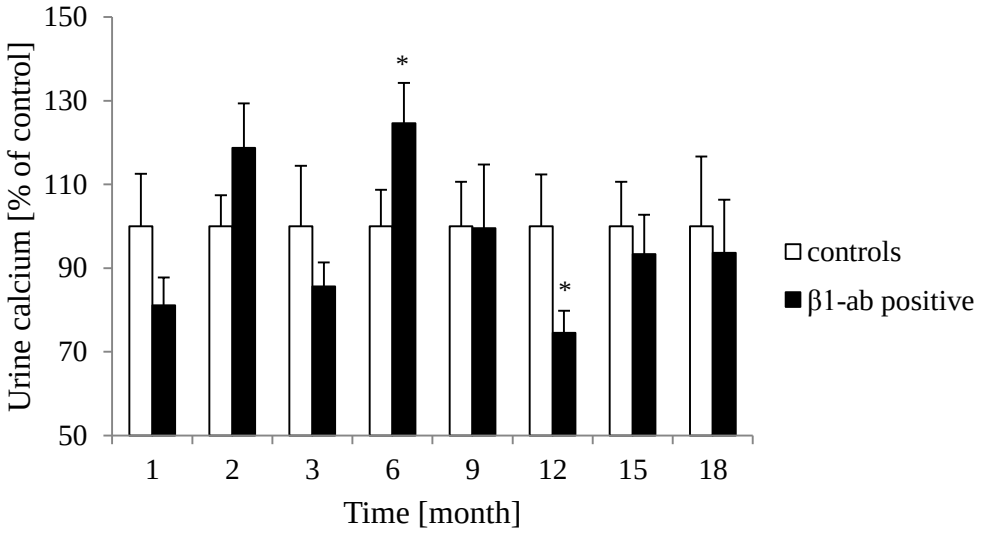

Figure 18: Calcium concentration in 24h urine.

Urine samples of each animal were collected on ice for 24 h. Columns represent urine calcium concentration of immunized anti-β_1-EC_{II}-ab-positive animals (black) given as percentage of the corresponding control animals (white), set at 100%. Results were adjusted to the total urine volume. Error bars depict ± SEM; *$p < 0.05$.

3.6.2.3 Potassium

Potassium is the most abundant cation in the body. Concentration gradients of potassium across cell membranes are essential for nerve excitation and muscle contraction. Accordingly, intracellular and extracellular potassium concentrations are continuously separately controlled to secure potassium homeostasis.

60–70% of the filtered K^+ are passively reabsorbed in the proximal tubule. There are no specific potassium transporters, and reabsorption parallels water absorption (solvent drag). 25–35% of the filtered potassium are reabsorbed in the loop of Henle by the Na-K-2Cl-cotransporter. 5–15% of the filtered potassium reaches the distal nephron, where potassium reabsorption and excretion is controlled by aldosterone. Besides the control by aldosterone, the potassium secretion strongly depends on distal sodium supply, explaining the fact that an increase in sodium concentration increases potassium secretion at the distal tubule [180-183].

In anti-β_1-EC_{II}-ab-positive animals, K^+ levels did not differ significantly from control rats within the first two months after immunization (Figure 19). Three months after immunization, the amount of free potassium in the sera increased significantly. Thereafter, serum K^+ levels decreased compared to control animals, attaining its lowest level nine months after immunization. This feature was then counterbalanced at month 12 and remained constant during the last months of the experiment (Figure 19).

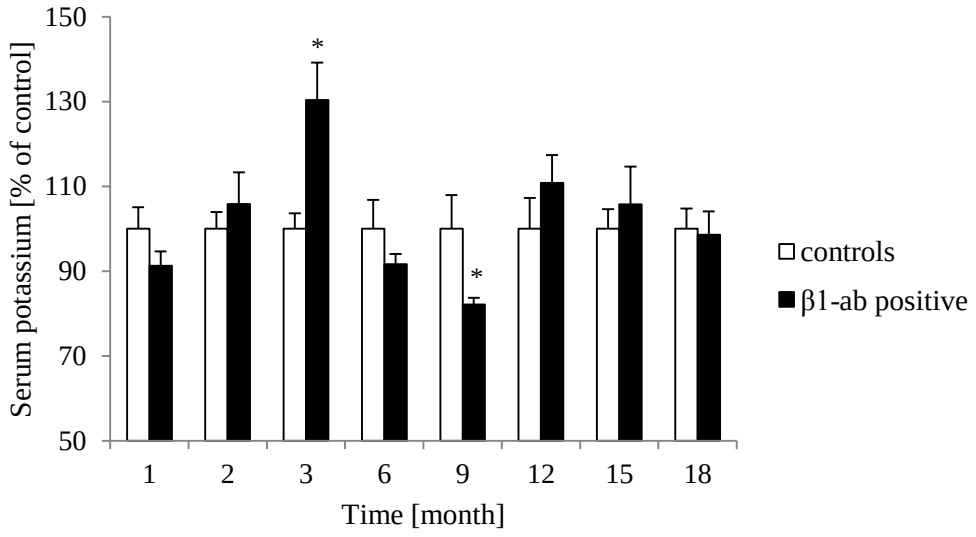

Figure 19: Serum potassium content.

Columns represent serum potassium concentrations of immunized anti-β_1-EC_{II}-ab-positive animals (black) given as percentage of the corresponding control animals (white), set at 100%. Error bars depict ± SEM. *$p < 0.05$.

Urinary excretion of potassium is not directly controlled along the proximal tubule. However, secondary flow-dependent modifications in potassium transport occur in distal nephron segments when sodium delivery increases [182, 184-186]. As urine sodium concentration did not significantly differ between anti-β_1-EC_{II}-ab-positive and control animals, similarly, no major differences in the excretion of potassium into the urine were observed throughout the experiment (Figure 20).

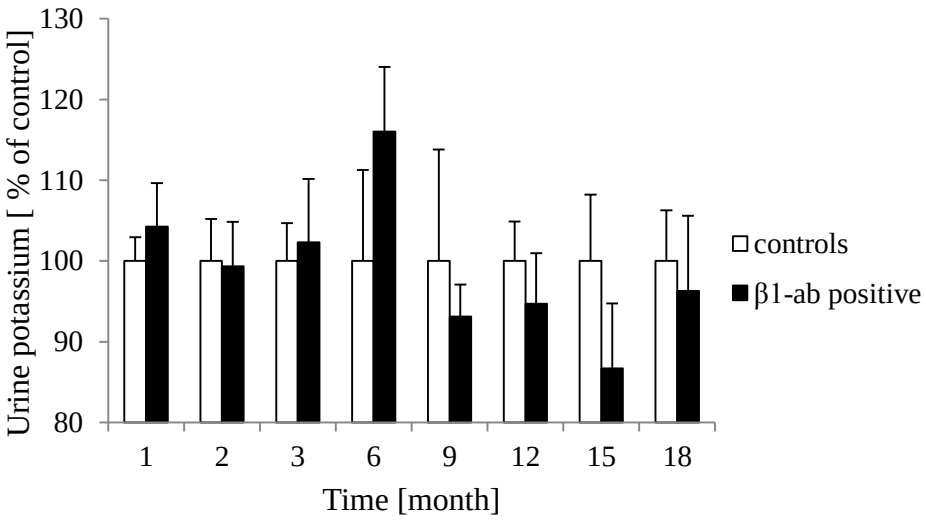

Figure 20: Potassium concentration in 24 h urine.

Urine samples of each animal were collected on ice for 24 h. Columns represent urine potassium concentrations of immunized anti-β_1-EC_{II}-ab-positive animals (black) given as percentage of the corresponding control animals (white), set at 100%. Results were adjusted to the total urine volume. Error bars depict ± SEM.

3.6.3 Further renal damage

Besides microscopic analysis of kidney tissues, "functional" renal damage can also be assessed by measuring the urinary secretion of proteins. Normal individuals usually excrete very small amounts of protein into the urine. Persistently increased protein excretion is an established marker for kidney damage. The excretion of specific types of protein, such as albumin or low molecular weight globulins, depends on the type of disease that is present. Increased excretion of albumin is a sensitive marker for kidney and nephron damage due to e.g. diabetes, certain glomerular diseases, and hypertension, whereas increased excretion of low molecular weight globulins is a sensitive marker for certain tubulointerstitial diseases.

Glomerular permeability is affected by molecular weight, size, shape, and electrical charge of molecules and, of course, is also affected by renal hemodynamics. Under physiological conditions, the renal filtration threshold is 68,000 daltons. Thus, the glomerular ultrafiltrate contains electrolytes (in a similar concentration as plasma) and low molecular weight proteins. All proteins with a higher molecular weight cannot pass through the membrane and are, therefore, not filtered out of the blood. Most of the filtered proteins, however, are reabsorbed in the proximal tubule, preventing their loss from the body through the urine.

3.6.3.1 Total protein

Assessment of urine total protein has been a cornerstone for the diagnosis and monitoring of renal diseases for decades. As proteins are generally filtrated in the glomeruli and reabsorbed in the proximal tubules, it is used as an indicator for possible alterations in filtration function in these particular areas.

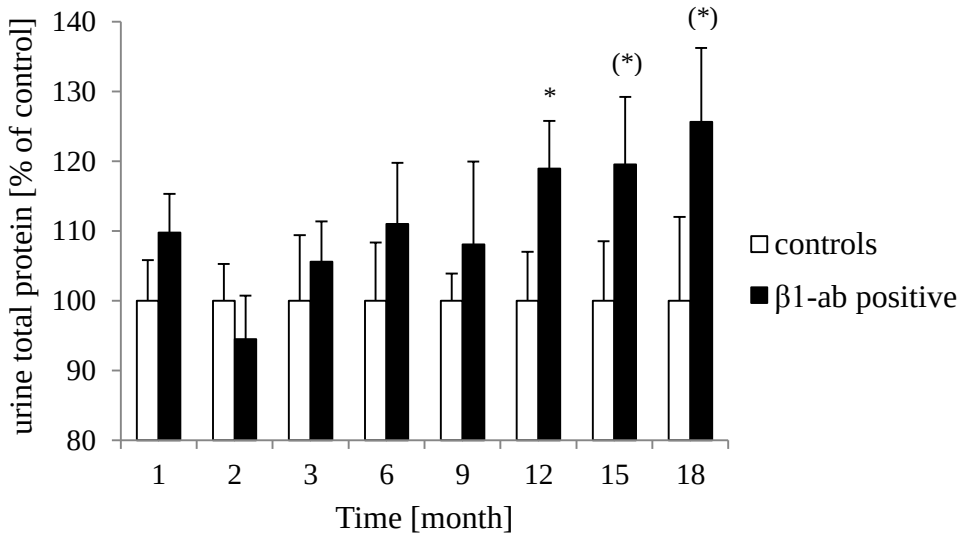

Figure 21: Total protein level measured in 24 h urine samples.

Columns represent total protein concentrations in the urine of immunized anti-β_1-EC_{II}-ab-positive animals (black) given as percentage of the corresponding control animals (white), set at 100%. Results were adjusted to the total urine volume. Error bars depict ± SEM. (*)$p < 0.1$, *$p < 0.05$.

In immunized anti-β_1-EC_{II}-ab-positive rats, significantly increased levels of urine total protein were observed from the 12^{th} immunization month on (Figure 21), and remained elevated until the end of the experiment.

To determine more precisely where the damage was situated in the nephron, we performed a differential analysis of the excreted urine proteins.

3.6.3.2 Albumin

Albumin is synthesized in the liver and is the most abundant plasma protein. It serves as carrier of metabolites, hormones, and vitamins, acts as an antioxidant, and is essential to maintain oncotic pressure and blood volume. It has a molecular weight of about 65 kDa, and its presence in

the urine is considered to be the result of a dysbalance between its glomerular filtration and its tubular reabsorption. In most cases, the level of albumin in the urine is directly related to the progression of the underlying renal disease.

Albumin filtered in the glomeruli is the major source of urinary albumin. In the rat, it is glomerularily filtered with a sieving coefficient of about 0.003 [187], resulting in an estimated albumin concentration in the ultrafiltrate between 1 and 50µg/ml [188]. Filtration of albumin is followed by tubular reabsorption. Thus, albuminuria reflects alterations of at least one of the two latter processes. Most often, however, increased urinary albumin levels are caused by a disease-induced dysfunction of the tubules and subsequently reduced tubular albumin reabsorption.

In immunized anti-β_1-EC_{II}-ab-positive rats, significant albuminuria was not observed during the study (Figure 22). After 12 months of immunization, however, the amount of urinary albumin largely increased in antibody-positive rats compared to the corresponding controls, and remained elevated until the end of the study, similarly as the urinary total protein levels, but this trend failed to reach significance.

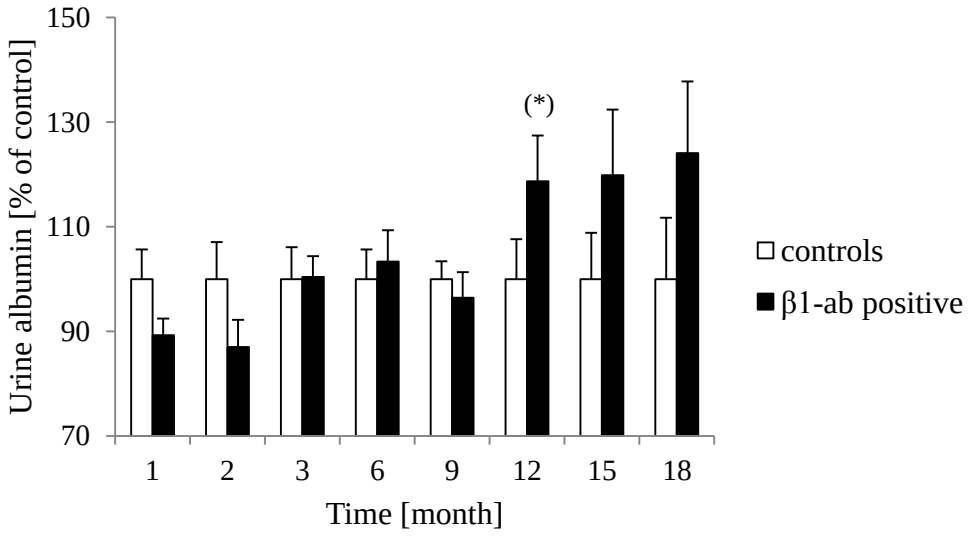

Figure 22: Urinary albumin levels in immunized *versus* control rats.

Columns represent albumin concentrations in the urine of immunized anti-β_1-EC_{II}-ab-positive animals (black) given as percentage of the corresponding control animals (white), set at 100%. Results were adjusted to the total urine volume. Error bars depict ± SEM. (*)$p < 0.1$.

3.6.4 Renin

Renin is the key regulator of the renin-angiotensin-aldosterone system, which is critically involved in salt, volume, and blood pressure homeostasis of the body. The adrenergic system is known to be one of the main modulators of renin stimulation and secretion. We, therefore, hypothesized that stimulating anti-β_1-EC_{II}-ab might also stimulate the secretion of renin (see also section 1.3).

Within the first months after induction of anti-β_1-EC_{II}-ab, renin activity levels were elevated in immunized ab-positive compared to control animals, but this initial stimulating effect seems to be counter-regulated after six months (Figure 23). Interestingly, PRA was already significantly increased one month after inducing anti-β_1-EC_{II}-abs, although ab-titers were still relatively low at this time-point (see Figure 10).

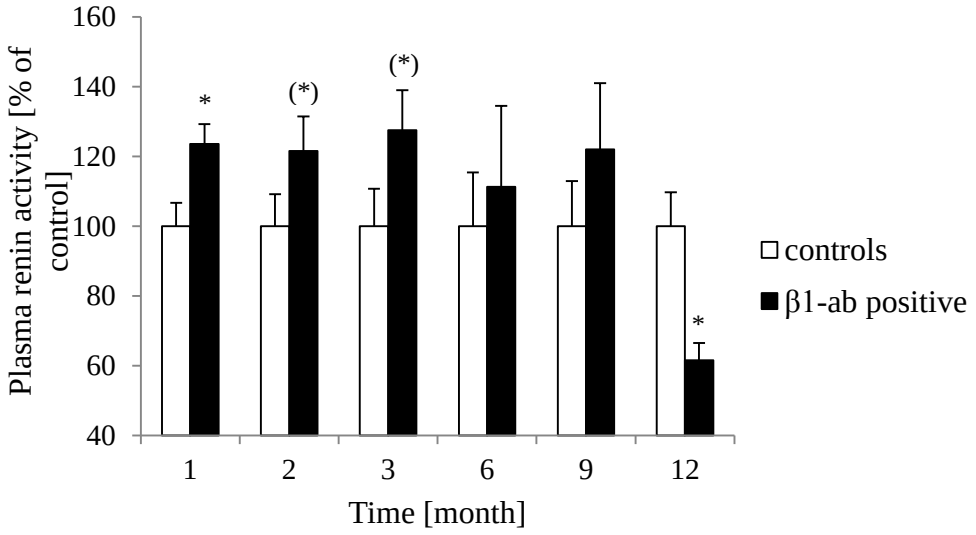

Figure 23: Plasma renin activity in immunized *versus* control animals over the course of time.

Plasma renin activity was determined by radioimmunoassay. Values were determined in triplicates. Columns represent PRA of immunized anti-β_1-EC_{II}-ab-positive animals (black) given as percentage of the corresponding control animals (white), set at 100%. Error bars represent ± SEM. N=20 animals per time point and group were analyzed; (*)$p < 0.1$, *$p < 0.05$.

This pattern fitted well to the qPCR analysis of renin expression: the kidney of immunized ab-positive rats revealed a significant increase in renin expression between two and six months after induction of stimulating anti-β_1-EC_{II}-abs compared to the corresponding controls (Figure 24).

From the ninth month on, renin expression decreased in the anti-β_1-EC_{II}-ab-positive rats (significant at month 12) and remained low until the study-end.

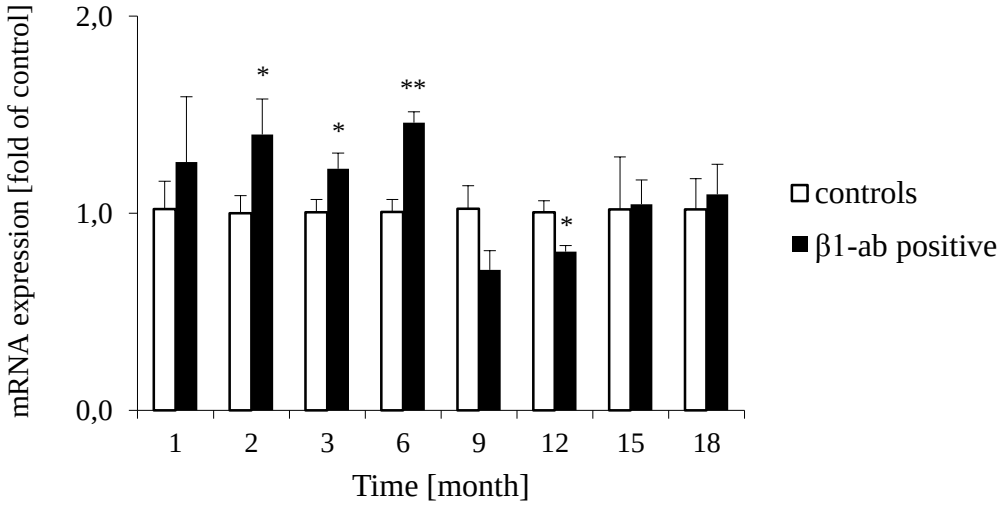

Figure 24: Renin mRNA levels in kidney tissues from anti-β_1-EC_{II}-ab-positive *versus* ab-negative rats.
Columns represent renin mRNA expression levels of immunized anti-β_1-EC_{II}-ab-positive animals (black) given as percentage of the corresponding control animals (white), set at 100%. Error bars depict ± SEM. N=5 animals per time point and group were analyzed; *$p < 0.05$, **$p<0.01$.

3.6.5 Isolated perfused kidney

In addition to effects of stimulating anti-β_1-EC_{II}-abs on the kidney under chronic conditions "*in vivo*", we also analyzed their acute renal effects in isolated perfused kidneys. This approach enabled us to directly assess functional effects of stimulating anti-β_1-EC_{II}-abs on one sole organ, almost unaffected by potential whole body-(auto-) regulatory mechanisms. The experiments were carried out in collaboration with the Institute of Physiology of the University of Regensburg. Kidneys of normal BL6 mice were isolated and perfused with different solutions (see methods-section 2.2.14). After the various experiments, the secretion rate of renin was determined in the respective eluates by radioimmunoassay. Perfusion with 10nM (-)isoproterenol was used as a positive control.

Perfusion of the isolated kidneys with whole sera of the anti-β_1-EC_{II}-ab-positive animals led to a significant increase in renin secretion, whereas control sera had no effect (Figure 25). To exclude other components than anti-β_1-EC_{II} abs present in the serum, ab-positive and –negative sera were

filtered (cut-off 100 kDa) in order to retain IgG molecules (> 150 kDa) and to get rid of smaller components potentially stimulating renin secretion, as e.g. catecholamines and prostaglandins. Analysis of the resuspended macromolecules (> 100 kDa) yielded the same results as whole sera. As there are no known substances larger than 100 kDa present in serum which might affect renin, it is justified to assume that the observed stimulating effect on renin secretion is indeed due to the binding of functional anti-β_1-EC_{II}-abs to renal β_1-ARs.

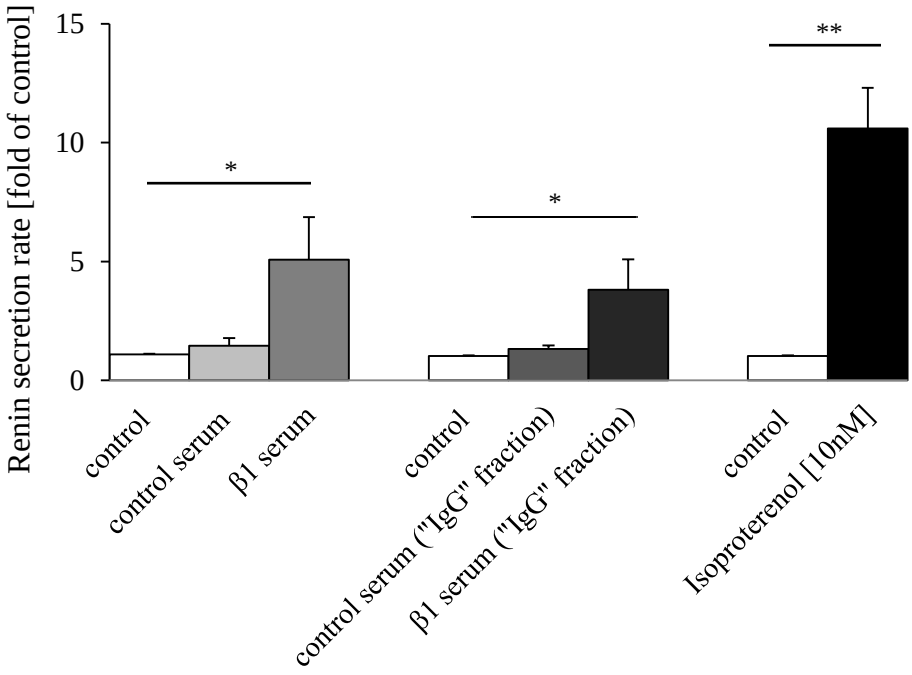

Figure 25: Renin secretion rate, measured in isolated perfused kidneys.

Kidneys of normal BL6-mice were isolated and perfused with various ab-containing solutions. Secreted renin was determined in the respective eluates by radioimmunoassay. Isoproterenol (10 nM) served to determine the maximal response. Columns represent mean renin secretion rates, given as fold over control (perfusion medium only, white columns), set at 1. Error bars represent ± SEM. N=5; *$p < 0.05$, **$p < 0.01$.

3.6.6 Glomerular filtration rate

GFR is defined as the plasma volume fully cleared of a particular substance by the kidneys in a given time interval. The clearance of exogenous substances such as inulin or iohexol serves as a gold standard for the determination of the GFR. In a single nephron, the filtration rate is a function of (a) the net filtration pressure, (b) the permeability of the filtration membrane, and (c) the surface area available for filtration. The GFR reflects all these factors, based on the total number of functioning nephrons. The GFR is autoregulated by the kidney in order to keep GFR steady over a wide range of different blood pressures. In case blood pressure drops too low (e.g. due to excessive fluid loss), the sympathetic nervous system will override renal autoregulation. Sympathetic nerves directly innervating the afferent arteriole through smooth muscle contraction cause narrowing of the afferent arteriole and, subsequently, a decrease in GFR. In addition, Ang II may affect both GFR and RBF by inducing constriction of the afferent and efferent arterioles. As described above (section 1.3), stimulation of β_1-ARs may lead to an activation of the RAAS, and thus to increased serum-levels of Ang II.

Because the SNS is constantly activated in the presence of stimulating anti-β_1-EC_{II}-abs, we also expected some β_1-AR mediated effects on GFR.GFR is assessed directly by measuring inulin clearance. Inulin is a plant carbohydrate that is neither reabsorbed nor secreted, thus the clearance of inulin (blood volume cleared from inulin per time unit) solely depends on filtration.

Within the first weeks after immunization GFR (determined by inulin-clearance) was clearly, but not significantly, reduced in anti-β_1-EC_{II}-abs positive compared to control animals (Figure 26). During the following months of the experiment, GFR fully recovered despite the presence of stimulating anti-β_1-EC_{II} abs. Towards the end of the experiment (15 and 18 months), GFR was again (significantly) reduced in the ab-positive rats compared to the corresponding controls.

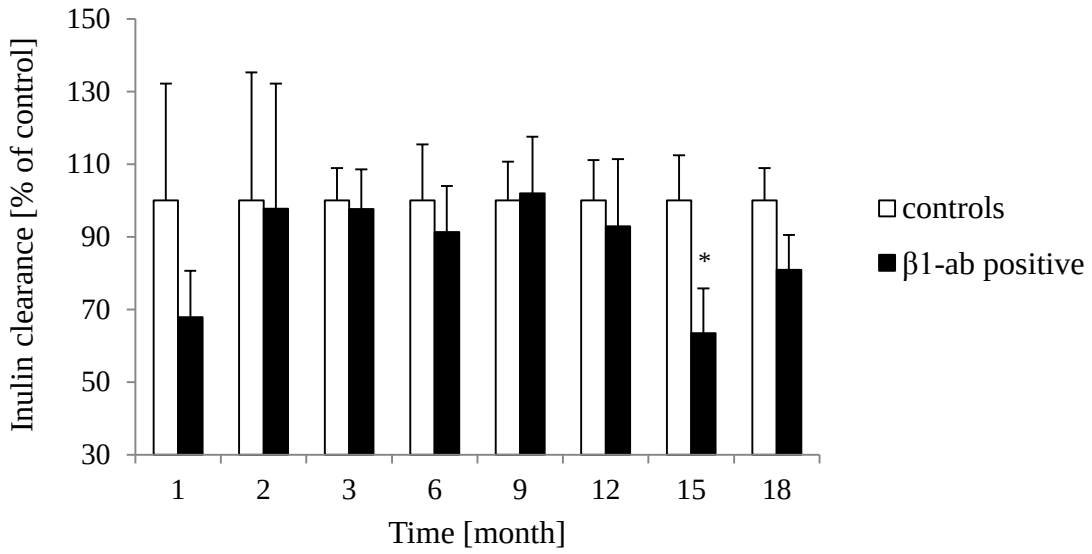

Figure 26: Measurement of GFR *via* bladder catheterization.

Renal inulin clearance was measured to determine GFR (described in detail in section 2.2.10). Columns represent mean inulin clearances of immunized anti-β_1-EC_{II}-ab-positive animals (black), given in percent of the values obtained for control animals (white), set at 100%. Error bars represent ± SEM. N=5 animals per time point and group were analyzed; *$p < 0.05$.

Besides GFR, also RBF is expected to be affected by the β_1-adrenergic system. As a consequence, we analyzed the effects of stimulating anti-β_1-EC_{II}-abs on PAH clearance. As for GFR, RBF was clearly but not significantly reduced in anti-β_1-EC_{II}-ab-positive rats during the first weeks of the experiment after successful immunization (Figure 27). Thereafter, at months three through nine, RBF recovered in anti-β_1-EC_{II}-ab-positive animals. From the 12^{th} month on – together with the development of HF and as observed for GFR – RBF progressively decreased in anti-β_1-EC_{II}-ab-positive compared to control rats.

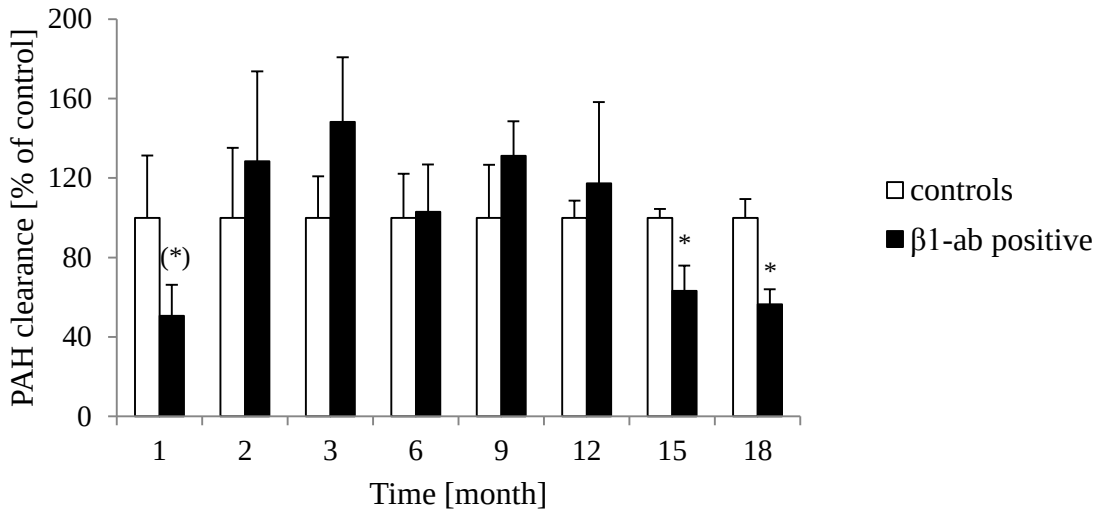

Figure 27: Assessment of RBF by measurement of PAH clearance.

Renal PAH clearance was measured to determine RBF (described in detail in section 2.2.10). Columns represent mean PAH clearances of immunized anti-β_1-EC_{II}-ab-positive animals (black), given in percent of the values obtained for control animals (white), set at 100%. Error bars represent ± SEM. N=5 animals per time point and group were analyzed; (*)$p < 0.1$, *$p < 0.05$.

A decrease in PAH clearance can result from reduced renal PAH supply or reduced PAH secretion from the proximal tubules. Determination of PNS serves as a measure of organic anion secretion by the renal proximal tubules. In accordance to inulin and PAH clearance, PNS was reduced within the first weeks after immunization in ab-positive compared to control animals (Figure 28). After a recovery phase between months three and nine, PNS decreased from the 12th month on, analogous to GFR (Figure 26) and RBF (Figure 27).

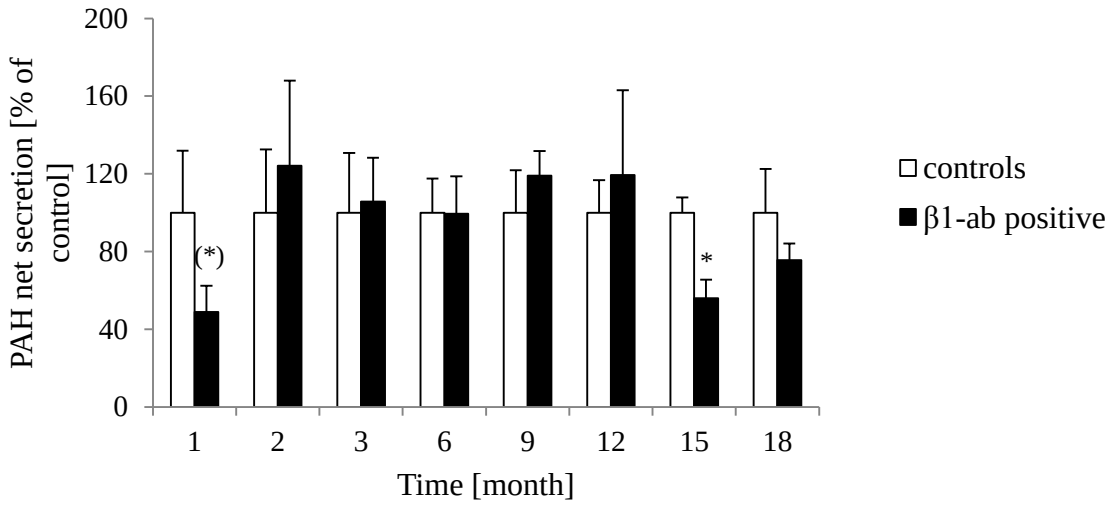

Figure 28: Effects of stimulating anti-β_1-EC_{II}-abs on PAH net secretion.

PNS was measured as described in detail in section 2.2.10. Columns represent mean PNS of immunized anti-β_1-EC_{II}-ab-positive animals (black), given in percent of the values obtained for control animals (white), set at 100%. Error bars represent ± SEM. N=5 animals per time point and group were analyzed; (*)$p < 0.1$, *$p < 0.05$.

3.7 Structural changes

Chronic stimulation of the β_1-ARs may lead to structural changes in different organs. Particularly the subsequent Ang II-generation is associated e.g. with the formation of fibrosis. The following sections present the potential effects of stimulating anti-β_1-EC_{II}-abs on kidney morphology and structure.

3.7.1 Formation of total fibrosis

Fibrosis is defined as the formation of excess connective tissue as a reparative or reactive process. It is also regarded as a failure of the physiological wound healing response. Fibroblasts have been recognized as key cells involved in the regulation of tissue fibrosis through, e.g., extracellular matrix deposition [189]. Characteristic features include the expression of vimentin in the absence of desmin and α-smooth muscle actin. Once activated, fibroblasts exhibit an abundant endoplasmic reticulum and prominent Golgi associated with the synthesis and secretion of ECM molecules including collagens, proteoglycans, and fibronectin, as well as proteases capable of degrading the ECM [190]. Renal fibrosis is characterized by glomerulosclerosis and tubulointerstitial fibrosis, and represents the final common path of a wide range of chronic kidney

diseases. The corresponding histopathological renal findings are often described as glomerulosclerosis, tubulo-interstitial fibrosis, renal inflammatory infiltrates, and loss of renal parenchyma characterized by tubular atrophy, capillary loss, and podocyte depletion. Although more than a dozen different pro-fibrotic factors have been identified including various cytokines, hormones, and metabolic products but also hemodynamic factors, it is widely accepted that TGF-β_1 and its downstream Smad signaling pathway play a crucial role, particularly in renal fibrosis [191, 192].

Molecular analysis of the mRNA expression levels in immunized anti-β_1-EC_{II}-ab-positive animals compared to 0.9% NaCl-injected control rats revealed an upregulation of a number of pro-fibrotic markers, most of them also known to be regulated by Ang II (Figure 29).

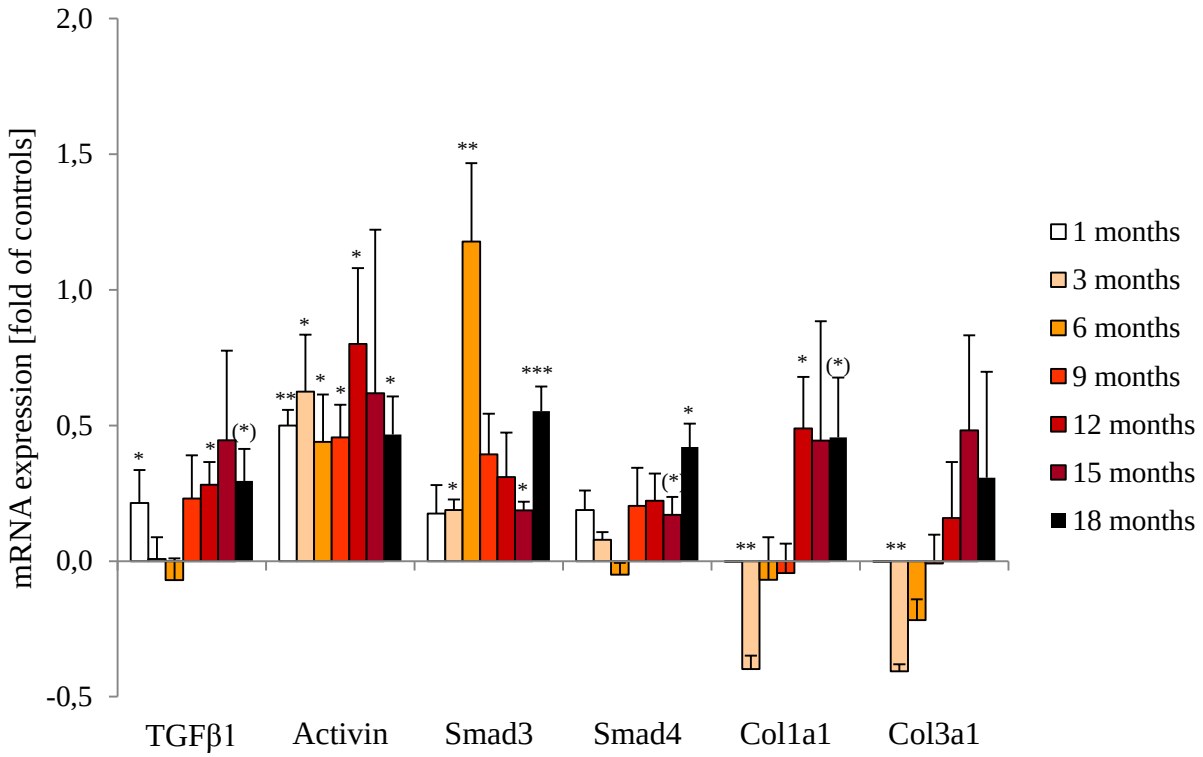

Figure 29: mRNA expression of selected pro-fibrotic markers in immunized animals.

RNA was isolated from kidney tissues and reverse transcription was performed as described in the Material & Methods section. QPCR was performed using 10 ng of DNA. Columns represent means of mRNA expression ± SEM in kidneys of immunized anti-β_1-EC_{II}-ab-positive animals, expressed as fold over corresponding control animals; with controls normalized to zero. N=5 animals per time point and group were analyzed; (*)$p < 0.1$, *$p < 0.05$, **$p < 0.01$, ***$p< 0.005$.

Expression levels in renal tissues of immunized anti-β_1-EC_{II}-ab-positive rats *versus* control rats showed an interesting pattern regarding the key components of fibrosis, Collagen type I and III:
Within the first months of immunization, renal Collagen type I/III expression of immunized anti-β_1-EC_{II}-ab-positive animals appeared to be decreased compared to the non-immunized rats. However, after 12 months, Collagen expression was significantly increased in the ab-positive animals, most likely secondary to the documented increase in TGFβ_1/Activin and Smad3/4 expression (Figure 29).
To analyze whether this molecular activation of pro-fibrotic pathways also results in visible alterations in kidney tissues, differentially stained tissue sections were analyzed by light microscopy. Kidney tissue sections were stained with Sirius Red (as described in section 2.2.11.1), a standard procedure for identifying fibrotic tissue. Sirius Red staining of renal tissue revealed no significant differences between immunized anti-β_1-EC_{II}-ab-positive and control animals (Figure 30). However, at time-points 15 and 18 months, slightly elevated levels of fibrosis could be observed in ab-positive animals.

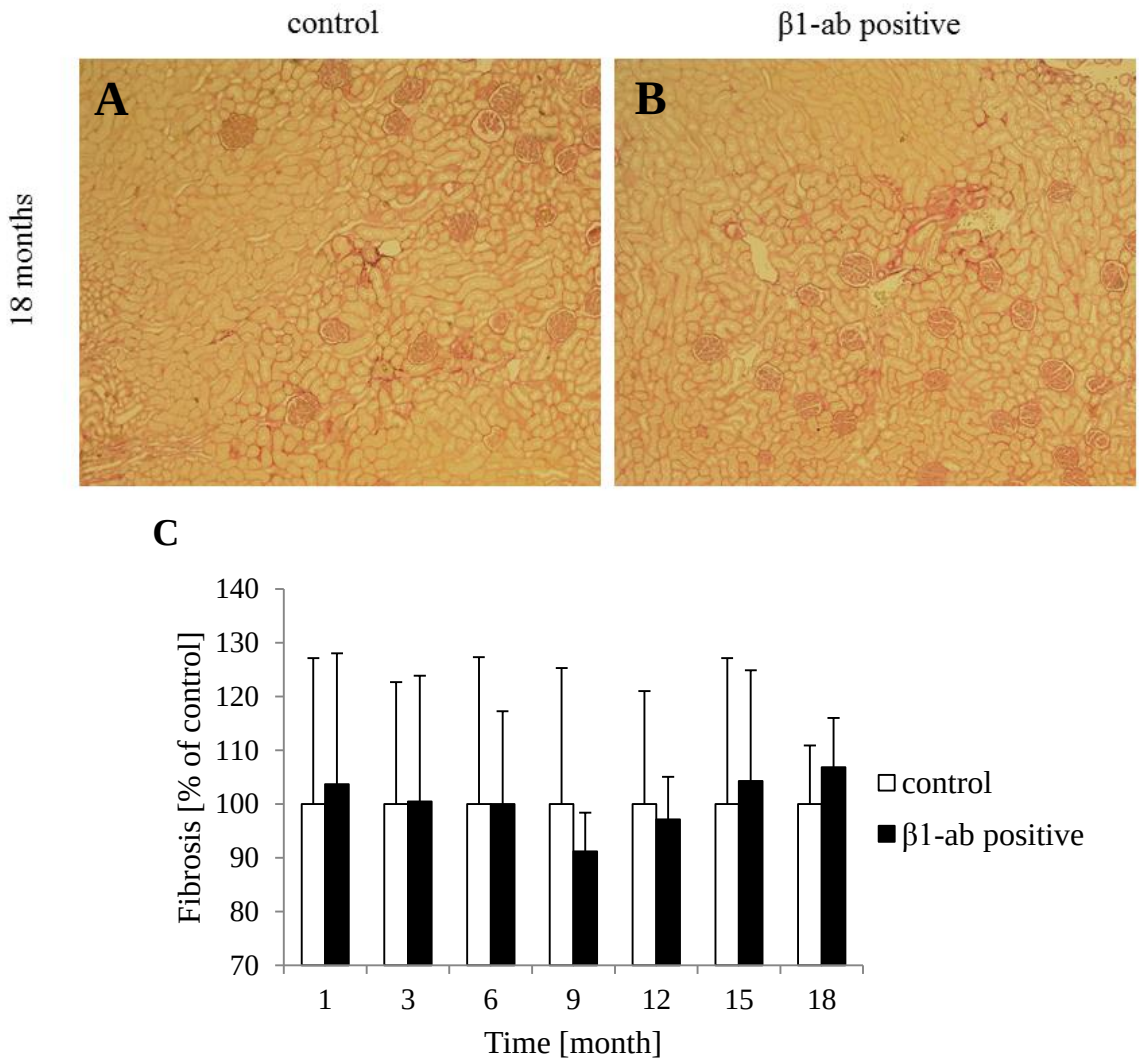

Figure 30: Development of fibrosis in renal tissue.

Representative microscopic images of a Sirius Red-stained kidney section of (A) a 0.9% NaCl-injected control and (B) an immunized ab-positive animal, 18 months after immunization. Total content of fibrous tissue was calculated computer-assisted using Adobe Photoshop (as described in section 2.2.11.2) (C). Columns represent mean of the collagen content in tissue sections of immunized anti-β_1-EC_{II}-ab-positive animals (black), expressed as percentage of the whole cross-sectional area compared to controls, set at 100%. Error bars represent ± SEM. N=5 animals per time point and group were analyzed.

Additional analysis of collagen deposits by a dye-binding-and-elution-method (see Material & Methods section 2.2.11.3) gave a comparable result: no significant differences were detected between ab-positive and control animals (Figure 31). From immunization month 15 on, however, the immunized rats showed increased levels of fibrosis compared to the corresponding control animals.

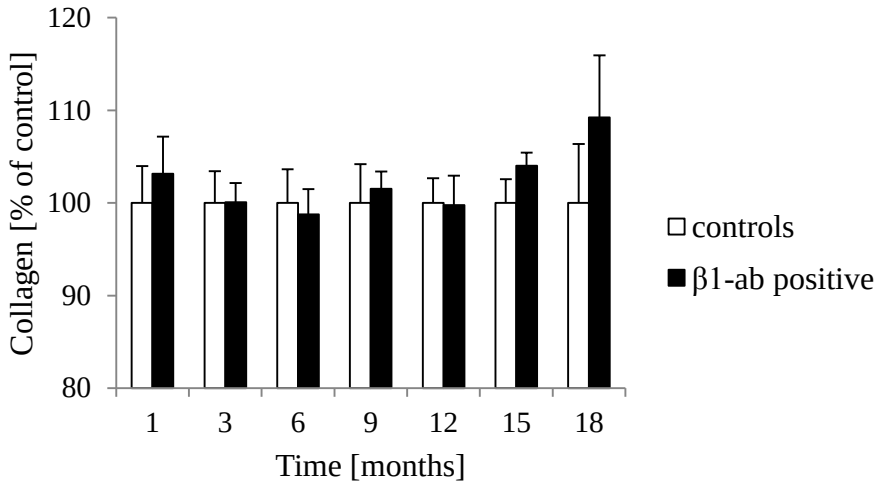

Figure 31: Collagen content of kidney cross-sections.

Analysis of fibrosis in the kidney cross-sections by the dye-binding-and-elution-method. Columns represent the mean collagen content in kidney cross sections of immunized anti-β_1-EC_{II}-ab-positive animals (black), given in percent of the values obtained for control animals (white), set at 100%. Error bars represent ± SEM. N=5 animals per time point and group were analyzed.

3.7.2 Glomerulosclerosis

The term glomerulosclerosis refers to the hardening or scarring of the glomerulus, a condition which leads to the impairment of filtration function and, subsequently, to proteinuria. One of the causes may be hypertension, leading to so-called "hypertensive nephrosclerosis". Characteristic morphological features of glomerulosclerosis may be formation of sclerosis, segmental capillary collapse, epithelial hyperplasia, thickening of the glomerular basement membranes, and mesangial deposits [159, 193], which are detected easily using PAS staining. In our study, we did not observe development of severe (neither general nor focal segmental) glomerulosclerosis (Figure 32). Nevertheless, the glomerulosclerotic index slightly increased over time, and was slightly but not significantly elevated after 12 months of immunization in the anti-β_1-EC_{II}-ab-positive animals compared to 0.9% NaCl-injected control animals.

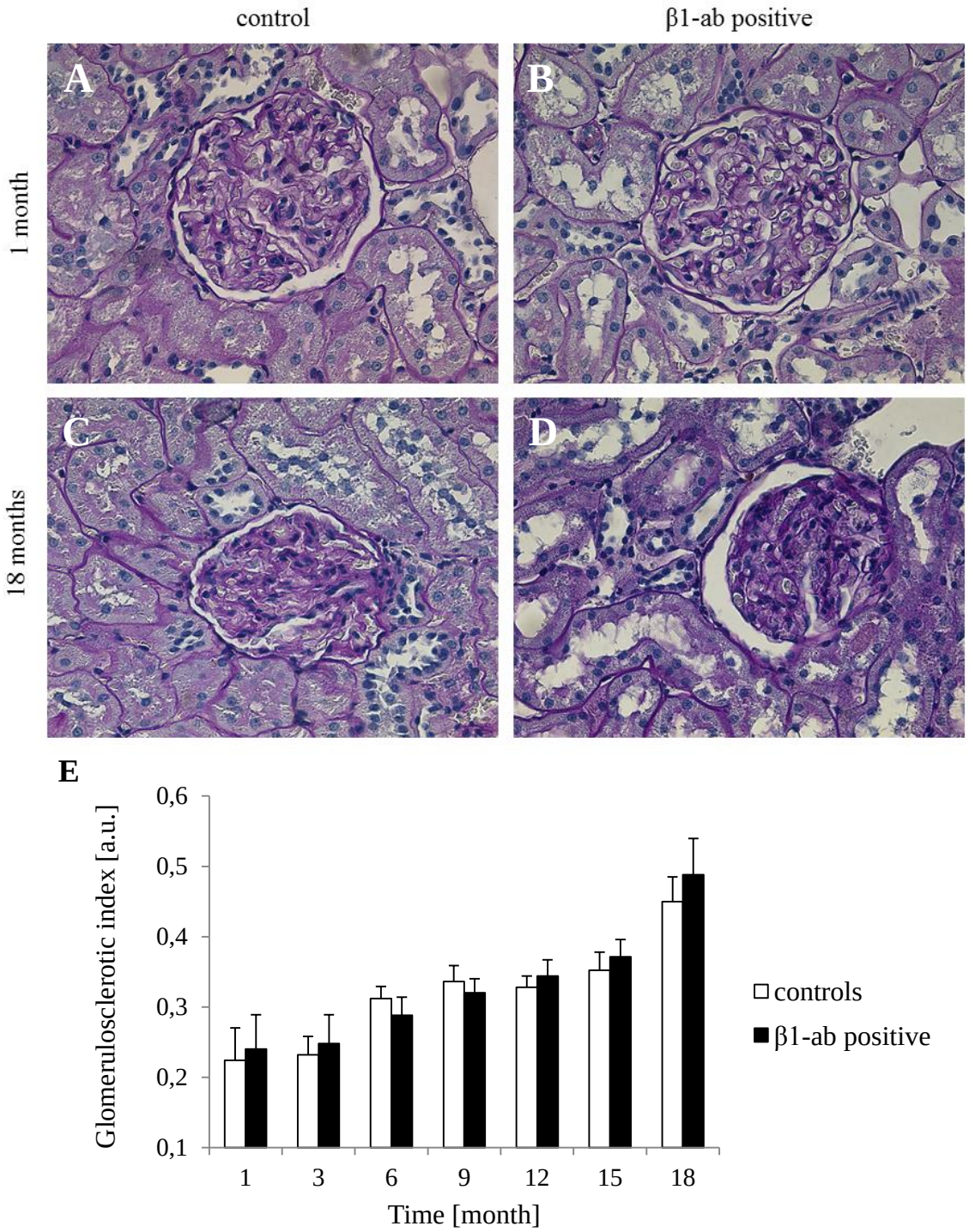

Figure 32: Glomerulosclerosis

Glomerulosclerotic index, assessed on PAS stained kidney cross-sections. Exemplary microscopic images showing a PAS-stained glomerulus of (A) a control and (B) of a immunized anti-β_1-EC_{II}-ab-positive rat 1 month after immunization, as well as after 18 months ((C) control, (D) immunized). (E) Columns represent the mean glomerulosclerotic index of immunized anti-β_1-EC_{II}-ab-positive animals (black) compared to corresponding control animals (white). Error bars represent ± SEM. N=5 animals per time point and group were analyzed.

The two distinct patterns of glomerulosclerosis are termed obsolescence and solidification [194]. Obsolescence is the predominant form of glomerulosclerosis in e.g. hypertensive nephropathy. Histopathologically, it is characterized by collapse of the glomerular tuft and by intracapsular fibrosis [195]. However, as a consequence of glomerular solidification, the glomerular tuft may expand due to increased accumulation of mesangial matrix cells, thought to occur subsequent to glomerular hyperfiltration when afferent arteriolar autoregulation has been lost.

The average size of the glomerular tuft of immunized anti-β_1-EC_{II}-ab-positive rats progressively decreased from immunization-month 12 on compared to 0.9% NaCl-injected control animals, however, without reaching significance (Figure 33).

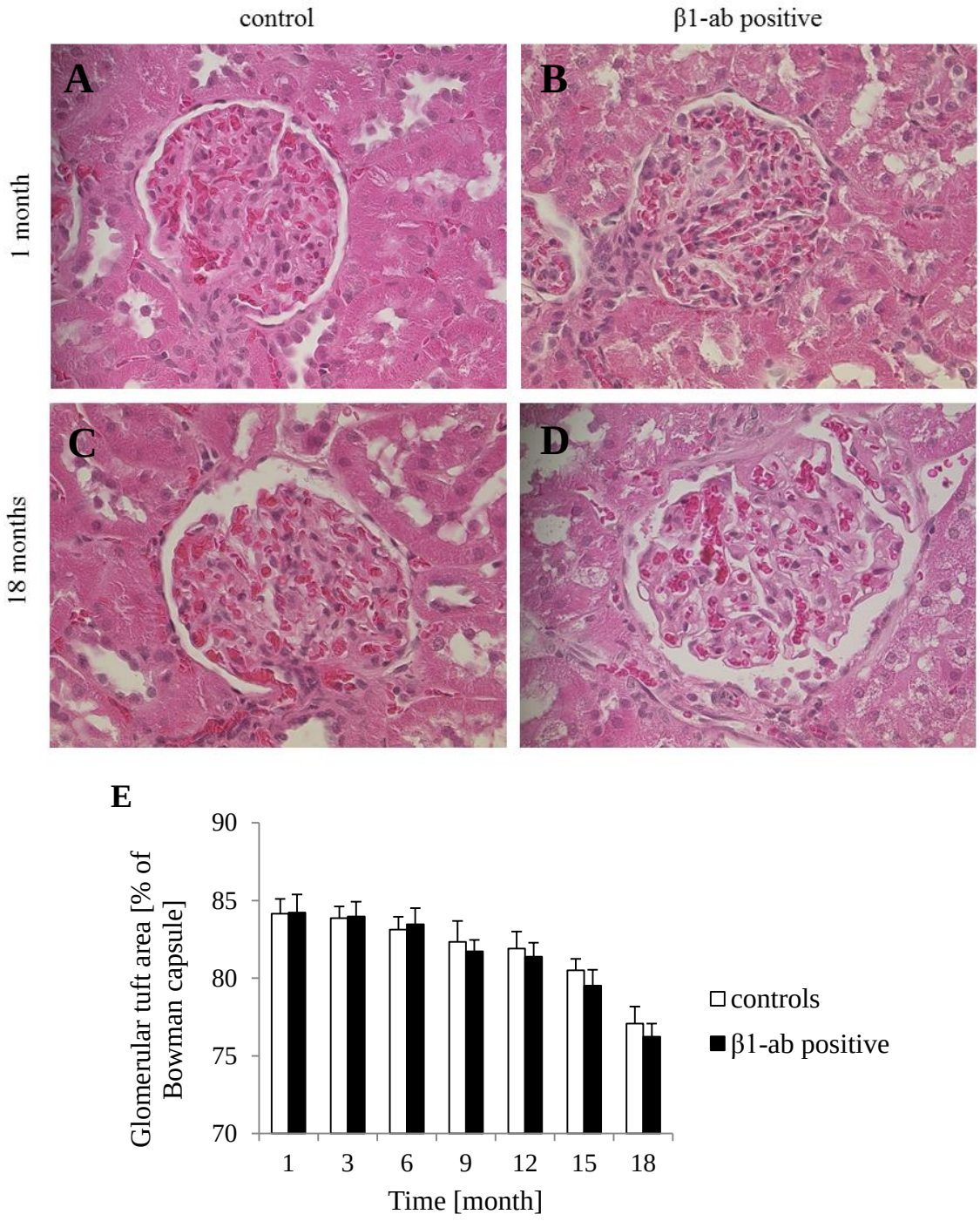

Figure 33: Glomerular atrophy.

Exemplary microscopic images of a HE-stained glomerulus of (A) a 0.9% NaCl-injected control and (B) of a immunized anti-β_1-EC_{II}-ab-positive animal 1 month after start of immunization, as well as after 18 months ((C) control, (D) immunized). (E) Columns represent mean glomerular tuft area, given as percentage of the corresponding Bowman capsule, of immunized anti-β_1-EC_{II}-ab-positive animals (black) and control animals (white). Error bars represent ± SEM. N=5 animals per time point and group were analyzed.

3.7.3 Tubulointerstitial fibrosis

Tubulointerstitial fibrosis occurs as a consequence of recurrent episodes of inflammation leading to progressive peritubular fibrosis and interstitial deposition of matrix proteins which inevitably deteriorate renal function. As for glomerulosclerosis, tubulointerstital fibrosis may also represent a feature of hypertension-induced renal damage. In the latter, an increased activity of the RAAS and the subsequent enhanced production of TGF-β_1 [196] results in tubulointerstitial fibrosis consistently predicting an irreversible loss of renal function and progression to end-stage renal failure [197].

As shown in Figure 34, renal interstitial fibrosis constantly increased in the course of the experiment; however, although the amount of tubulointerstitial fibrosis tended to be higher in immunized anti-β_1-EC_{II}-ab-positive *versus* 0.9% NaCl-injected control, the differences did not reach statistical significance.

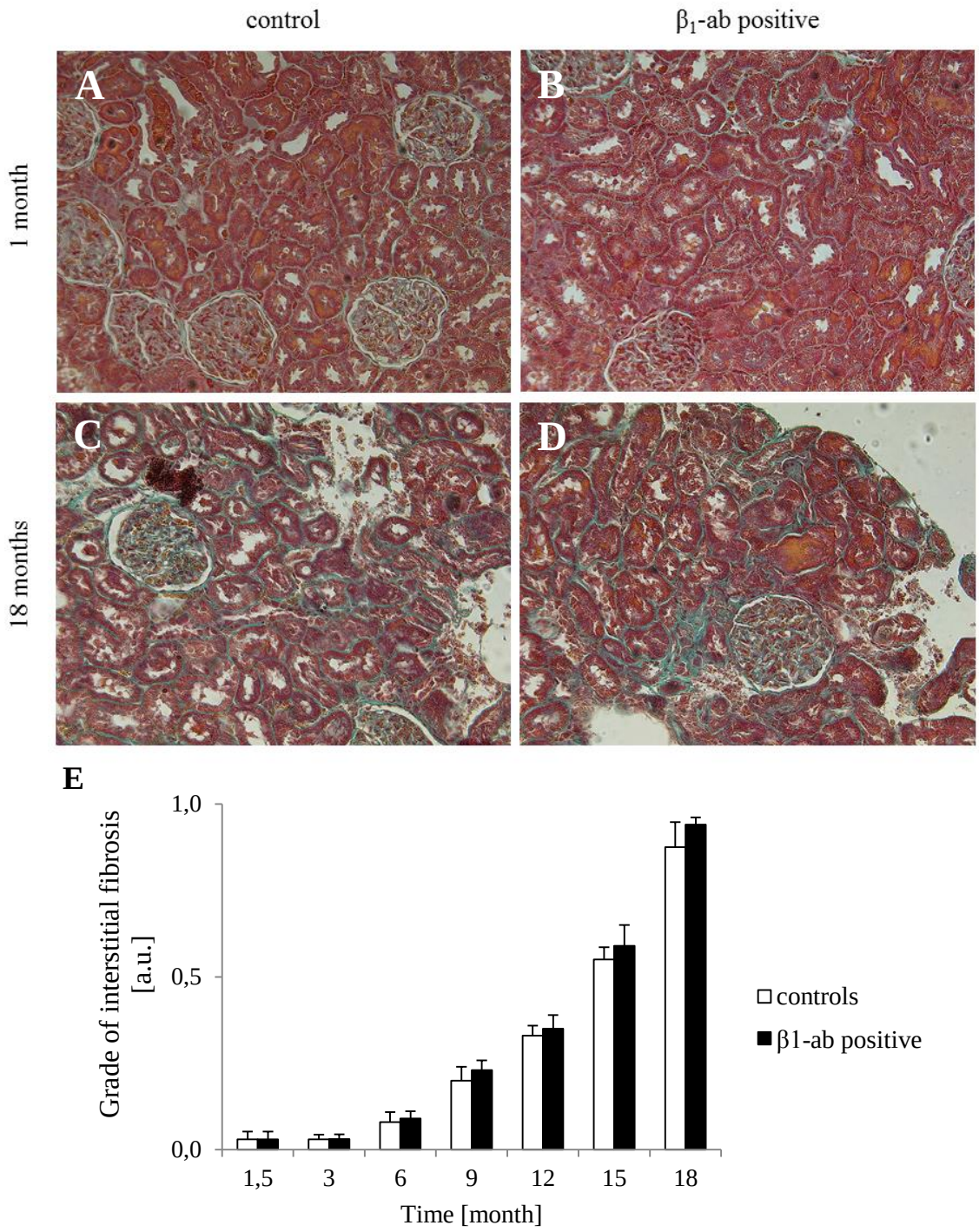

Figure 34: Tubulointerstitial fibrosis in anti-β_1-EC_{II}-ab-positive *versus* control rats.

Representative images of Masson-Goldner Trichrome stainings of kidneys from immunized anti-β_1-EC_{II}-ab-positive rats and corresponding 0.9% NaCl-injected controls (A-D). (A) Control animal and (B) immunized ab-positive animal, 1 month after immunization; (C) control and (D) ab-positive animal, 18 months after start of immunization. (E) Columns represent mean grade of tubulointerstitial fibrosis of immunized anti-β_1-EC_{II}-ab-positive animals (black) and corresponding control animals (white). Error bars represent ± SEM. N=5 animals per time point and group were analyzed.

3.7.4 Perivascular fibrosis

In the hearts of immunized anti-β_1-EC_{II}-ab-positive rats we have shown that cardiac fibrosis starts in the perivascular area of middle-sized and intramural arteries subsequently extending into the interstitial space [198]. Histological analysis of the rat hearts revealed a significantly higher amount of fibrosis around smaller vessels in immunized ab-positive compared to control animals, 15 months after the induction of stimulating anti-β_1-EC_{II}-abs. Perivascular fibrosis may be the consequence of hormonal stimuli (e.g. activation of the RAAS [198]), of a hemodynamic stimulus, or by local inflammatory processes [199]. Thus, direct involvement of stimulating anti-β_1-EC_{II}-abs in perivascular fibrosis can be imagined. Detailed analysis of Sirius Red stained cross-sections of the kidneys revealed an increase in perivascular fibrosis in the kidneys of immunized anti-β_1-EC_{II}-ab-positive compared to corresponding control animals from immunization-month 15 on (Figure 35), which, again, failed to attain statistical significance.

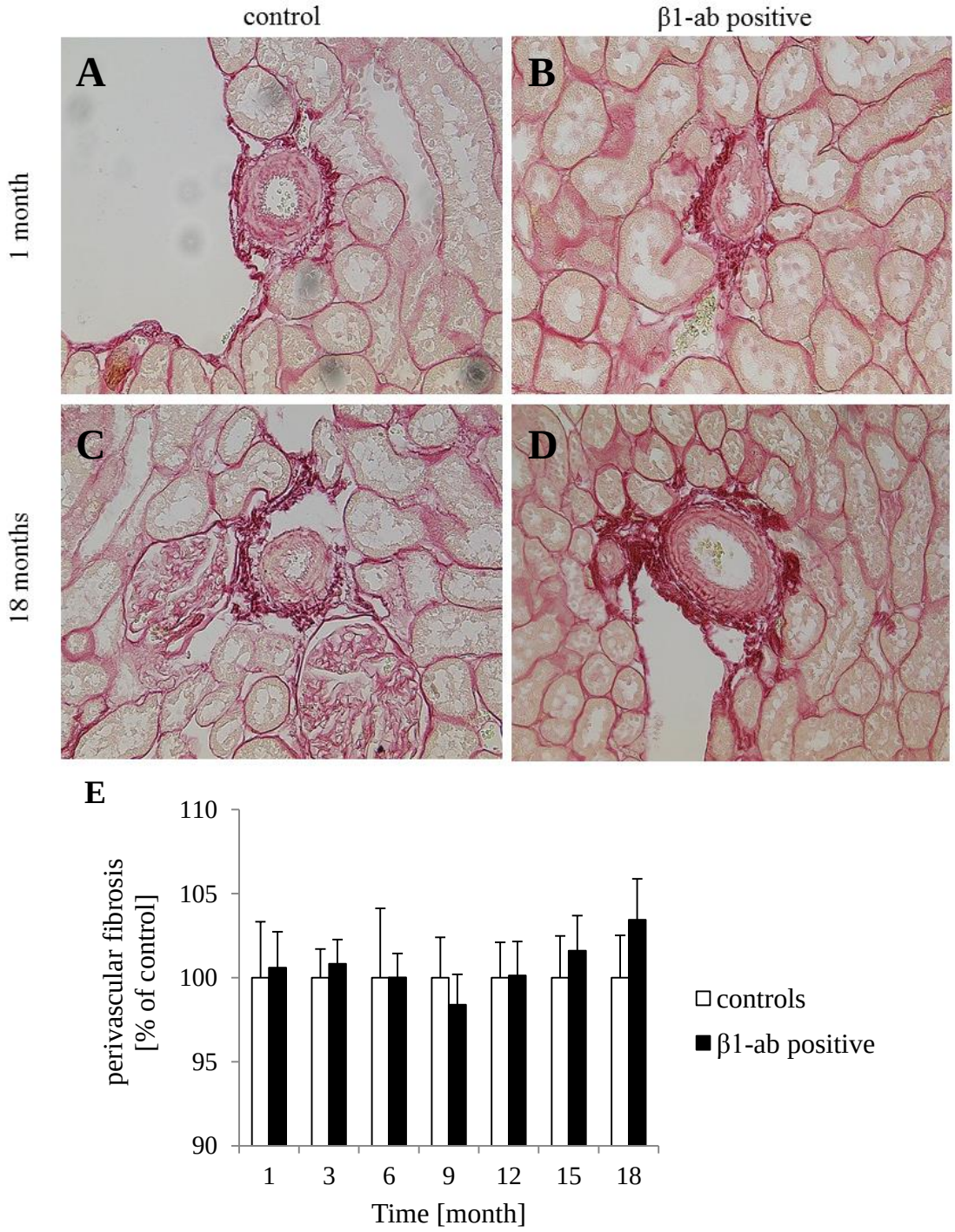

Figure 35: Renal perivascular fibrosis in anti-β_1-EC_{II}-ab-positive *versus* control rats.

Exemplary light-microscopic pictures of perivascular fibrosis of (A) a 0.9% NaCl-injected control animal and of (B) an ab-positive animals after 1 month of immunization. Perivascular fibrosis of (C) a control and (D) an ab-positive animal, 18 months after start of immunization. (E) Columns represent mean values of perivascular fibrosis of immunized anti-β_1-EC_{II}-ab-positive rats (black), given in percent of the blood vessel area compared to the values obtained for control animals (white), set at 100%. Error bars represent ± SEM. N=5 animals per time point and group were analyzed.

4 Discussion

4.1 Role of anti-β_1-abs in cardiac and kidney disease

In human heart failure (HF), more and more experimental and clinical data obtained during the past decades point towards a pathophysiologic relevance of functional auto-antibodies targeting the β_1-AR. The prevalence of functional anti-β_1-aabs, while negligible in the healthy population, attains 30% in patients with idiopathic cardiomyopathy. The prognostic significance of such antibodies in DCM was demonstrated in a pilot-study, which revealed an about 3-fold increased cardiovascular mortality risk in anti-β_1-aab-positive patients [1]. Because β_1-ARs are also highly expressed in the kidney, a potential pathophysiological relevance and clinical implication of anti-β_1-aabs for renal function cannot be denied. However, so far the effect of stimulating anti-β_1-aabs on kidney function has been almost completely neglected. My present work aimed at revealing the potential (patho-)physiologic effects of antibodies directed against the β_1-AR for kidney function and its inter-relationship with autoimmune DCM.

Inbred rats immunized against the human β_1-EC_{II} develop receptor-stimulating anti-β_1-EC_{II}-abs after one month (Figure 10). As we could show by echocardiographic follow-up, ab-positive animals developed a hypertensive phenotype within the first six months of immunization, which evolved into LV dilatation and cardiac dysfunction after about 9 months of regular immunization (Figure 11). This dysfunction slowly but steadily progressed during the course of the study, resulting in the end in a DCM phenotype (Figure 9). Our findings fit very well with results obtained by other groups [200, 201] and are, moreover, comparable with the cardiac phenotype seen in low-dose isoprenaline-induced heart failure [202]. Hence, the generated anti-β_1-EC_{II}-abs may be regarded as mild β_1-AR-agonists, which initiate and – over time – worsen the vicious circle of sympathetic overdrive and progressive HF. The homology of the human and rat β_1-AR and the fact that the antibodies induced in our model were equally able to recognize native human β_1-ARs [131] makes this animal model well suited to gain more insight into the (patho-) physiological processes induced by such agonist-like anti-β_1-EC_{II}-abs depending on the organ/organ system regarded.

It is known that the kidneys express high levels of β_1-ARs in certain segments of the nephron known to be involved in the regulation of renal function. The specific localization of these receptors tempts to speculate that the stimulating anti-β_1-EC_{II}-abs generated in our animals might also have an effect on renin secretion, salt excretion, GFR, and urinary pH regulation [35]. Besides these direct effects, it can be imagined that other functional parameters may be altered indirectly by stimulating anti-β_1-AR antibodies, at least through effects on the cardiovascular system in general.

4.2 Effects of anti-β_1-EC_{II}-abs on renin secretion and activity

The protease renin is the key enzyme of the renin-angiotensin system and is critically involved in volume, salt, and blood pressure regulation of the body. The release of renin can be modulated by a variety of intrarenal and extrarenal factors [203]. Catecholamines and other renin-stimulating hormones induce renin release from renal JG cells *via* GPCRs, Gs_α mediated activation of adenylyl cyclases, and an increase in intracellular cAMP [204]. As functional antibodies targeting the β_1-AR mediate their effects *via* this pathway, it is tempting to speculate that they also affect renin secretion and activity to some extent. Our data show that anti-β_1-EC_{II}-abs induce the expression of renin within the first six months of immunization (Figure 24). More importantly, they contribute to an increased renin secretion at a very initial stage, which in the kidney is rapidly counter-regulated, however (Figure 23).

Besides a direct β_1-AR-mediated effect on renin secretion, alterations in blood sodium concentration would be able to cause the observed effect on renin, as its secretion is under tight control of NaCl-sensing by macula densa cells. $Beta_1$-ARs located in the proximal and distal tubules are supposed to affect sodium reabsorption and excretion [58]. However, measurement of sodium levels in blood and 24 h urine samples showed no significant differences in the initial stages, indicating that the observed increase in plasma renin activity does not rely on an increase in renal sodium. Thus, from our data it seems conceivable that the generated anti-β_1-EC_{II}-abs are able to stimulate renin secretion directly *via* the receptors located in the renin-producing cells of the juxtaglomerular apparatus. Due to the tight regulatory networks of the kidney it is not surprising that this effect is immediately counter-regulated to reconstitute normal kidney function. Although the stimulation of renin was not sustained in the long run, we cannot exclude that it might have contributed to the development of the initial hypertensive phenotype. The fact

that antibody-induced renin secretion is detected already very early after starting immunization with only a small amount of functional anti-β_1-EC_{II}-abs present in the circulation indicates that the total amount of circulating anti–β_1-EC_{II}-abs appears to be less important than the individual stimulating potential of each receptor-antibody. Our results from experiments in isolated perfused kidneys support this concept: with a final experimental antibody-concentration of only 1/33rd of the original serum concentration, a considerable effect on renin secretion was obtained (Figure 25).

4.3 Anti-β_1-EC_{II}-ab-effects on electrolyte reabsorption

Balanced salt concentrations in the bloodstream are crucial for the maintenance of fluid equilibrium of the body, ensuring proper functionality of heart, nerves, muscles, etc. The lead organ for electrolyte homeostasis and – subsequently – water balance is the kidney. The regulation of renal electrolyte excretion/reabsorption, however, is rather complex and involves a vast number of regulatory mechanisms.

Sodium reabsorption takes place along the entire nephron, with 60 – 75% being reabsorbed in the proximal tubules, 25% in the thick ascending limb of the loop of Henle, and the rest in the distal tubules and the collecting duct. The elimination of sodium by the kidneys is mainly a function of glomerular filtration, Ang II and subsequent aldosterone release [205, 206], and the concentration of the natriuretic hormone [207]. The main regulator of sodium reabsorption is aldosterone. It mediates its effects through the cells of the distal tubules and the cortical collecting duct. Even though these sites only account for approximately 2% of sodium reabsorption, they represent the key site for the regulation of the Na^+ balance. The secretion of aldosterone from the *zona glomerulosa* of the renal cortex is stimulated by Ang II, with renin being the limiting step of Ang II-generation. In our study, increased renin levels were detected one month after the start of immunization (Figure 24). However, at the same time, blood and urine concentrations of sodium did not differ between immunized anti-β_1-EC_{II}-abs positive rats and corresponding 0.9% NaCl-injected control animals (Figures 15 and 16), indicating that the reabsorption of sodium was either not affected by the circulating antibodies (neither directly nor indirectly *via* aldosterone, Ang II, or ANP), or that the antibody-mediated stimulatory effects have been abolished immediately by counter-regulatory mechanisms. The differences in serum sodium concentrations in the course of the experiment (3 and 9 months after immunization)

remained within a physiological range [208, 209], making a pathophysiological significance of the anti-β_1-EC_{II}-abs unlikely.

Potassium channels are key members of the transport systems integrated in renal epithelial cells. They participate in the generation of the cell membrane potential, the regulation of the cell volume, K^+-recycling (which is essential for maintaining the function of transport proteins), and potassium secretion in the distal nephron. One of the most important potassium channels controlling K^+-secretion, the renal outer medullary potassium channel (ROMK), is activated – among others – by PKA [210] and aldosterone [211, 212], resulting in increased excretion of potassium. Because of this paramount importance, a variety of mechanisms have evolved to preserve the extracellular concentration of potassium within a normal range [213]. In our rat model, serum potassium concentration was strongly increased 3 months after the start of immunization in anti-β_1-EC_{II}-ab-positive animals compared to their controls, and decreased after 9 months of immunization (Figure 19). These changes were not reflected in the urine samples (Figure 20), indicating that the changes in blood potassium were due to changes in (internal) cellular uptake rather than to alterations in potassium excretion. It is known that catecholamines affect potassium uptake by activating PKA, which in turn induces phosphorylation of FXYD1 (phospholemman) [214]. FXYD1, in its dephosphorylated form, binds to the Na^+/K^+-ATPase and modulates its activity. Phosphorylation disrupts this interaction resulting in an increase in the affinity of the Na^+/K^+-ATPase for intracellular Na^+. The enhanced export of intracellular sodium increases the negative voltage in the cells and causes a translocation of K^+ into the cells. This mechanism might have contributed to the low serum potassium levels observed in immunized animals at 9 months. However, the significant increase in serum potassium 3 months after start of immunization in our model cannot be explained by changes in cellular uptake. Even though this increase was not accompanied by a respective decrease in urinary potassium, it might still be caused by a stimulation of K^+-reabsorption: type-A intercalated cells – also expressing high levels of β_1-ARs [35] – are mainly responsible for the secretion of hydrogen ions, but are also responsible for K^+-reabsorption. To do so, they express two isoforms of the K^+/H^+-ATPase. Their activation is modulated by several factors including catecholamines [215, 216]. Thus, agonistic anti-β_1-EC_{II}-abs might indeed have contributed to an increase in K^+-reabsorption in the initial phase.

Furthermore, the kidneys play a crucial role in the maintenance of the calcium balance by regulating Ca^{2+}-excretion. The β_1-adrenergic system is directly involved in the regulation of Ca^{2+}-

reabsorption/excretion in the kidney [179]. Thus, a possible inter-relationship with the reabsorption of sodium cannot be ruled out in our study. However, as shown in Figures 17 and 18, there were no changes in the amount of calcium in sequentially collected serum and urine samples; all measurements gave values within standard physiological ranges [209, 217], precluding a relevance for anti-β_1-EC_{II}-abs for Ca^{2+}-homeostasis.

4.4 Anti-β_1-EC_{II}-ab-effects on water-intake, urine production, and pH

Renin stimulates the sensation of thirst through the generation of Ang II, thereby augmenting water intake [218, 219]. This might lead to an – albeit rather small – increase in blood pressure [220]. However, the ab-positive rats in our study did not show any changes in water consumption (Figure 12). This can be explained by the fact that the stimulation of drinking in response to sympathetic activation probably depends on an activation of β_2-ARs rather than β_1-ARs [221]. The generally higher water-intake in the first months of the study can be explained by the higher demand of water in developing animals, rather than by the presence of stimulating anti-β_1-EC_{II}-abs because the water-intake was similar in 0.9% NaCl-injected control rats.

In addition, the 24 h urine excretion rates did not differ significantly between immunized rats and the corresponding controls (Figure 13). It should be mentioned, however, that the excreted urine volumes were subject to considerable fluctuations, precluding any meaningful conclusions.

Extracellular pH and systemic acid-base balance are critical for normal organ and cellular function. The renal collecting system serves to fine-tune renal acid-base balance. Type A-intercalated cells (or α-intercalated cells) secrete acid by an apically expressed H^+-ATPase proton pump and a basolaterally expressed Cl^--HCO_3^- exchanger. Type B intercalated cells (or β-intercalated cells) secrete HCO_3^-, mediated by an apically expressed Cl^--HCO_3^- exchanger and a basolaterally expressed vacuolar H^+-ATPase, also called V-ATPase. The almost exclusive expression of the β_1-AR subtype in type A intercalated cells [35] as well as the findings that β_1-adrenergic stimulation increases acid excretion [176, 178] made an assessment of this parameter of interest for the immunized-rat-model. However, as shown in Figure 14, the pH value in 24 h urine samples did not differ significantly between anti-β_1-EC_{II}-abs-positive rats and corresponding controls throughout the course of the study. This indicates, that the stimulation of

β_1-ARs by circulating anti-β_1-EC_{II}-abs does not affect acid-base status, or – as the antibodies act as mild agonists [131] – their stimulatory effect seems not strong enough to influence the pH of the urine.

4.5 Anti-β_1-EC_{II}-ab-effects on renal filtration

GFR is generally accepted to be the most suited parameter for the assessment of kidney function. A reduction in GFR is generally detectable before the onset of clinical symptoms of renal failure, and even a moderate impairment of renal function has been shown to strongly predict mortality and outcome in cardiovascular diseases [222, 223]. To determine GFR as well as RBF we sequentially assessed renal inulin- and PAH-clearances in both, immunized ab-positive animals and their corresponding controls. Within the first month after successful immunization, both, PAH and inulin clearance, were markedly reduced in anti-β_1-EC_{II}-ab-positive rats (Figures 26 and 27). On the one hand, the observed reduced RBF might have contributed to the reduced filtration-rate. This is, because reduced clearance of inulin and PAH as a measure for GFR and RBF can be caused both, by impaired renal perfusion (e.g. by activation of β_1-ARs located in the afferent arteriole leading to vasoconstriction, and by diminished proximal tubular secretion of these marker-substances, or by a combination thereof. On the other hand, contraction of glomerular mesangial cells, which are also richly endowed with β_1-ARs, might have reduced the area available for filtration, thus lowering GFR [61].

In order to assess the effects of altered glomerular filtration by using the PAH clearances, we determined the PAH net secretion (PNS). In our study, PNS was slightly diminished during the first months after immunization (Figure 28); the values recovered to those of the control rats from month 3 on (as it was the case for the inulin and PAH clearances). 15 months after immunization, the PNS of anti-β_1-EC_{II}-ab-positive animals significantly decreased compared to controls. Hence, we assume that in our model, reduced proximal tubular PAH-secretion rather than reduced renal perfusion accounts for the decreased PAH-clearance in anti-β_1-EC_{II}-ab-positive rats.

Proteinuria is strongly associated with progression of kidney disease [224] and has proven to represent an independent risk factor for all-cause and cardiovascular mortality in the general population [225]. The origin of proteinuria can be glomerular (e.g., resulting from an impairment of the glomerular filtration apparatus), tubular (e.g., resulting from a diminished tubular resorption of low-molecular-weight proteins), or due to “overflow” in case the resorptive capacity

is saturated by large amounts of filtered proteins [226, 227]. With albumin being the main protein in the blood, microalbuminuria – by definition 30 to 300 mg/d urinary albumin in humans – represents another very common and suited marker to predict progressive cardiovascular and renal disease in the general population. Damage of the glomerular filtration barrier or failure of proximal tubular reabsorption accounts for most cases of pathological albuminuria [228]. By sequential measurement of both total protein as well as albumin concentrations in 24 h urine samples, in immunized anti-β_1-EC_{II}-ab-positive rats, we were able to detect an alteration of glomerular filtration from immunization-month 12 on, the time-point from which on the animals developed cardiac dysfunction (Figures 21 and 22). This filtration deficiency remained rather mild throughout the experiment, and in the last months of the experiment most likely relied on the progressive cardiac dysfunction observed in immunized rats.

Taken together, it seems that despite chronic stimulation of renal β_1-AR by stimulating anti-β_1-EC_{II}-abs the impact on the kidney is rather weak compared to the development of progressive cardiac dysfunction, which starts about 9 months after regular immunization,.

4.6 Structural renal changes induced by anti-β_1-EC_{II}-abs

Activation of the RAAS is generally associated with an increase in extracellular matrix proteins and inflammatory markers. By binding to the AT_1-receptor (irrespective of its localization), Ang II has been shown to promote e.g. proliferation, inflammation, and fibrosis, thereby contributing to the development of a number of chronic diseases like hypertension, cardiac hypertrophy, and renal failure [229]. Fibrosis is a typical feature of chronic inflammation, which is (a) defined as an immune response that persists for several months, and (b) as a process, in which inflammation, tissue remodeling, and tissue repair occur simultaneously. Tissue fibrosis and organ dysfunction may occur during the inflammatory response in case there is an instantaneous over-production and deposition of collagen. Regardless of the underlying etiology, most forms of (chronic) kidney disease and most chronic cardiac pathologies are characterized by progressive fibrosis. One common feature of all fibrotic processes (independent of the affected organ) is the induction of TGF-β_1 [230-233]. TGF-β_1 is upregulated by Ang II in both the heart [234, 235] and the kidney [236]. The expression of TGF-β_1, Activin, and of Smad3/Smad4 (the corresponding second messengers), and also of collagen type 1 and type 3 was significantly upregulated in immunized ab-positive rats (Figure 29), indicating an activation of pro-fibrotic

pathways by stimulating anti-β_1-EC_{II}-abs. However, direct histomorphological analysis of renal tissues did not reveal significant excess collagen deposition (Figures 30 and 31). However, detailed examination of the kidney tissues for glomerulosclerosis (Figure 32), glomerular atrophy (Figure 33), tubulointerstitial fibrosis, and tubular atrophy (Figure 34), revealed markedly (but not significantly) increased levels of damage in the immunized animals compared to the 0.9% NaCl-injected controls during the last months of the experiment (15 and 18 months after induction of anti-β_1-EC_{II}-abs). Several renal and cardiac disorders, like membranous nephropathy [237], IgA nephropathy [238], or hypertension [239] are associated with severe (focal) histomorphological changes including development of renal fibrosis. In particular, hypertension is a common cause of renal disease; chronic exposure of the kidney to elevated blood pressure-levels leads to morphological changes that start in the juxtamedullary cortex (where the pressure gradient along the afferent arterioles is greatest, eventually causing arteriolar hypertrophy), followed by segmental glomerulosclerosis, and then tubular atrophy and interstitial fibrosis [240]. As the development of glomerulosclerosis, glomerular atrophy, tubulointerstitial fibrosis, and tubular atrophy in anti-β_1-EC_{II}-ab-positive rats is noted only after 15 months, when the hypertensive phenotype has already evolved into the DCM-phenotype, hypertension does not seem to account for the observed structural changes. It is, therefore, possible that these late effects are indeed anti-β_1-EC_{II}-ab-mediated. Regarding cardiac fibrosis, in our animal model we were able to show that the anti-β_1-EC_{II}-ab-positive rats developed significant amounts of perivascular fibrosis, especially around small vessels (arterioles), whereas the amount of total collagen did not differ significantly between immunized and 0.9% NaCl-injected control rats. A possible explanation for the exclusive occurrence of perivascular fibrosis around small vessels in the hearts of anti-β_1-EC_{II}-ab-positive rats may be the spatial proximity of these areas to the circulating abs. Generally, perivascular deposition of collagen might represent a response to direct or indirect hormonal, hemodynamic, and/or inflammatory stress or injury [199], induced by stimulating anti-β_1-EC_{II}-abs. Thus, such effects are expected to take place in the kidney as well. However, from a clinical point of view, perivascular fibrosis appears less relevant for kidney function. In agreement with this hypothesis, the kidneys from immunized anti-β_1-EC_{II}-ab-positive rats only showed a trend for an increase in collagen deposits around renal vessels compared to the corresponding control animals (Figure 35), which, however, (and in contrast to cardiac micro-vessels) did not reach statistical significance.

Taken together, there is an undeniable tendency towards the development of renal fibrosis in immunized the anti-β_1-EC_{II}-ab-positive animals. However, these alterations are relatively weak compared to the damage seen in other (human) pathologies. The mild stimulating effect of anti-β_1-EC_{II}-abs together with the rather slow progress of renal damage might not be sufficient to induce severe fibrosis in our model. It is furthermore possible that – even in the advancing states of autoimmune HF – the kidneys represent only a secondary target for stimulating anti-β_1-EC_{II}-abs.

4.7 Effects of anti-β_1-EC_{II}-abs on cardio-renal phenotypes

Another aspect of the present work was to analyze the potential contribution of renal anti-β_1-EC_{II}-ab-effects to the ab-induced cardiac phenotype. One question was, whether stimulation of renal β_1-ARs by anti-β_1-EC_{II}-abs might have triggered the development of the initial hypertensive phenotype seen within the first six months of the study.

The paramount role of the kidney in the regulation of blood pressure has been recognized since a long time [241]. The main renal effector of "blood pressure control" is the RAAS. Along with its importance in maintaining normal circulatory conditions, any abnormal activation of the RAAS may result in the development of hypertension. Being an important blood pressure control system on its own, the RAAS also interacts extensively with other blood pressure control mechanisms, including the sympathetic nervous system (SNS) and the baroreceptor reflexes. The clinical relevance of the SNS for the pathophysiology and treatment of hypertension can be derived from the current attempts to perform renal sympathetic denervation in patients with treatment-resistent hypertension [242].

Several groups have established that Ang II, the major bioactive product of the RAAS, causes hypertension [243, 244]. In addition, some animal experiments (mostly performed in the rat) have shown, that sustained hypertension may even develop several weeks to months after short-term Ang II administration [245, 246]. Thus, it is tempting to speculate, that – similarly – the increase in renin activity observed in our anti-β_1-EC_{II}-ab-positive rats (Figure 23) and the subsequent increase in Ang II-levels has indeed contributed to the initial hypertensive phenotype in our model (Figure 9). The fact that renin activity in our immunized rats decreased within the first 3 months of continued immunization is in line with clinical findings (hypertensive patients). Ang II contributes to the regulation of renin and controls its own synthesis *via* the so-called short-loop

feedback mechanism by activating AT_1-receptors expressed at the JGA, serving to suppress further renin release [247, 248]. The elevated renin levels seen within the first 3 months of the experiment (Figure 23) underscore the initial directly anti-β_1-EC_{II}-ab-mediated activation of the RAAS in successfully immunized rats.

Another factor contributing to the initial hypertensive phenotype might be the initial decrease in GFR and RBF in immunized anti-β_1-EC_{II}-ab-positive rats (Figures 26 and 27). The decrease in GFR (observed during the first few months after immunization) activates stretch receptors located in the macula densa, which in turn stimulate renin secretion (Figure 23). Activation of the RAAS induces peripheral vasoconstriction (mainly through small arterioles), thereby increasing peripheral vascular resistance and, subsequently, systemic blood pressure.

4.8 Clinical relevance

The aim of this study was to analyze the potential (patho-)physiological relevance of stimulating antibodies targeting the β_1-AR for renal function. As the renal actions of functionally active anti-β_1-abs have been almost completely neglected so far, our experiments represent a first attempt to address this issue and serves to analyze in depth how renal effects of anti-β_1-EC_{II}-abs may contribute to – that is, enhance or diminish their effects on – cardiac function. Even though the chronic effects of stimulating anti-β_1-EC_{II}-abs on the myocardium may be detrimental, here we show that such antibodies have no major effect on kidney structure and function. Although our results were obtained in a rat model, they might be useful to better understand the situation in anti-β_1-EC_{II}-aab-positive human patients. Having the results of our rat experiments in mind, future therapeutic strategies in autoimmune DCM should focus on the direct and – as specific as possible – neutralization/elimination of stimulating anti-β_1-AR-aabs or at least comprise strategies that counteract their effects on the heart by standard treatment of heart failure according to current guidelines [88, 89]. For the direct neutralization of anti-β_1-EC_{II}-aabs, application of cyclic peptides mimicking the β_1-EC_{II} target epitope represents a novel promising approach. Such peptides are supposed to not just abolish the cardiac, but probably also the renal effects of stimulating anti-β_1-EC_{II}-aabs.

5 Summary

Functionally active (conformational) autoantibodies directed against the β_1-adrenergic receptor (β_1-AR) are supposed to have a pathogenic relevance in human heart failure, particularly in idiopathic dilated cardiomyopathy (DCM). Prevalence of anti-β_1-autoantibodies (anti-β_1-aabs) in the healthy population is almost negligible, whereas it amounts to up to 30% in heart failure patients with idiopathic DCM. As β_1-ARs are not restricted to the heart and are also highly expressed in particular segments of the nephron, it is conceivable that such autoantibodies might also affect kidney function to some extent through the activation of renal β_1-ARs.

In the kidney, β_1-ARs are highly abundant in the juxtaglomerular apparatus, the distal convoluted tubules, the collecting duct, and the renal arteries. However, the functional significance of β_1-ARs at these particular sites along the nephron is poorly understood, as are the effects of conformational stimulating anti-β_1-aabs on renal β_1-ARs. From the available literature, it is well known that the β_1-adrenergic system is involved in, e.g., the regulation of renin-secretion from juxtaglomerular cells. In addition, the β_1-adrenergic system is thought to be involved in the regulation of the urine pH *via* type B-intercalated cells in the collecting duct. In contrast, the regulation of salt- and fluid-secretion in the medullary collecting duct appears to occur independently from the SNS.

As a consequence, the present work aimed to unravel the potential pathophysiological links between renal function, alterations in the cardiovascular system, and circulating agonist-like anti-β_1-abs. We analyzed possible renal effects of anti-β_1-abs in a human-analogous rat model. After immunization with a GST-fusion protein containing the second extracellular loop (β_1-EC_{II}) of the human β_1-AR, Lewis-rats develop functionally active, stimulating, conformational anti-β_1-EC_{II}-abs. Within the first 6 months, anti-β_1-EC_{II}-ab-positive animals develop a hypertensive phenotype, which after 9 months evolves into a DCM phenotype.

In n=40 GST/ β_1-EC_{II}-immunized Lewis rats and n=40 age-matched, 0.9% NaCl-injected control animals, we sequentially (i.e. at months 1, 2, 3, 6, 9, 12, 15, and 18 after start of immunization) analyzed the changes in renal function on a molecular, functional, and structural level. We could show that the presence of stimulating anti-β_1-EC_{II}-abs – even though having detrimental effects on the heart – has only a minor impact on kidney function and structure. Within the first 3 months after induction of anti-β_1-EC_{II}-abs, the levels and activity of renin were

significantly increased in immunized compared to corresponding control animals, which was confirmed by experiments on isolated perfused kidneys, in which anti-β_1-EC_{II}-abs were able to directly induce the liberation of renin. However, within several weeks the initial anti-β_1-EC_{II}-ab-mediated RAAS activation was counter-regulated by auto-regulatory mechanisms activated in the kidney. Similarly, glomerular filtration rate (GFR) and renal blood flow (RBF) were initially decreased in the presence of the stimulating anti-β_1-EC_{II}-abs, but returned to control values within 3 months after immunization of the animals. Although expression of several pro-fibrotic markers was significantly up-regulated in anti-β_1-EC_{II}-ab-positive rats, no significant differences were noted on a histomorphological level with regard to the occurrence of renal fibrosis, glomerular damage, tubular damage, and perivascular fibrosis. Only a mild decrease in glomerular filtration function was observed in the kidneys of anti-β_1-EC_{II}-ab-positive animals from immunization-month 12 on, apparent by increased levels of urinary protein.

Even though anti-β_1-EC_{II}-abs were able to induce mild changes in renal function, their effects were not strong enough to critically damage the kidneys in our rat-model. Differences between immunized anti-β_1-EC_{II}-ab-positive and corresponding control rats at later time-points (that is, from immunization-month 12 on) are most likely secondary to the progressive heart failure phenotype that immunized animals develop in the course of the experiment.

The present study is the first to focus on the effects of stimulating anti-β_1-EC_{II}-abs on the kidney, and on the prevalence of these effects for the heart (referred to as cardio-renal crosstalk). Although our results were obtained in a rat model, they might contribute to better understand the situation in anti-β_1-AR-aab-positive human patients. Following the results of our experiments, treatment of such patients should focus on direct and specific neutralization/elimination of stimulating anti-β_1-EC_{II}-aab or at least comprise therapeutic strategies that counteract the anti-β_1-EC_{II}-aab-effects on the heart by standard treatment for heart failure (i.e. ACE inhibitors, AT_1-receptor blockers, and β-blockers) according to current guidelines.

6 Zusammenfassung

Funktionell aktive, konformationelle Autoantikörper, die gegen den β_1-adrenergen Rezeptor (β_1-AR) gerichtet sind, sind vermutlich pathologisch relevant bei Herzinsuffizienz, insbesondere bei der idiopathischen Dilativen Kardiomyopathie (DCM). Die Prävalenz solcher Antikörper ist in der gesunden Population vernachlässigbar, wohingegen sie bei der idiopathischen DCM 30% erreicht. Da β_1-AR nicht nur im Herzen, sondern auch in der Niere stark exprimiert werden, ist naheliegend, dass solche Antikörper über eine Stimulation renaler β_1-AR auch die Nierenfunktion beeinflussen können.

In der Niere werden β_1-AR überwiegend im juxtaglomerulären Apparat, im distalen Tubulus, in den Sammelrohren und in den renalen Arterien exprimiert. Die Bedeutung der in diesen Bereichen hohen Expression von β_1-AR für die Nierenfunktion ist noch nicht vollständig geklärt, ebenso wie die renalen Effekte von stimulierenden β_1-AR-Antikörpern. Aus der Literatur ist bekannt, dass das β_1-adrenerge System unter anderem an der Renin-Sekretion der juxtaglomerulären Zellen beteiligt ist. Außerdem wird vermutet, dass das β_1-adrenerge System in die Regulation des pH-Wertes des Urins über die Typ B-interkalierenden Zellen des Sammelrohrs eingreift, wohingegen die Regulation der Salz- und Wasserexkretion im medullären Sammelrohr wahrscheinlich unabhängig vom sympathischen Nervensystem abläuft.

Die vorliegende Arbeit zielt darauf ab, die potentiellen pathophysiologischen Zusammenhänge zwischen renaler Funktion, Änderungen innerhalb des kardiovaskulären Systems und zirkulierenden, agonist-ähnlichen anti-β_1-Autoantikörpern darzustellen. Wir haben die möglichen renalen Effekte der anti-β_1-AK in einem human-ähnlichen Ratten-Modell untersucht. Nach Immunisierung mit einem GST-Fusionsprotein, welches den zweiten extrazellulären Loop des β_1-AR beinhaltet, entwickeln Lewis-Ratten funktionell aktive, stimulierende Antikörper gegen β_1-EC_{II}. Anti-β_1-EC_{II}-AK-positive Tiere entwickeln nach ca. 6 Monaten einen hypertensiven Phänotyp, welcher nach 9 Monaten in einen DCM Phänotyp übergeht.

Wir haben Änderungen der renalen Funktion auf molekularer, funktioneller, und struktureller Ebene in n=40 GST/ β_1-EC_{II}-immunisierten Lewis-Ratten und n=40 altersgleichen 0.9% NaCl-injizierten Kontrolltieren sequenziell (d.h. 1, 2, 3, 6, 9, 12, 15 und 18 Monate nach Beginn der Immunisierung) analysiert. Wir konnten zeigen, dass die stimulierenden anti-β_1-EC_{II}-Antikörper – obwohl sie eine schädigende Wirkung auf das Herz haben – die Nierenfunktion und -struktur

nur gering beeinflussen. In den ersten Monaten nach Induktion der anti-β_1-EC_{II}-AK stieg die Reninkonzentration und -aktivität in den immunisierten Tieren im Vergleich zu den entsprechenden Kontrollen signifikant an. Dieses Ergebnis konnte im Model der isolierten perfundierten Niere bestätigen werden, in dem anti-β_1-EC_{II}-AK eine direkte Freisetzung von Renin induzierten. Diese frühe AK-vermittelte Aktivierung des RAAS wurde jedoch innerhalb weniger Wochen durch autoregulatorische Mechanismen der Niere aufgehoben. Ebenso waren anfangs die glomeruläre Filtrationsrate und der renale Blutfluss in anti-β_1-EC_{II}-AK-positiven Ratten vermindert, kehrten jedoch nach 3 Monaten zu den Werten der Kontrolltiere zurück. Obwohl die Expression mehrerer pro-fibrotischer Marker signifikant erhöht war, konnten keine signifikanten Veränderungen auf histomorphologischer Ebene hinsichtlich des Auftretens renaler Fibrose, glomerulärer und tubulärer Schädigung, oder perivaskulärer Fibrose festgestellt werden. Lediglich die glomeruläre Filtrationsfunktion war ab dem 12. Immunisierungsmonat zunehmend beeinträchtigt, was sich an einer progredienten Proteinurie zeigte.

Obwohl anti-β_1-EC_{II}-AK durchaus einen gewissen Effekt auf die Nierenfunktion haben, ist ihr Einfluss nicht stark genug um die Niere kritisch zu schädigen. Unterschiede zwischen immunisierten und Kontrolltieren, welche zu späteren Zeitpunkten (d.h. ab dem 12. Immunisierungsmonat) auftreten, sind wahrscheinlich sekundäre Effekte der progredienten Herzinsuffizienz, die die immunisierten Tiere im Verlauf des Experiments entwickeln.

Unsere Studie ist die Erste, die sich mit den Effekten von stimulierenden anti-β_1-AK auf die Niere und ihre Zusammenhänge mit der antikörper-induzierten Herzinsuffizienz (dem sogenannten kardio-renalen „Crosstalk“) befasst. Obwohl unsere Ergebnisse in einem Tiermodell erzielt wurden, könnten sie von großem Nutzen sein, um die Krankheitsentwicklung von anti-β_1-Autoantikörper-positiven Patienten besser zu verstehen. Unseren Ergebnissen zufolge sollte die Behandlung von Autoimmun-DCM auf eine möglichst direkte und spezifische Neutralisierung/Eliminierung von anti-β_1-Autoantikörpern abzielen und gleichzeitig alle kardio- und renal-protektiven Elemente der Standard-Therapie der Herzinsuffizienz (d.h. Gabe von ACE-Hemmern, AT_1-Rezeptor-Inhibitoren und β-Blockern) einschließen.

7 References

1. Störk, S., et al., *Stimulating autoantibodies directed against the cardiac beta1-adrenergic receptor predict increased mortality in idiopathic cardiomyopathy.* Am. Heart J., 2006. **152**: p. 697-704.
2. Ninomiya, T., et al., *Impact of kidney disease and blood pressure on the development of cardiovascular disease: an overview from the Japan Arteriosclerosis Longitudinal Study.* Circulation, 2008. **118**(25): p. 2694-701.
3. Cannon, W.B., *Bodily Changes in Pain, Hunger, Fear and Rage: An Account on Recent Researches into the Function of Emotional Excitement*. 1915, New York: D. Appleton And Company.
4. Zimmer, C., *Soul Made Flesh.* . 2004, London: The Random House (Arrow Books).
5. College, O., *Anatomy & Physiology*. June 19, 2013, OpenStax College: http://cnx.org/content/col11496/1.6/.
6. Chrousos, G.P. and P.W. Gold, *The concepts of stress and stress system disorders. Overview of physical and behavioral homeostasis.* JAMA, 1992. **267**(9): p. 1244-52.
7. Tyndall, J.D. and R. Sandilya, *GPCR agonists and antagonists in the clinic.* Med Chem, 2005. **1**(4): p. 405-21.
8. Overington, J.P., B. Al-Lazikani, and A.L. Hopkins, *How many drug targets are there?* Nat Rev Drug Discov, 2006. **5**(12): p. 993-6.
9. Lagerstrom, M.C. and H.B. Schioth, *Structural diversity of G protein-coupled receptors and significance for drug discovery.* Nat Rev Drug Discov, 2008. **7**(4): p. 339-57.
10. *"The Nobel Prize in Chemistry 2012 - Press Release"* 2013.
11. Worth, C.L., G. Kleinau, and G. Krause, *Comparative sequence and structural analyses of G-protein-coupled receptor crystal structures and implications for molecular models.* PLoS One, 2009. **4**(9): p. e7011.
12. Jahns, R., V. Boivin, and M.J. Lohse, *Beta 1-adrenergic receptor-directed autoimmunity as a cause of dilated cardiomyopathy in rats.* Int J Cardiol, 2006. **112**(1): p. 7-14.
13. Jacoby, E., et al., *The 7 TM G-protein-coupled receptor target family.* ChemMedChem, 2006. **1**(8): p. 761-82.
14. Pierce, K.L., R.T. Premont, and R.J. Lefkowitz, *Seven-transmembrane receptors.* Nat Rev Mol Cell Biol, 2002. **3**(9): p. 639-50.
15. Vauquelin, G. and I. Van Liefde, *G protein-coupled receptors: a count of 1001 conformations.* Fundam Clin Pharmacol, 2005. **19**(1): p. 45-56.
16. Kobilka, B.K. and X. Deupi, *Conformational complexity of G-protein-coupled receptors.* Trends Pharmacol Sci, 2007. **28**(8): p. 397-406.
17. Vilardaga, J.P., et al., *GPCR and G proteins: drug efficacy and activation in live cells.* Mol Endocrinol, 2009. **23**(5): p. 590-9.
18. Hamm, H.E., *The many faces of G protein signaling.* J. Biol. Chem., 1998. **273**: p. 669-672.
19. Clapham, D.E. and E.J. Neer, *New roles for G-protein βγ-dimers in transmembrane signaling.* Nature, 1993. **365**(6445): p. 403-406.
20. Chisari, M., et al., *G protein subunit dissociation and translocation regulate cellular response to receptor stimulation.* PLoS One, 2009. **4**(11): p. e7797.

21. Spiegel, A.M., *Signal transduction by guanine nucleotide binding proteins.* Mol Cell Endocrinol, 1987. **49**(1): p. 1-16.
22. Krupnick, J.G. and J.L. Benovic, *The role of receptor kinases and arrestins in G protein-coupled receptor regulation.* Annu Rev Pharmacol Toxicol, 1998. **38**: p. 289-319.
23. Lefkowitz, R.J. and S.K. Shenoy, *Transduction of receptor signals by beta-arrestins.* Science, 2005. **308**(5721): p. 512-7.
24. Liggett, S.B., *Phosphorylation barcoding as a mechanism of directing GPCR signaling.* Sci Signal, 2011. **4**(185): p. pe36.
25. Gurevich, V.V. and E.V. Gurevich, *The new face of active receptor bound arrestin attracts new partners.* Structure, 2003. **11**(9): p. 1037-42.
26. Lands, A., et al., *Differentiation of receptor systems by sympathomimetic amines.* Nature, 1967. **241**: p. 597-598.
27. Ahlquist, R.P., *Study of adrenotropic receptors.* Am.J.Physiol., 1948. **153**: p. 586-600.
28. Bylund, D.B., et al., *International Union of Pharmacology nomenclature of adrenoceptors.* Pharmacol Rev, 1994. **46**(2): p. 121-36.
29. Fain, J.N. and J.A. Garcia-Sainz, *Role of phosphatidylinositol turnover in alpha 1 and of adenylate cyclase inhibition in alpha 2 effects of catecholamines.* Life Sci, 1980. **26**(15): p. 1183-94.
30. Hein, L. and B.K. Kobilka, *Adrenergic receptor signal transduction and regulation.* Neuropharmacology, 1995. **34**(4): p. 357-66.
31. Lefkowitz, R.J., *Editorial: Selectivity in beta-adrenergic responses: clinical implications.* Circulation, 1974. **49**(5): p. 783-6.
32. Bristow, M.R., et al., *β_1- and β_2-adrenergic receptor subpopulations in nonfailing and failing human ventricular myocardium: coupling of both receptor subtypes to muscle contraction and selective β_1-receptor down-regulation in heart failure.* Circ. Res., 1986. **59**: p. 297-309.
33. Meister, B., et al., *Patterns of messenger RNA expression for adrenergic receptor subtypes in the rat kidney.* J. Pharmacol. Exp. Ther., 1994. **268**: p. 1605-1611.
34. Strader, C.D., et al., *Antibodies to the b-adrenergic receptor: Attenuation of catecholamine-sensitive adenylate cyclase and demonstration of post synaptic receptor localization in brain.* Proc. Natl. Acad. Sci. U.S.A., 1983. **80**: p. 1840-1844.
35. Boivin, V., et al., *Immunofluorescent imaging of beta1- and beta2-adrenergic receptors in rat kidney.* Kidney Int., 2001. **59**: p. 515-531.
36. Zhao, X.L., et al., *The alpha 1-subunit of skeletal muscle L-type Ca channels is the key target for regulation by A-kinase and protein phosphatase-1C.* Biochem Biophys Res Commun, 1994. **198**(1): p. 166-73.
37. Gerhardstein, B.L., et al., *Identification of the sites phosphorylated by cyclic AMP-dependent protein kinase on the beta 2 subunit of L-type voltage-dependent calcium channels.* Biochemistry, 1999. **38**(32): p. 10361-70.
38. Simmerman, H.K. and L.R. Jones, *Phospholamban: protein structure, mechanism of action, and role in cardiac function.* Physiol Rev, 1998. **78**(4): p. 921-47.
39. Sulakhe, P.V. and X.T. Vo, *Regulation of phospholamban and troponin-I phosphorylation in the intact rat cardiomyocytes by adrenergic and cholinergic stimuli: roles of cyclic nucleotides, calcium, protein kinases and phosphatases and depolarization.* Mol Cell Biochem, 1995. **149-150**: p. 103-26.
40. Jahns, R., et al., *Targeting receptor antibodies in immune cardiomyopathy.* Semin Thromb Hemost, 2010. **36**(2): p. 212-8.

41. Churchill, P.C., *Second messengers in renin secretion.* Am J Physiol, 1985. **249**(2 Pt 2): p. F175-84.
42. Rad, A., *The renin-angiotensin-aldosterone system*. 2006: Wikimedia Commons.
43. Coote, J.H., et al., *Effect of renal nerve stimulation, renal blood flow and adrenergic blockade on plasma renin activity in the cat.* J Physiol, 1972. **226**(1): p. 15-36.
44. Henrich, W.L. and W.B. Campbell, *The systemic beta-adrenergic pathway to renin secretion: relationships with the renal prostaglandin system.* Endocrinology, 1983. **113**(6): p. 2247-54.
45. Healy, D.P., P.A. Munzel, and P.A. Insel, *Localization of beta 1- and beta 2-adrenergic receptors in rat kidney by autoradiography.* Circ Res, 1985. **57**(2): p. 278-84.
46. Summers, R.J., J.A. Stephenson, and M.J. Kuhar, *Localization of beta adrenoceptor subtypes in rat kidney by light microscopic autoradiography.* J Pharmacol Exp Ther, 1985. **232**(2): p. 561-9.
47. Meister, B., et al., *Patterns of messenger RNA expression for adrenergic receptor subtypes in the rat kidney.* J Pharmacol Exp Ther, 1994. **268**(3): p. 1605-11.
48. Klar, J., et al., *Cyclic AMP stimulates renin gene transcription in juxtaglomerular cells.* Pflugers Arch, 2002. **444**(3): p. 335-44.
49. Chen, L., et al., *Regulation of renin in mice with Cre recombinase-mediated deletion of G protein Gsalpha in juxtaglomerular cells.* Am J Physiol Renal Physiol, 2007. **292**(1): p. F27-37.
50. Weinberger, M.H., W. Aoi, and D.P. Henry, *Direct effect of beta-adrenergic stimulation on renin release by the rat kidney slice in vitro.* Circ Res, 1975. **37**(3): p. 318-24.
51. Kim, S.M., et al., *Regulation of renin secretion and expression in mice deficient in beta1- and beta2-adrenergic receptors.* Hypertension, 2007. **50**(1): p. 103-9.
52. Hackenthal, E., et al., *Morphology, physiology, and molecular biology of renin secretion.* Physiol Rev, 1990. **70**(4): p. 1067-116.
53. Friis, U.G., et al., *Prostaglandin E2 EP2 and EP4 receptor activation mediates cAMP-dependent hyperpolarization and exocytosis of renin in juxtaglomerular cells.* Am J Physiol Renal Physiol, 2005. **289**(5): p. F989-97.
54. Kurtz, A., et al., *Rat juxtaglomerular cells are endowed with DA-1 dopamine receptors mediating renin release.* J Cardiovasc Pharmacol, 1988. **12**(6): p. 658-63.
55. Jensen, B.L., B.K. Kramer, and A. Kurtz, *Adrenomedullin stimulates renin release and renin mRNA in mouse juxtaglomerular granular cells.* Hypertension, 1997. **29**(5): p. 1148-55.
56. Schnermann, J.B.J., *Function of the juxtaglomerular apparatus: Control of glomerular hemodynamics and renin secretion.*, in *Seldin and Giebisch's The Kidney (Fourth Edition)*, A.H.S. Alpern, Editor. 2008, ,: Elsevier Academic Press. p. 589 - 626.
57. Bell, P.D., J.Y. Lapointe, and J. Peti-Peterdi, *Macula densa cell signaling.* Annu Rev Physiol, 2003. **65**: p. 481-500.
58. Bailly, C., et al., *Isoproterenol increases Ca, Mg, and NaCl reabsorption in mouse thick ascending limb.* Am J Physiol, 1990. **258**(5 Pt 2): p. F1224-31.
59. Besarab, A., et al., *Effect of catecholamines on tubular function in the isolated perfused rat kidney.* Am J Physiol, 1977. **233**(1): p. F39-45.
60. Schor, N., I. Ichikawa, and B.M. Brenner, *Mechanisms of action of various hormones and vasoactive substances on glomerular ultrafiltration in the rat.* Kidney Int, 1981. **20**(4): p. 442-51.
61. Pelayo, J.C., B.J. Tucker, and R.C. Blantz, *Effects of beta-adrenergic stimulation with isoproterenol on glomerular hemodynamics.* Am J Physiol, 1989. **257**(5 Pt 2): p. F866-73.

62. Alper, S.L., et al., *Subtypes of intercalated cells in rat kidney collecting duct defined by antibodies against erythroid band 3 and renal vacuolar H+-ATPase.* Proc Natl Acad Sci U S A, 1989. **86**(14): p. 5429-33.
63. Teng-umnuay, P., et al., *Identification of distinct subpopulations of intercalated cells in the mouse collecting duct.* J Am Soc Nephrol, 1996. **7**(2): p. 260-74.
64. Muto, S., et al., *Electrophysiological identification of alpha- and beta-intercalated cells and their distribution along the rabbit distal nephron segments.* J Clin Invest, 1990. **86**(6): p. 1829-39.
65. Schuster, V.L., *Bicarbonate reabsorption and secretion in the cortical and outer medullary collecting tubule.* Semin Nephrol, 1990. **10**(2): p. 139-47.
66. Maron, B.J., et al., *Contemporary definitions and classification of the cardiomyopathies: an American Heart Association Scientific Statement from the Council on Clinical Cardiology, Heart Failure and Transplantation Committee; Quality of Care and Outcomes Research and Functional Genomics and Translational Biology Interdisciplinary Working Groups; and Council on Epidemiology and Prevention.* Circulation, 2006. **113**(14): p. 1807-16.
67. Richardson, P., et al., *Report of the 1995 World Health Organization/International Society and Federation of Cardiology Task Force on the Definition and Classification of cardiomyopathies.* Circulation, 1996. **93**(5): p. 841-2.
68. *The Criteria Committee of the New York Heart Association. (1994). Nomenclature and Criteria for Diagnosis of Diseases of the Heart and Great Vessels.* 9th ed. 1994, Boston, Massachussetts: Little, Borwn & Co.
69. Schrier, R.W., *Cardiorenal versus renocardiac syndrome: is there a difference?* Nat Clin Pract Nephrol, 2007. **3**(12): p. 637.
70. Engelhardt, S., et al., *Analysis of beta-adrenergic receptor mRNA-levels in human ventricular biopsies by RT-PCR: progressive reduction of beta1-adrenergic receptor mRNA in heart failure.* J. Am. Coll. Cardiol., 1996. **27**: p. 146-154.
71. Brodde, O.E., *Beta-adrenoceptors in cardiac disease.* Pharmacol Ther, 1993. **60**(3): p. 405-30.
72. Böhm, M., et al., *Increase of Giα in human hearts with dilated but not ischemic cardiomyopathy.* Circulation, 1990. **82**(4): p. 1249-1265.
73. Eschenhagen, T., *G proteins and the heart.* Cell Biol Int, 1993. **17**(8): p. 723-49.
74. Allen, D.G. and J.C. Kentish, *The cellular basis of the length-tension relation in cardiac muscle.* J Mol Cell Cardiol, 1985. **17**(9): p. 821-40.
75. Hillege, H.L., et al., *Renal function, neurohormonal activation, and survival in patients with chronic heart failure.* Circulation, 2000. **102**(2): p. 203-10.
76. Damman, K., et al., *Decreased cardiac output, venous congestion and the association with renal impairment in patients with cardiac dysfunction.* Eur J Heart Fail, 2007. **9**(9): p. 872-8.
77. Packer, M., *Why do the kidneys release renin in patients with congestive heart failure? A nephrocentric view of converting-enzyme inhibition.* Eur Heart J, 1990. **11 Suppl D**: p. 44-52.
78. Curtiss, C., et al., *Role of the renin-angiotensin system in the systemic vasoconstriction of chronic congestive heart failure.* Circulation, 1978. **58**(5): p. 763-70.
79. Brilla, C.G., et al., *Collagen metabolism in cultured adult rat cardiac fibroblasts: response to angiotensin II and aldosterone.* J Mol Cell Cardiol, 1994. **26**(7): p. 809-20.
80. Lijnen, P. and V. Petrov, *Induction of cardiac fibrosis by aldosterone.* J Mol Cell Cardiol, 2000. **32**(6): p. 865-79.

81. Dries, D.L., et al., *Prognostic impact of diabetes mellitus in patients with heart failure according to the etiology of left ventricular systolic dysfunction.* J Am Coll Cardiol, 2001. **38**(2): p. 421-8.
82. McAlister, F.A., et al., *Renal insufficiency and heart failure: prognostic and therapeutic implications from a prospective cohort study.* Circulation, 2004. **109**(8): p. 1004-9.
83. Smilde, T.D., et al., *Prognostic importance of renal function in patients with early heart failure and mild left ventricular dysfunction.* Am J Cardiol, 2004. **94**(2): p. 240-3.
84. Herzog, C.A., et al., *Cardiovascular disease in chronic kidney disease. A clinical update from Kidney Disease: Improving Global Outcomes (KDIGO).* Kidney Int, 2011. **80**(6): p. 572-86.
85. Dries, D.L., et al., *The prognostic implications of renal insufficiency in asymptomatic and symptomatic patients with left ventricular systolic dysfunction.* J Am Coll Cardiol, 2000. **35**(3): p. 681-9.
86. Heywood, J.T., et al., *High prevalence of renal dysfunction and its impact on outcome in 118,465 patients hospitalized with acute decompensated heart failure: a report from the ADHERE database.* J Card Fail, 2007. **13**(6): p. 422-30.
87. Heywood, J.T., *The cardiorenal syndrome: lessons from the ADHERE database and treatment options.* Heart Fail Rev, 2004. **9**(3): p. 195-201.
88. McMurray, J.J., et al., *ESC Guidelines for the diagnosis and treatment of acute and chronic heart failure 2012: The Task Force for the Diagnosis and Treatment of Acute and Chronic Heart Failure 2012 of the European Society of Cardiology. Developed in collaboration with the Heart Failure Association (HFA) of the ESC.* Eur Heart J, 2012. **33**(14): p. 1787-847.
89. Yancy, C.W., et al., *2013 ACCF/AHA guideline for the management of heart failure: a report of the American College of Cardiology Foundation/American Heart Association Task Force on practice guidelines.* Circulation, 2013. **128**(16): p. e240-327.
90. *Effect of enalapril on survival in patients with reduced left ventricular ejection fractions and congestive heart failure. The SOLVD Investigators.* N Engl J Med, 1991. **325**(5): p. 293-302.
91. *Effects of enalapril on mortality in severe congestive heart failure. Results of the Cooperative North Scandinavian Enalapril Survival Study (CONSENSUS). The CONSENSUS Trial Study Group.* N Engl J Med, 1987. **316**(23): p. 1429-35.
92. Teerlink, J.R. and B.M. Massie, *The role of beta-blockers in preventing sudden death in heart failure.* J Card Fail, 2000. **6**(2 Suppl 1): p. 25-33.
93. Foody, J.M., M.H. Farrell, and H.M. Krumholz, *beta-Blocker therapy in heart failure: scientific review.* JAMA, 2002. **287**(7): p. 883-9.
94. Pitt, B., et al., *The effect of spironolactone on morbidity and mortality in patients with severe heart failure. Randomized Aldactone Evaluation Study Investigators.* N Engl J Med, 1999. **341**(10): p. 709-17.
95. Pitt, B., et al., *Eplerenone, a selective aldosterone blocker, in patients with left ventricular dysfunction after myocardial infarction.* N Engl J Med, 2003. **348**(14): p. 1309-21.
96. Ezekowitz, J.A. and F.A. McAlister, *Aldosterone blockade and left ventricular dysfunction: a systematic review of randomized clinical trials.* Eur Heart J, 2009. **30**(4): p. 469-77.
97. Cohn, J.N. and G. Tognoni, *A randomized trial of the angiotensin-receptor blocker valsartan in chronic heart failure.* N Engl J Med, 2001. **345**(23): p. 1667-75.

98. Pitt, B., et al., *Effect of losartan compared with captopril on mortality in patients with symptomatic heart failure: randomised trial--the Losartan Heart Failure Survival Study ELITE II.* Lancet, 2000. **355**(9215): p. 1582-7.
99. Jong, P., et al., *Angiotensin receptor blockers in heart failure: meta-analysis of randomized controlled trials.* J Am Coll Cardiol, 2002. **39**(3): p. 463-70.
100. Packer, M., et al., *Effect of oral milrinone on mortality in severe chronic heart failure. The PROMISE Study Research Group.* N Engl J Med, 1991. **325**(21): p. 1468-75.
101. Felker, G.M. and C.M. O'Connor, *Inotropic therapy for heart failure: an evidence-based approach.* Am Heart J, 2001. **142**(3): p. 393-401.
102. Bradley, D.J., et al., *Cardiac resynchronization and death from progressive heart failure: a meta-analysis of randomized controlled trials.* JAMA, 2003. **289**(6): p. 730-40.
103. Cleland, J.G., et al., *The effect of cardiac resynchronization on morbidity and mortality in heart failure.* N Engl J Med, 2005. **352**(15): p. 1539-49.
104. Connolly, S.J., et al., *Meta-analysis of the implantable cardioverter defibrillator secondary prevention trials. AVID, CASH and CIDS studies. Antiarrhythmics vs Implantable Defibrillator study. Cardiac Arrest Study Hamburg . Canadian Implantable Defibrillator Study.* Eur Heart J, 2000. **21**(24): p. 2071-8.
105. Kadish, A., et al., *Prophylactic defibrillator implantation in patients with nonischemic dilated cardiomyopathy.* N Engl J Med, 2004. **350**(21): p. 2151-8.
106. Strickberger, S.A., et al., *Amiodarone versus implantable cardioverter-defibrillator:randomized trial in patients with nonischemic dilated cardiomyopathy and asymptomatic nonsustained ventricular tachycardia--AMIOVIRT.* J Am Coll Cardiol, 2003. **41**(10): p. 1707-12.
107. Bansch, D., et al., *Primary prevention of sudden cardiac death in idiopathic dilated cardiomyopathy: the Cardiomyopathy Trial (CAT).* Circulation, 2002. **105**(12): p. 1453-8.
108. Hosenpud, J.D., et al., *The Registry of the International Society for Heart and Lung Transplantation: eighteenth Official Report-2001.* J Heart Lung Transplant, 2001. **20**(8): p. 805-15.
109. Levy, D., et al., *Long-term trends in the incidence of and survival with heart failure.* N Engl J Med, 2002. **347**(18): p. 1397-402.
110. Poole-Wilson, P.A., et al., *Comparison of carvedilol and metoprolol on clinical outcomes in patients with chronic heart failure in the Carvedilol Or Metoprolol European Trial (COMET): randomised controlled trial.* Lancet, 2003. **362**(9377): p. 7-13.
111. Kawai, C. and T. Takatsu, *Clinical and experimental studies on cardiomyopathy.* N Engl J Med, 1975. **293**(12): p. 592-7.
112. Fowles, R.E., C.P. Bieber, and E.B. Stinson, *Defective in vitro suppressor cell function in idiopathic congestive cardiomyopathy.* Circulation, 1979. **59**(3): p. 483-91.
113. Anderson, J.L., J.F. Carlquist, and E.H. Hammond, *Deficient natural killer cell activity in patients with idiopathic dilated cardiomyopathy.* Lancet, 1982. **2**(8308): p. 1124-7.
114. Limas, C.J., I.F. Goldenberg, and C. Limas, *Soluble interleukin-2 receptor levels in patients with dilated cardiomyopathy. Correlation with disease severity and cardiac autoantibodies.* Circulation, 1995. **91**(3): p. 631-4.
115. Neumann, D.A., et al., *Circulating heart-reactive antibodies in patients with myocarditis or cardiomyopathy.* J. Am. Coll. Cardiol., 1990. **16**: p. 839-846.
116. Caforio, A.L., et al., *Circulating cardiac autoantibodies in dilated cardiomyopathy and myocarditis: pathogenetic and clinical significance.* Eur J Heart Fail, 2002. **4**(4): p. 411-7.
117. Okazaki, T., et al., *Autoantibodies against cardiac troponin I are responsible for dilated cardiomyopathy in PD-1-deficient mice.* Nat. Med., 2003. **9**(12): p. 1477-1483.

118. Li, Y., et al., *Mimicry and antibody-mediated cell signaling in autoimmune myocarditis.* J. Immunol., 2006. **177**: p. 8234-8240.
119. Schultheiss, H.P., et al., *Antibody-mediated enhancement of calcium permeability in cardiac myocytes.* J. Exp. Med., 1988. **168**: p. 2102-2109.
120. Pohlner, K., et al., *Identification of mitochondrial antigens recognized by the antibody in sera of patients with dilated cardiomyopathy by two-dimensional gel electrophoresis and protein sequencing.* Am. J. Cardiol., 1997. **80**: p. 1040-1045.
121. Magnusson, Y., et al., *Autoimmunity in idiopathic dilated cardiomyopathy. Characterization of antibodies against the beta 1-adrenoceptor with positive chronotropic effect.* Circulation, 1994. **89**(6): p. 2760-7.
122. Jahns, R., et al., *Autoantibodies activating human beta1-adrenergic receptors are associated with reduced cardiac function in chronic heart failure.* Circulation, 1999. **99**(5): p. 649-54.
123. Fu, L.X.M., et al., *Localization of a functional autoimmune epitope on the second extracellular loop of the human muscarinic acetylcholine receptor 2 in patients with idiopathic dilated cardiomyopathy.* J. Clin. Invest., 1993. **91**: p. 1964-1968.
124. Limas, C.J., I.F. Goldenberg, and C. Limas, *Autoantibodies against beta-adrenoceptors in human idiopathic dilated cardiomyopathy.* Circ. Res., 1989. **64**(1): p. 97-103.
125. Schulze, K., et al., *Antibodies to ADP-ATP carrier - an autoantigen in myocarditis and dilated cardiomyopathy- impair cardiac function.* Circulation, 1990. **81**: p. 959-969.
126. Magnusson, Y., et al., *Predictive role of beta1-autoantibodies in patients with idiopathic dilated cadiomyopathy treated with metoprolol (abstract).* Circulation, 1994. **90**(4 pt 2): p. I-543.
127. Wallukat, G., et al., *Anti-beta1-adrenoceptor autoantibodies with chronotropic activity from the serum of patients with dilated cardiomyopathy: mapping of epitopes in the first and second extracellular loops.* J. Mol. Cell Cardiol., 1995. **27**: p. 397-406.
128. Matsui, S., et al., *Peptides derived from cardiovascular G-protein-coupled receptors induce morphological cardiomyopathic changes in immunized rabbits.* J. Mol. Cell Cardiol., 1997. **29**: p. 641-655.
129. Muller, J., et al., *Immunoglobulin adsorption in patients with idiopathic dilated cardiomyopathy.* Circulation, 2000. **101**(4): p. 385-91.
130. Felix, S.B., et al., *Hemodynamic effects of immunoadsorption and subsequent immunoglobulin substitution in dilated cardiomyopathy: three-month results from a randomized study.* J. Am. Coll. Cardiol., 2000. **35**: p. 1590-1598.
131. Jahns, R., et al., *Direct evidence for a beta 1-adrenergic receptor-directed autoimmune attack as a cause of idiopathic dilated cardiomyopathy.* J Clin Invest, 2004. **113**(10): p. 1419-29.
132. Limas, C.J., *Cardiac autoantibodies in dilated cardiomyopathy.* Circulation, 1997. **95**: p. 1979-1980.
133. Jahns, R., et al., *Modulation of beta1-adrenoceptor activity by domain-specific antibodies and heart failure-associated autoantibodies.* J Am Coll Cardiol, 2000. **36**(4): p. 1280-7.
134. Chiale, P.A., et al., *Differential profile and biochemical effects of antiautonomic membrane receptor antibodies in ventricular arrhythmias and sinus node dysfunction.* Circulation, 2001. **103**: p. 1765-1771.
135. Iwata, M., et al., *Autoantibodies against the second extracellular loop of beta1-adrenergic receptors predict ventricular tachycardia and sudden death in patients with idiopathic dilated cardiomyopathy.* J. Am. Coll. Cardiol., 2001. **37**: p. 418-424.

136. Witebsky, E., et al., *Chronic thyreoiditis and autoimmunization.* J. Am. Med. Assoc., 1957. **164**: p. 1439-1447.
137. Rose, N.R. and C. Bona, *Defining criteria for autoimmune diseases (Witebsky's postulates revisited).* Immunol Today, 1993. **14**(9): p. 426-30.
138. Parrillo, J.E., et al., *A prospective, randomized, controlled trial of prednisone for dilated cardiomyopathy.* N Engl J Med, 1989. **321**(16): p. 1061-8.
139. Camargo, P.R., et al., *Favorable effects of immunosuppressive therapy in children with dilated cardiomyopathy and active myocarditis.* Pediatr Cardiol, 1995. **16**(2): p. 61-8.
140. Kleinert, S., et al., *Myocarditis in children with dilated cardiomyopathy: incidence and outcome after dual therapy immunosuppression.* J Heart Lung Transplant, 1997. **16**(12): p. 1248-54.
141. Deswal, A., et al., *Safety and efficacy of a soluble P75 tumor necrosis factor receptor (Enbrel, etanercept) in patients with advanced heart failure.* Circulation, 1999. **99**(25): p. 3224-6.
142. Skudicky, D., et al., *Beneficial effects of pentoxifylline in patients with idiopathic dilated cardiomyopathy treated with angiotensin-converting enzyme inhibitors and carvedilol: results of a randomized study.* Circulation, 2001. **103**(8): p. 1083-8.
143. Kaplan, A.A., *Toward the Rational Prescription of Therapeutic Plasma Exchange: The Kinetics of Immunoglobulin Removal.* Seminars in Dialysis, 1992. **5**: p. 227-229.
144. Doerffel, W.V., et al., *Short-term hemodynamic effects of immunoadsorption in dilated cardiomyopathy.* Circulation, 1997. **95**: p. 1994-1997.
145. Felix, S.B., et al., *Removal of cardiodepressant antibodies in dilated cardiomyopathy by immunoadsorption.* J Am Coll Cardiol, 2002. **39**(4): p. 646-52.
146. Larsson, L., et al., *Beneficial effect on cardiac function by intravenous immunoglobulin treatment in patients with dilated cardiomyopathy is not due to neutralization of anti-receptor autoantibody.* Autoimmunity, 2004. **37**(6-7): p. 489-93.
147. Arnson, Y., Y. Shoenfeld, and H. Amital, *Intravenous immunoglobulin therapy for autoimmune diseases.* Autoimmunity, 2009. **42**(6): p. 553-60.
148. Haberland, A., et al., *Aptamer neutralization of beta1-adrenoceptor autoantibodies isolated from patients with cardiomyopathies.* Circ Res, 2011. **109**(9): p. 986-92.
149. Keefe, A.D. and R.G. Schaub, *Aptamers as candidate therapeutics for cardiovascular indications.* Curr Opin Pharmacol, 2008. **8**(2): p. 147-52.
150. Bouchard, P.R., R.M. Hutabarat, and K.M. Thompson, *Discovery and development of therapeutic aptamers.* Annu Rev Pharmacol Toxicol, 2010. **50**: p. 237-57.
151. Anderton, S.M., *Peptide-based immunotherapy of autoimmunity: a path of puzzles, paradoxes and possibilities.* Immunology, 2001. **104**(4): p. 367-76.
152. Jahns, R., et al., *A new cyclic receptor-peptide prevents development of heart dilatation and failure induced by antibodies activating cardiac beta1-adrenergic receptors.* Circulation, 2005. **112, suppl.II**: p. 5 (120).
153. Jahns, R., et al., *Immuno-modulating cyclopeptides: new biomolecules to combat stimulatory beta1-receptor antibodies in heart failure.* Eur. Heart J., 2006. **26, suppl.1**: p. 452 (4083).
154. Jahns, R., et al., *Probing human beta 1- and beta 2-adrenoceptors with domain-specific fusion protein antibodies.* Eur J Pharmacol, 1996. **316**(1): p. 111-21.
155. Litwin, S.E., et al., *Serial echocardiographic Doppler assessment of left ventricular geometry and function in rats with pressure-overload hypertrophy.* Circulation, 1995. **91**: p. 2642-2654.

156. Morse, E.E., *Anthrone in Estimating Low Concentrations of Sucrose.* Anal. Chem., 1947. **19**(12): p. 1012 - 1013.
157. Rasband, W.S., *Image J*. 1997 - 2012, U. S. National Institutes of Health, Bethesda, Maryland, USA.
158. Raij, L., S. Azar, and W. Keane, *Mesangial immune injury, hypertension, and progressive glomerular damage in Dahl rats.* Kidney Int, 1984. **26**(2): p. 137-43.
159. Dijkman, H., et al., *The parietal epithelial cell is crucially involved in human idiopathic focal segmental glomerulosclerosis.* Kidney Int, 2005. **68**(4): p. 1562-72.
160. Racusen, L.C., et al., *The Banff 97 working classification of renal allograft pathology.* Kidney Int, 1999. **55**(2): p. 713-23.
161. Shih, W., W.H. Hines, and E.G. Neilson, *Effects of cyclosporin A on the development of immune-mediated interstitial nephritis.* Kidney Int, 1988. **33**(6): p. 1113-8.
162. Lopez-De Leon, A. and M. Roijkind, *A simple micromethod for collagen and total protein determination in formalin-fixed paraffin-embedded sections.* J. Histochem. Cytochem., 1985. **33**: p. 737-743.
163. Morrison, T.B., J.J. Weis, and C.T. Wittwer, *Quantification of low-copy transcripts by continuous SYBR Green I monitoring during amplification.* Biotechniques, 1998. **24**(6): p. 954-8, 960, 962.
164. Pfaffl, M.W., *A new mathematical model for relative quantification in real-time RT-PCR.* Nucleic Acids Res, 2001. **29**(9): p. e45.
165. Brodde, O.E. and M.C. Michel, *Adrenergic and muscarinic receptors in the human heart.* Pharmacol Rev, 1999. **51**(4): p. 651-90.
166. Xiao, R.P. and E.G. Lakatta, *β_1-adrenoceptor stimulation and β_2-adrenoceptor stimulation differ in their effects on contraction,cytosolic Ca^{2+}, and Ca^{2+} current in single rat ventricular cells.* Circ. Res., 1993. **73**: p. 286-300.
167. Xiao, R.P., et al., *Recent advances in cardiac β_2-adrenergic signal transduction.* Circ. Res., 1999. **85**: p. 1092-1100.
168. Reid, I.A., *Actions of angiotensin II on the brain: mechanisms and physiologic role.* Am J Physiol, 1984. **246**(5 Pt 2): p. F533-43.
169. Morel, F., *Sites of hormone action in the mammalian nephron.* Am J Physiol, 1981. **240**(3): p. F159-64.
170. Thibonnier, M., et al., *Signal transduction pathways of the human V1-vascular, V2-renal, V3-pituitary vasopressin and oxytocin receptors.* Prog Brain Res, 1998. **119**: p. 147-61.
171. Bailey, J.L., *Metabolic acidosis: an unrecognized cause of morbidity in the patient with chronic kidney disease.* Kidney Int Suppl, 2005(96): p. S15-23.
172. Arnett, T.R., *Extracellular pH regulates bone cell function.* J Nutr, 2008. **138**(2): p. 415S-418S.
173. Jehle, S., et al., *Partial neutralization of the acidogenic Western diet with potassium citrate increases bone mass in postmenopausal women with osteopenia.* J Am Soc Nephrol, 2006. **17**(11): p. 3213-22.
174. Verlander, J.W., K.M. Madsen, and C.C. Tisher, *Structural and functional features of proton and bicarbonate transport in the rat collecting duct.* Semin Nephrol, 1991. **11**(4): p. 465-77.
175. Hamm, L.L., I.D. Weiner, and V.M. Vehaskari, *Structural-functional characteristics of acid-base transport in the rabbit collecting duct.* Semin Nephrol, 1991. **11**(4): p. 453-64.
176. Manger, T.M., C.A. Pappas, and B.M. Koeppen, *Beta-adrenergic regulation of H+ secretion by cultured outer medullary collecting duct cells.* Am J Physiol, 1992. **263**(6 Pt 2): p. F1011-9.

177. Schuster, V.L., *Cyclic adenosine monophosphate-stimulated bicarbonate secretion in rabbit cortical collecting tubules.* J Clin Invest, 1985. **75**(6): p. 2056-64.
178. Tago, K., V.L. Schuster, and J.B. Stokes, *Regulation of chloride self exchange by cAMP in cortical collecting tubule.* Am J Physiol, 1986. **251**(1 Pt 2): p. F40-8.
179. van der Hagen, E.A., et al., *beta1-Adrenergic Receptor Signaling Activates the Epithelial Calcium Channel, Transient Receptor Potential Vanilloid Type 5 (TRPV5), via the Protein Kinase A Pathway.* J Biol Chem, 2014. **289**(26): p. 18489-18496.
180. Duarte, C.G., F. Chomety, and G. Giebisch, *Effect of amiloride, ouabain, and furosemide on distal tubular function in the rat.* Am J Physiol, 1971. **221**(2): p. 632-40.
181. Giebisch, G., et al., *Renal and extrarenal sites of action of diuretics.* Cardiovasc Drugs Ther, 1993. **7 Suppl 1**: p. 11-21.
182. Malnic, G., R.W. Berliner, and G. Giebisch, *Distal perfusion studies: transport stimulation by native tubule fluid.* Am J Physiol, 1990. **258**(6 Pt 2): p. F1523-7.
183. Giebisch, G., *Renal potassium transport: mechanisms and regulation.* Am J Physiol, 1998. **274**(5 Pt 2): p. F817-33.
184. Giebisch, G. and W. Wang, *Potassium transport: from clearance to channels and pumps.* Kidney Int, 1996. **49**(6): p. 1624-31.
185. Khuri, R.N., W.N. Strieder, and G. Giebisch, *Effects of flow rate and potassium intake on distal tubular potassium transfer.* Am J Physiol, 1975. **228**(4): p. 1249-61.
186. Malnic, G., R.W. Berliner, and G. Giebisch, *Flow dependence of K+ secretion in cortical distal tubules of the rat.* Am J Physiol, 1989. **256**(5 Pt 2): p. F932-41.
187. Tanner, G.A., *Glomerular sieving coefficient of serum albumin in the rat: a two-photon microscopy study.* Am J Physiol Renal Physiol, 2009. **296**(6): p. F1258-65.
188. Maack, T., *Renal handling of proteins and polypeptides.* Windhager EE (ed). Handbook of Physiology. Renal Physiology, 1992: p. 2039–2082.
189. Hinz, B. and G. Gabbiani, *Fibrosis: recent advances in myofibroblast biology and new therapeutic perspectives.* F1000 Biol Rep, 2010. **2**: p. 78.
190. McAnulty, R.J., *Fibroblasts and myofibroblasts: their source, function and role in disease.* Int J Biochem Cell Biol, 2007. **39**(4): p. 666-71.
191. Bottinger, E.P. and M. Bitzer, *TGF-beta signaling in renal disease.* J Am Soc Nephrol, 2002. **13**(10): p. 2600-10.
192. Schnaper, H.W., et al., *TGF-beta signal transduction and mesangial cell fibrogenesis.* Am J Physiol Renal Physiol, 2003. **284**(2): p. F243-52.
193. Daskalakis, N. and M.P. Winn, *Focal and segmental glomerulosclerosis.* Cell Mol Life Sci, 2006. **63**(21): p. 2506-11.
194. Hughson, M.D., *Hypertension and Vascular Diseases of Kidney*, in *Silva's Diagnostic Renal Pathology*, D.A.V. Silva FG, Nadasdy T, Laszik Z, Zhou XJ, Editor. 2009: New York. p. 436-464.
195. Jennette, J.C., *The kidney*, in *Rubin's Pathology. Clinicopathologic Foundations of Medicine*. 2008, Rubin, R.; Strayer, D.S.; Rubin, E.: Philadelphia.
196. Izzo, J.L., Jr.; Sica, D.A.; Black H.R. , *Hypertension Primer: The Essentials of High Bloodpressure 4th Edition*. 4 ed. 2008, Dallas, Texas: Lippincott, Williams & Wilkins.
197. Nangaku, M., *Mechanisms of tubulointerstitial injury in the kidney: final common pathways to end-stage renal failure.* Intern Med, 2004. **43**(1): p. 9-17.
198. Weber, K.T. and C.G. Brilla, *Pathological hypertrophy and cardiac interstitium. Fibrosis and renin-angiotensin-aldosterone system.* Circulation, 1991. **83**(6): p. 1849-65.
199. Nicoletti, A. and J.B. Michel, *Cardiac fibrosis and inflammation: interaction with hemodynamic and hormonal factors.* Cardiovasc Res, 1999. **41**(3): p. 532-43.

200. Buvall, L., et al., *Antibodies against the beta1-adrenergic receptor induce progressive development of cardiomyopathy.* J Mol Cell Cardiol., 2007. **42**: p. 1001-1007.
201. Christ, T., et al., *Autoantibodies against the beta1-adrenoceptor from patients with dilated cardiomyopathy prolong action potential duration and enhance contractility in isolated cardiomyocytes.* J. Mol. Cell. Cardiol., 2001. **33**: p. 1515-1525.
202. Woodiwiss, A.J., et al., *Reduction in myocardial collagen cross-linking parallels left ventricular dilatation in rat models of systolic chamber dysfunction.* Circulation, 2001. **103**: p. 155-160.
203. Castrop, H., et al., *Physiology of kidney renin.* Physiol Rev, 2010. **90**(2): p. 607-73.
204. Schweda, F. and A. Kurtz, *Regulation of renin release by local and systemic factors.* Rev Physiol Biochem Pharmacol, 2011. **161**: p. 1-44.
205. de Wardener, H.E., *Control of sodium reabsorption.* Br Med J, 1969. **3**(5672): p. 676-83.
206. Hall, J.E., *Control of sodium excretion by angiotensin II: intrarenal mechanisms and blood pressure regulation.* Am J Physiol, 1986. **250**(6 Pt 2): p. R960-72.
207. Buckalew, V.M., Jr. and K.A. Gruber, *Natriuretic hormone.* Annu Rev Physiol, 1984. **46**: p. 343-58.
208. Ewringmann, A.G., B., *Leitsymptome bei Hamster, Ratte, Maus und Rennmaus: Diagnostischer Leitfaden und Therapie*. 2008, Stuttgart, ermany: Enke Verlag.
209. Waynforth, H.B.F., P.A., *Experimental and Surgical Technique in the Rat*. 1992, San Diego, California, USA: Academic Press.
210. Xu, Z.C., Y. Yang, and S.C. Hebert, *Phosphorylation of the ATP-sensitive, inwardly rectifying K+ channel, ROMK, by cyclic AMP-dependent protein kinase.* J Biol Chem, 1996. **271**(16): p. 9313-9.
211. Beesley, A.H., D. Hornby, and S.J. White, *Regulation of distal nephron K+ channels (ROMK) mRNA expression by aldosterone in rat kidney.* J Physiol, 1998. **509 (Pt 3)**: p. 629-34.
212. Ring, A.M., et al., *An SGK1 site in WNK4 regulates Na+ channel and K+ channel activity and has implications for aldosterone signaling and K+ homeostasis.* Proc Natl Acad Sci U S A, 2007. **104**(10): p. 4025-9.
213. Sahni, V.G., A.; Rosa, R.M., *Extrarenal Potassium Metabolism,* in *Seldin and Giebisch's The Kidney (5th Edition),* R.J.M. Alpern, O.W.; Caplan, M., Editor. 2013, Academic Press.
214. Bibert, S., et al., *Phosphorylation of phospholemman (FXYD1) by protein kinases A and C modulates distinct Na,K-ATPase isozymes.* J Biol Chem, 2008. **283**(1): p. 476-86.
215. Doucet, A., *H+, K(+)-ATPASE in the kidney: localization and function in the nephron.* Exp Nephrol, 1997. **5**(4): p. 271-6.
216. Wingo, C.S. and B.D. Cain, *The renal H-K-ATPase: physiological significance and role in potassium homeostasis.* Annu Rev Physiol, 1993. **55**: p. 323-47.
217. Boehm, O., et al., *Clinical chemistry reference database for Wistar rats and C57/BL6 mice.* Biol Chem, 2007. **388**(5): p. 547-54.
218. McKinley, M.J., et al., *Physiological and pathophysiological influences on thirst.* Physiol Behav, 2004. **81**(5): p. 795-803.
219. Rettig, R., D. Ganten, and A.K. Johnson, *Isoproterenol-induced thirst: renal and extrarenal mechanisms.* Am J Physiol, 1981. **241**(3): p. R152-7.
220. Jormeus, A., et al., *Doubling of water intake increases daytime blood pressure and reduces vertigo in healthy subjects.* Clin Exp Hypertens, 2010. **32**(7): p. 439-43.

221. Thunhorst, R.L., et al., *Effects of beta-adrenergic receptor agonists on drinking and arterial blood pressure in young and old rats.* Am J Physiol Regul Integr Comp Physiol, 2011. **300**(4): p. R1001-8.
222. Go, A.S., et al., *Chronic kidney disease and the risks of death, cardiovascular events, and hospitalization.* N Engl J Med, 2004. **351**(13): p. 1296-305.
223. Weiner, D.E., et al., *Chronic kidney disease as a risk factor for cardiovascular disease and all-cause mortality: a pooled analysis of community-based studies.* J Am Soc Nephrol, 2004. **15**(5): p. 1307-15.
224. Peterson, J.C., et al., *Blood pressure control, proteinuria, and the progression of renal disease. The Modification of Diet in Renal Disease Study.* Ann Intern Med, 1995. **123**(10): p. 754-62.
225. Matsushita, K., et al., *Association of estimated glomerular filtration rate and albuminuria with all-cause and cardiovascular mortality in general population cohorts: a collaborative meta-analysis.* Lancet, 2010. **375**(9731): p. 2073-81.
226. Carroll, M.F. and J.L. Temte, *Proteinuria in adults: a diagnostic approach.* Am Fam Physician, 2000. **62**(6): p. 1333-40.
227. Abuelo, J.G., *Proteinuria: diagnostic principles and procedures.* Ann Intern Med, 1983. **98**(2): p. 186-91.
228. Glassock, R.J., *Is the presence of microalbuminuria a relevant marker of kidney disease?* Curr Hypertens Rep, 2010. **12**(5): p. 364-8.
229. Ruiz-Ortega, M., et al., *Angiotensin II: a key factor in the inflammatory and fibrotic response in kidney diseases.* Nephrol Dial Transplant, 2006. **21**(1): p. 16-20.
230. Rosenkranz, S., et al., *Alterations of beta-adrenergic signaling and cardiac hypertrophy in transgenic mice overexpressing TGF-beta(1).* Am J Physiol Heart Circ Physiol, 2002. **283**(3): p. H1253-62.
231. Wolf, G., *New insights into the pathophysiology of diabetic nephropathy: from haemodynamics to molecular pathology.* Eur J Clin Invest, 2004. **34**(12): p. 785-96.
232. Bataller, R. and D.A. Brenner, *Liver fibrosis.* J Clin Invest, 2005. **115**(2): p. 209-18.
233. Vallance, B.A., et al., *TGF-beta1 gene transfer to the mouse colon leads to intestinal fibrosis.* Am J Physiol Gastrointest Liver Physiol, 2005. **289**(1): p. G116-28.
234. Campbell, S.E. and L.C. Katwa, *Angiotensin II stimulated expression of transforming growth factor-beta1 in cardiac fibroblasts and myofibroblasts.* J Mol Cell Cardiol, 1997. **29**(7): p. 1947-58.
235. Kim, S., et al., *Angiotensin II induces cardiac phenotypic modulation and remodeling in vivo in rats.* Hypertension, 1995. **25**(6): p. 1252-9.
236. Wolf, G., *Link between angiotensin II and TGF-beta in the kidney.* Miner Electrolyte Metab, 1998. **24**(2-3): p. 174-80.
237. Bonegio, R.G., et al., *Rapamycin ameliorates proteinuria-associated tubulointerstitial inflammation and fibrosis in experimental membranous nephropathy.* J Am Soc Nephrol, 2005. **16**(7): p. 2063-72.
238. Donadio, J.V. and J.P. Grande, *IgA nephropathy.* N Engl J Med, 2002. **347**(10): p. 738-48.
239. Lekgabe, E.D., et al., *Relaxin reverses cardiac and renal fibrosis in spontaneously hypertensive rats.* Hypertension, 2005. **46**(2): p. 412-8.
240. Bohle, A., et al., *Renal morphology in essential hypertension: analysis of 1177 unselected cases.* Kidney Int Suppl, 1998. **67**: p. S205-6.
241. Cowley, A.W., Jr. and R.J. Roman, *The role of the kidney in hypertension.* JAMA, 1996. **275**(20): p. 1581-9.

242. Esler, M.D., et al., *Renal sympathetic denervation in patients with treatment-resistant hypertension (The Symplicity HTN-2 Trial): a randomised controlled trial.* Lancet, 2010. **376**(9756): p. 1903-9.
243. Luft, F.C., et al., *Angiotensin-induced hypertension in the rat. Sympathetic nerve activity and prostaglandins.* Hypertension, 1989. **14**(4): p. 396-403.
244. Coffman, T.M. and S.D. Crowley, *Kidney in hypertension: guyton redux.* Hypertension, 2008. **51**(4): p. 811-6.
245. Lombardi, D., et al., *Salt-sensitive hypertension develops after short-term exposure to Angiotensin II.* Hypertension, 1999. **33**(4): p. 1013-9.
246. Koletsky, S., J.M. Rivera-Velez, and W.H. Pritchard, *Production of hypertension and vascular disease by angiotensin.* Arch Pathol, 1966. **82**(1): p. 99-106.
247. Shricker, K., et al., *The role of angiotensin II in the feedback control of renin gene expression.* Pflugers Arch, 1997. **434**(2): p. 166-72.
248. Oliverio, M.I., et al., *Renal growth and development in mice lacking AT1A receptors for angiotensin II.* Am J Physiol, 1998. **274**(1 Pt 2): p. F43-50.

8 Appendix

8.1 Materials

8.1.1 Chemicals, solvents and enzymes

Substance	Catalog Number	Company
2-Methylbutane	A0440	Applichem
Acetic acid	33209	Sigma
Acetone	8003	Baker
Acrylamide	A0385	Applichem
Ammonium-amidosulfonate	101220	Merck
Ammoniumperoxidsulfate (APS)	9592.1	Roth
Ampicillin	A9518	Sigma
β-mercaptoethanol	15433	Merck
Bovine serum albumin	A1391	Applichem
Bromphenolblue	15375	Serva
Caprylic acid	C2875	Sigma
Calciumchloride ($CaCl_2$)	2387	Merck
Direct Red	365548	Sigma
Dithiothreitol (DTT)	A1101	Applichem
DNase	DN25	Sigma
EDTA disodiumsalt dihydrate	8043.2	Roth
Ethanol	32205	Sigma
Eukitt	03989	Fluka
Fast Green FCF	F7252	Sigma
Freud’s Adjuvands complete	F5881	Sigma
Freud’s Adjuvands incomplete	F5506	Sigma
Glucose	8337	Merck
Glutathione	G4251	Sigma
Glycerol	D10-313	Pharmacy

Glycin	A1067	Applichem
Hematoxylin	3816.1	Roth
Hydrochloride (HCl)	4625.1	Roth
Hydrogen peroxide (H_2O_2)	A1134	Applichem
Inulin	F3272	Sigma
IPTG	A4773	Applichem
L-malate	02315	Sigma
Magnesium sulfate	A963086	Merck
Methanol	32213	Sigma
2- (n-morpholino) ethanesulfonic acid (MES)	M3885	Sigma
N-(1-naphthyl) ethylenediamino dihydrochloride	N5889	Sigma
Non-fat dried milk powder	A0830	Applichem
O.C.T Compound	4583	Sakara
o-Phenylenediamine	P-9029	Sigma
Para-aminohippuric acid (PAH)	61789	Sigma
Paraformaldehyde (PFA)	P-6148	Sigma
Perchloric acid	100514	Merck
Periodic acid	HP00.1	Roth
Picric acid	74069	Fluka
Phenylmethylsulfonylfluoride (PMSF)	P-7626	Sigma
Ponceau S	P-3504	Sigma
Potassium chloride (KCl)	A2939	Applichem
Potassium dihydrogen phosphate (KH_2PO_4)	A776073	Merck
RNase	A3832	Applichem
Schiff's reagent	X900.1	Roth
Sodium acetate	6268	Merck
Sodium azide	6688	Merck
Sodium dodecylsulfate (SDS)	A7249	Applichem
Sodium chloride (NaCl)	A3597	Applichem
Sodium hydrogen carbonate (Na_2HCO3)	A1940	Applichem
Sodium hydrogen phosphate dihydrate (Na_2HPO_4)	A4732	Applichem
Sodium-L-lactate	L7022	Sigma

Sodium nitrite	8604	Roth
Sodium pyruvate	P2256	Sigma
TEMED	A1148	Applichem
n-tris(hydroxymethyl)methyl-2-aminoethanesulfonic acid (TES)	T1375	Sigma
Trichloroacetic acid	A1431	Applichem
Tris base	A1086	Applichem
Tris-HCl	A1087	Applichem
TritonX-100	T-9284	Sigma
Tween20	A1389	Applichem
Urea	A1361	Applichem
Xylol	A2476	Applichem

8.1.2 Buffers

Blocking Buffer (ELISA)	3% (w/v) non-fat dried milk powder 1x PBS 0.1% (v/v) Tween10
Bovine Serum Albumin	5% (w/v) BSA (Fraction V) 0.2% (v/v) 1x TBS
Coating Buffer	15 mM Na_2CO_3 35 mM $NaHCO_3$
Dialysis hose buffer	5 mM EDTA 200 mM $NaHCO_3$
Elutionbuffer	10 mM Glutathion 50 mM Tris-HCl 200 mM NaCl

		1 mM EDTA
		2 mM DTT
		→ pH adjusted to 8.0
Krebs-Henseleit-Buffer (modified)		118 mM NaCl
		4.7 mM KCl
		1.2 mM $MgSO_4$
		1.25 mM $CaCl_2$
		1.2 mM KH_4PO_4
		25 mM $NaHCO_3$
		8.7 mM Glucose
		0.3 mM sodium-pyruvate
		2 mM L-lactate
		1 mM α-ketoglutarate
		1 mM sodium-L-malate
		6 mM urea
Lysis Buffer		1x PBS
		0.5 M $MgSO_4$
		DNase
		100 mM PMSF
	After disruption:	1% TritonX
		100 µg/ml RNase
		5 mM EDTA
Measuring Buffer (GFR)		5 mM TES
		4.6 mM MES
		→ pH adjusted to 7.4
PFA 4%		4% (w/v) PFA
		1x PBS

Phosphate Buffered Saline (PBS) (10x)	1.4 M NaCl 27 mM KCl 101 mM Na_2HPO_4 $2H_2O$ 18 mM KH_2PO_4 → pH adjusted to 7.3
Relaxing Buffer	5% Glucose 25 mM KCl 10x PBS 1 ml/l Proteinaseinhibitor 1x IBX/PPI
Tris-buffered Saline (20x)	0.5 M Tris base 2.7 M NaCl 54 mM KCl → pH adjusted to 7.4
Washing Buffer (ELISA)	1x PBS 0.1% (v/v) Tween 20
Washingbuffer (induction of fusionproteins)	50 mM Tris-HCl 200 mM NaCl 1 mM EDTA 2 mM DTT → pH adjusted to 8.0

8.1.3 Primers

Primer	5’ – 3’ sequence	Accession number
Activin		
sense	GATGTGCGGATTGCTTGTGA	NM_024486
antisense	TCTTCTTGCCCAGGAGCACTA	
Collagen 1a1		
sense	AAGGCAACAGTCGATTCACC	NM_053304
antisense	ATGACTGTCTTGCCCCAAGT	
Collagen3a1		
sense	GAAATTCTGCCACCCTGAAC	NM_032085
antisense	GCATGTTTCTCCGGTTTCC	
GAPDH		
sense	CTCCCTCAAGATTGTCAGCA	NM_017008
antisense	TGATGGCATGGACTGTGG	
Hprt1		
sense	GACTTTGCTTTCCTTGGTCA	NM_012583
antisense	AGTCAAGGGCATATCCAACA	
Pgk1		
sense	TAAAGTCAGCCATGTGAGCA	NM_053291
antisense	ATGAATCCCGATGCAGTAAA	
Renin		
sense	TCTCTCCCAGAGGGTGCTAA	NM_012642
antisense	TTGCCCTGGTAATGTTGAGG	
Smad3		
sense	TCCAGTCTCCCAACTGCAAC	P84025
antisense	GAGCTAGGAGGGCAGCAAA	
Smad4		
sense	GCCGTCTTCGTGCAGAGT	NP_062148
antisense	ACACTGCCGCAAATCAAAG	

TGF-β_1		
sense	AAGAAGTCACCCGCGTGCTA	NM_021578
antisense	TGTGTGATGTCTTTGGTTTTGTCA	

8.1.4 Kits and markers

Name	Supplier
Albumin Standard	Pierce
BCA Protein Assay Kit	Thermo Scientific
Bradford Protein Detection Kit	Biorad
Brillant III SYBR Green QPCR Master Mix	Agilent Technologies
Masson-Goldner-Trichrome Staining Kit	Merck
High Capacity RNA to cDNA Kit	Applied Biosystems
Periodic acid Schiff's Staining Kit	Roth
Plasma Renin-Activity-RIA	DiaSorin
RNase-free DNase Set	Qiagen
RNeasy mini kit	Qiagen

8.1.5 Software

Name	Supplier
Photoshop CS4	Adobe Systems
Prism 6.0	GraphPad Software Inc.
Image J	Wayne Rasband (NIH)
LabChart	AD Instruments
Lauris	Swiss Lab
Office 2010	Microsoft

8.1.6 Equipment

Name	Model	Manufacturer
Analytical system	Cobas Integra 800	Roche
Autoclave	KSF 317	J. Thieme
Bacterial incubator	ISF-1-V	Adolf Kühner AG
Blood Gas Analyzer	ABL 520	Radiometer
Centrifuges	Centrifuge 5417	Eppendorf
	Rotina 48R	Hettich
	Avanti J-25	Beckman
Cooling plate	EG 1140C	Leica
Cryomicrotome	CM 3050S	Leica
Data acquisition device	Power Lab 4135	AD Instruments
French Press	Cell Press	SLM Aminco
γ-counter	1480 Wizard 3”	Perkin Elmer
Heart catheter	-	Millar Instruments
Heating plate	14501	Medax
Ice machine	MF30	Scotsman
Incubator	Kelvitron t	Heraeus Instruments
Magnetic stirrer	Ikamag RCT	Janke & Kunkel GmbH
Microscope	DM 4000B	Leica
Microscope camera	K4-F75U	JVC
Microscope light source	Codix	Kübler
Microtome	RM 2165	Leica
Microwave	Micromat	AEG
Nanodrop	2000C	Peqlab
Nephelometer	BN2-Behring II	Siemens
PCR cycler	CTX 384	Biorad
Perfusor	Perfusor® F	Braun
pH electrode	InLab Routine pro	Mettler Toledo
Photoaccustic imaging system	Vevo LAZR	Visual Sonics

Photometer	Victor^2 1420	Wallace
Pipetteboy	Accu-jet pro	Brand
Pipettes	Pitet lite	Rainin
	Research	Eppendorf
	Multipette plus	Eppendorf
Shaking table	WT12	Biometra
Spectrophotometer	SpectraMax plus	Molecular Devices
Thermo mixer	Thermomixer 5436	Eppendorf
Tissue Lyser	TissueLyser II	Quiagen
Transducer Coupler	-	Föhr Medical Instruments
Vortex	VTX-3000L	LMS
Water bath	1083	GFL

8.1.7 Consumables

Name	**Supplier**
384-well plates	Biozym
96-well plates	Thermo Scientific
Centrifugal filter units	Millipore
Cover slips	Nunc
Cryotubes	Nunc
Cuvettes	Sarstedt
Embedding cassettes	Roth
Hypodermic syringes	BD
Microscope slides	R. Langenbrinck
Microtome blades	Hartenstein
Monovettes	Sarstedt
Polypropylene tubes (Falcons),	BD
Reaction tubes	Eppendorf

8.2 Affidavit/Eidesstattliche Erklärung

8.2.1 Affidavit

I hereby confirm that my thesis entitled „Relevance of antibodies targeting the β_1-adrenergic receptor for renal function" is the result of my own work. I did not receive any help or support from commercial consultants. All sources and/or materials applied are listed and specified in the thesis.

I furthermore confirm that this thesis complies with the Guidelines of the University of Würzburg about Good Scientific Practice.

Furthermore I confirm that this thesis has not been submitted as part of another examination process neither in identical nor in similar form.

No further academic degrees were taken besides Master of Science with distinction in Biology.

8.2.2 Eidesstattliche Erklärung

Hiermit erkläre ich an Eides statt, die Dissertation „Relevanz von Antikörpern gegen den β_1-adrenergen Rezeptor für die Nierenfunktion" eigenständig, d.h. insbesondere selbständig und ohne Hilfe eines kommerziellen Promotionsberaters, angefertigt und keine anderen als die von mir angegebenen Quellen und Hilfsmittel verwendet zu haben.

Ich versichere an Eides statt, dass mir die Möglichkeit zur Promotion und deren Betreuer nicht durch kommerzielle Stellen vermittelt wurde. Weiterhin erkläre ich, dass die Richtlinien der Universität Würzburg über gute wissenschaftliche Praxis eingehalten wurden.

Ich erkläre außerdem, dass die Dissertation weder in gleicher noch in ähnlicher Form bereits in einem anderen Prüfungsverfahren vorgelegen hat.

Es wurden neben dem Grad des Diplom-Biologen bisher keine weiteren akademischen Grade erworben.

Würzburg, Juli 2014

8.3 Curriculum Vitae

PERSONAL DATA

Name	Sonja Hartmann
Date of birth	05/14/1985
Place of birth	Forchheim, Germany
Nationality	German

EDUCATION

11/2013 – present	PostDoc Position CHFC, University Hospital Würzburg, Germany
04/2010 – 10/2013	Ph.D. Julius Maximilian University, Würzburg, Germany Advisors: Roland Jahns, Thomas Müller
10/2004 – 11/2009	German diploma (equivalent to M.Sc.) in biology Julius Maximilian University Würzburg, Germany Majors: biotechnology, bioinformatics, pharmacology and toxicology
09/1995 – 07/2004	Eichendorff-Gymnasium, Bamberg, Germany Graduation: Abitur

8.4 List of Publications

Hartmann S., Schwarzbach V., Schneider R., Held C., Zechmeister C., Bitterer C., Lohse M.J., Jahns R., Boivin V., *Effects of antibodies targeting the β_1-adrenergic receptor on heart and kidney* (manuscript in preparation).

Panjwani P.A., Higuchi T., Helluy X., Ye Y., Zechmeister C., **Hartmann S.**, Kaiser F., Lohse M.J., Hiller K.H., Jakob P., Jahns R., Boivin V., *Detailed Histomorphologic and Molecular Analysis of Myocarditis as an approach to Identify Novel Molecular Targets Facilitating Imaging of Myocardial Inflammation* (manuscript in preparation).

Boivin-Jahns V., Schlipp A., **Hartmann S.**, Panjwani P., Klingel K., Lohse MJ., Ertl G.,Jahns R. *Antibodies to cardiac receptors.* Herz 2012. **37**(8): p. 843-8.

8.5 Conference Proceedings (Selection)

Hartmann S., Schneider R., Held C., Schweda F., Zechmeister C., Bitterer C., Lohse MJ., Ertl G., Jahns R., Boivin V. (2013), *Relevance of β_1-adrencopector auto-antibodies for renal function;* Poster presented at the Scientific Sessions, American Heart Association, Dallas, Texas, USA

Hartmann S., Schneider R., Held C., Zechmeister C., Bitterer C., Lohse MJ., Ertl G., Jahns R., Boivin V. (2012), *Stimulating anti-β_1-receptor antibodies and kidney function: reno-cardial crosstalk and its relevance for worsening cardiac function;* Poster presented at the European Society of Cardiology Congress, Munich, Germany

Hartmann S., Schneider R., Held C., Zechmeister C., Bitterer C., Lohse MJ., Ertl G., Jahns R., Boivin V. (2012), *Reno-cardial crosstalk in stimulating β_1-antibody-induced cardiomyopathy;* Poster presented at the Heart Failure Congress, European Society of Cardiology, Belgrade, Serbia

Hartmann S., Schneider R., Held C., Zechmeister C., Bitterer C., Lohse MJ., Ertl G., Jahns R., Boivin V. (2012), *Reno-cardial crosstalk in stimulating β_1-antibody-induced cardiomyopathy;* Poster presented at the 78th Annual Meeting, German Cardiac Society, Mannheim, Germany

Hartmann S., Boivin V., Schlipp A., Zechmeister C., Ullrich J., Schwarzbach V., Lohse MJ., Jahns R. (2010), *Endoplasmic reticulum stress is a key mediator of increased myocyte apoptosis in anti- β_1-antibody induced cardiomyopathy;* Poster presented at the European Society of Cardiology Congress, Stockholm, Sweden

Hartmann S., Boivin V., Schlipp A., Zechmeister C., Ullrich J., Schwarzbach V., Lohse MJ., Jahns R. (2010), *Sequential cardiac protein analysis in anti- β_1-antibody induced cardiomyopathy reveals endoplasmic reticulum stress as a key mediator of increased myocyte apoptosis;* Poster presented at the 76th Annual Meeting, German Cardiac Society, Mannheim, Germany

8.6 Acknowledgments

First of all, I must thank Prof. Roland Jahns for giving me the opportunity to work on this highly interesting topic. His supervision and constant support during my PhD thesis were unequaled, and especially his willingness to give his time so generously has been very much appreciated.

My sincere thanks go to Prof. Thomas Müller for offering to be my second supervisor, and for all his constructive recommendations and support on this project.

I thank Prof. Martin J. Lohse for the opportunity to do my PhD at the Institute of Pharmacology, and for all the useful discussions and ideas regarding my project.

Special thanks should be given to Dr. Valérie Jahns for all the helpful discussions and valuable input during the planning and development of this research project.

I would like to express my deep gratitude to all the former and current members of the AG Jahns, not just for their experimental help, but also for their friendship and constant encouragement during the past years. I also thank all the members of the Department of Pharmacology and Toxicology for their help and support in the past years; especially Anni, Evelyn, Marthe, and Tanja. Furthermore, I'd like to thank Alice, Anja, and Nadine for their support in the "final phase".

I'd like to say a big thank you to Dr. Reinhard Schneider and Christopher Held for the pleasant collaboration and all the (experimental) help. The same accounts for Enrico Wagner, Dr. Michael Neumann and the team of the Central Laboratory of the University Hospital Würzburg.
My heartfelt thanks go to Prof. Frank Schweda and Robert Götz for their support and especially for performing the experiments on the isolated perfused kidneys.

Many thanks to go Teresa, Lissy, Tommy, and David, for always being there for me and for keeping me sane.

Above all, my thanks go to my parents and brothers. You are the best family I could have ever wished for. I wouldn't be where I am without you.

Stephen, thank you for going through all this with me…